Fluorescence detection of trace aluminium using a sequential injection analyser

by
Tara de Jongh

Thesis presented in fulfilment of the requirements for the degree of Masters of Earth Sciences, at Stellenbosch University

Supervisor: Prof. Alakendra Roychoudhury

Co-supervisor: Dr Saumik Samanta

December 2022

Declaration

By submitting this assignment electronically, I declare that the entirety of the work contained therein is my own, original work, that I am the sole author thereof (save to the extent explicitly otherwise stated), that reproduction and publication thereof by Stellenbosch University will not infringe any third-party rights and that I have not previously in its entirety or in part submitted it for obtaining any qualification.

Tara de Jongh
Date:

Acknowledgements

I would like to thank my supervisor, Prof. Alakendra Roychoudhury for giving me the opportunity to work on this project, and for allowing me to be creative and exploratory in my approach to the project. I would like to give my deepest gratitude to my co-supervisor, Dr Saumik Samanta for the endless support and guidance, and for believing in me. Without your support and guidance this project would have not been possible. I am extremely grateful and thankful for the funding I received from Stellenbosch University and the National Research Foundation (NRF). I would also like to thank Dr Jan-Lukas Menzel for initiating this project and for the initial guidance. I express my gratitude to GlobalFIA, Fox Island, WA, USA for designing the miniSIA-2. To Erhardt Joubert for your support, expertise on pumps and assistance in writing the “abstraksie”. The SA Agulhas II crew and the TraceEx team for making science possible, and to the Antarctic chickens (Houda, Jennifer, Asmita, Raya, Zandria, and Marti) for making cruise life filled with fun and laughter. A special thanks to Simone Louw, words cannot express how appreciative I am of your friendship, support and motivation which you have given me throughout this project and for never letting me give-up. To my family for giving me support and understanding throughout this project and my studies. Finally, I would like to thank my dad for his support and unconditional love, who I know would have been very proud.

Abstract

Analytical instruments are either expensive to operate, prone to interferences, require a separate offline preconcentration step, or are not suitable for use onboard a ship when measuring dissolved Aluminium (Al_d; < 0.2 µm fraction) in seawater. Thus far, Al_d measurements have been performed most commonly using flow injection analysis (FIA), as it combines preconcentration, fluorometry and spectroscopy in a single manifold. Despite FIA's compact and comprehensive design, the manifold has several drawbacks, including its laminar flow regime and the peristaltic pump, which causes tube stretching and generates measurement drift. As a result of these limitations, a third-generation flow analyser was developed, known as a miniaturized two-line sequential injection analyser (miniSIA-2). The miniSIA-2 incorporates similar design features to that of FIA, however, it operates on a bidirectional flow regime, enabling reverse fluid flow and encourages turbulence to allow complete sample and reagents reaction, while reducing the reagent consumption and waste generation. Thus far, the miniSIA-2 has only been used to measure trace concentrations of Zinc (Zn) (Grand et al., 2011; Grand et al., 2016) and Iron (Fe) (Oliveira et al., 2015; Hatta et al., 2018) in seawater. This project therefore involves a novel and systematic approach to measuring Al_d in seawater through fluorescence detection by an advanced miniSIA-2 manifold of Grand et al., (2016). The systematic approach involved integrating the experimental procedures outlined by Hatta et al., (2018) and the experimental protocols of Grand et al., (2011 & 2016) first and second design of Zn_d for measurements of Al_d. This led to a method approach initiated with optimizing the batch method, followed by the Stop in Holding coil (SHC) procedure and finally incorporating a Solid Phase extraction (SPE) step with the SHC to ensure a fully automated instrument for measuring Al_d in seawater. However, this project focused on developing and applying the well-established batch method from Hydes & Liss, (1976). The method details the development of a two-step method. Initially, a basic analytical setup was established by systematically adjusting parameters to achieve measurements at relatively higher Al_d concentrations. During this step, a limit of detection (LOD = 9 nM) was achieved. The above-mentioned analytical setup was then used to achieve instrumental detection limits similar to the lowest Al_d concentrations measured in global oceans (0.1 nM). In this second instant a lower LOD (7 nM) was achieved, however, the improvement was much less than the initial aim. This was the result of the instruments fluctuating baseline values, high Relative Standard Deviation (RSD), and

the manifold's inability to self-regulate internal temperatures during analysis time causing a weak peak configuration that resembled that of photobleaching and quenching.

Opsomming

Analitiese gereedskap is gewoonlik duur om te gebruik, sensitief vir inmenging of benodig ‘n voorkonsentrasie proses wanneer dit kom by die meet van opgelosde aluminium (Al_d < 0.2 µm fraction) in seewater. Tot dusver word vloei inspuiting analiese (FIA) verkies om Al_d in seewater te meet omdat dit die voorkonsentrasie, flourometrie en spektroskopie in ‘n enkel manifold kombineer. Ten spyte van FIA manifold kompakte en omvattende ontwerp, die manifold het verskeie nadele, insluitend die laminêre vloei regime en die peristaltiese pomp wat die vloei aandryf en die pype kan strek en dus en metingsdrywing genereer. As gevolg van hierdie beperkings, het die derde generasie van flow analiseerders tot weeg gebring wat bekend staan as die miniSIA-2 (miniatuur twee-lyn opeenvolgende inspuitings analiseerder). Die miniSIA-2 bevat soortgelyke ontwerpkenmerke van dit van FIA, maar werk op en tweerigting-vloeiregime, wat omgekeerde vloeistofvloei moontlik maak en turbulensie aanmoedig om volledige monster-en reagensreaksie toe te laat,terwyl die reagensverbruik en afvalgenerering verminder word. So vêr, was die miniSIA-2 voorheen gebruik om die konsentrasie Zink (Zn) (Grand et al., 2011; Grand et al., 2016) en Yster (Fe) (Oliveira et al., 2015; Hatta et al., 2018) in seewater te meet. Hierdie projek behels dus ń nuwe en sistematiese benadering om Al_d in seewater te meet deur fluoressensie-opsporing deur ń gevorderde miniSIA-2 spruitstuk van Grand et al., (2016). Die sistematiese benadering behels die integrasie van die eksperimentele prosedures soos uiteengesit deur Hatta et al., (2018) en die eksperimentele protokolle van Grand et al., (2011 & 2016) eerste en tweede ontwerp van Zn_d vir metings van Al_d. Dit het gelei tot ń metodebenadering wat begin het met die optimering van die “Batch”-metode, gevolg deur die “Stop in Holding-spoel” (SHC)-prosedure en uiteindelik ń “Solid Phase-ekstraksie- stap (SPE) by die SHC ingesluit het om ń ten volle outomatiese instrument vir Al_d in seewater te verseker. Weens tydsbeperkings het hierdie projek egter gefokus op die ontwikkeling en toepassing van die goed gevestigde “Batch”-metode van Hydes & Liss, (1976). Die metode beskryf die ontwikkeling van ń twee-stap metode. Aanvanklik was ‘n basiese opstelling ontwikkel deur sistematies die parameters te verander vir relatiewe hoë Al_d waardes. Gedurende hierdie fase, was die laagste konsentrasie Al_d wat beroubaar opgespoor kon word in die oplossing, 9nM. Die bogenoemde analitiese opstelling was toe uitgebrei om aluminium te kan meet tot die laagste Al_d konsentrasie wat in die wêreld se oseane gemeet word (0.1 nM). In hierdie geval was die laagste konsentrasie wat gemeet kon word, 7 nM. Die 7 nM Al_d is veel meer as die 0.1 nM waarvoor gemik was. Die rede vir hierdie tekortkoming was die

wisselvallige grondvlak waardes, hoë Relatiewe standaardafwyking (RSD) waardes en die manifold se onvermoë om die temperatuur te reguleer. Hierdie het ‘n onbetroubare piek in die gemete grafiek teweeg bring wat “photobleaching” en “quenching kan voorstel.

Table of Contents

List of Figures

List of Tables

List of Equations

Abbreviations and Acronyms

AAS	Atomic Absorption Spectrometry
adCSV	Adsorptive Cathodic Stripping Voltammetry
Al_d	Dissolved Aluminium
Al-F	Al-Fluorescein Final
Al-LMG	Aluminium-Lumogallion
Al-O	Al-Fluorescein Original
AS	Atomic Spectroscopy
Brij-35	Polyoxyethylene(23) lauryl ether
CC	Central Channel
CTD	Conductivity-Temperature-Depth
DASA	1,2-Dihydroxyanthraquinone-3-sulfonic acid
EDTA	2,2',2",2'"-(1,2-Ethanediyldinitrilo)tetraacetic acid
ET AAS	Electrothermal Atomic Absorption Spectrometry
F AAS	Flame Atomic Absorption Spectrometry
Fe_d	Dissolved Iron
FIA	Flow Injection Analysis
GF AAS	Graphite Tube Furnace Atomic Absorption Spectrometry
HC	Holding coil
HDPE	High Density Polyethylene
HF	High flow
HR-ICP-MS	High Resolution Inductively Coupled Plasma Mass Spectrometry
ICP-MS	Inductively Coupled Plasma Mass Spectrometry
IDA	2,2'-Iminodiacetic acid
LDPE	Low Density Polyethylene
LLE	Liquid-Liquid solvent Extraction
LMG	Lumogallion
LOV	Lab-on-Valve
miniSIA-2	Miniaturized two-line Sequential Injection Analyser
PFA	Perfluoro Alkoxy
PMT	Photomultiplier tube

PP	Polypropylene
PTFE	Polytetrafluoroethylene
RT	Room Temperature
SCALE	Southern oCean seAsonal Experiment
SFC	Stop in Flow cell
SHC	Stop in Holding coil
SIA	Sequential Injection Analysis
SI-LOV	Sequential Injection Lab-on-Valve
SO	Southern Ocean
SPE	Solid Phase Extraction
TM_d	Dissolved Trace Metal
TM	Trace Metal
µSI-LOV	Micro-Sequential Injection – Lab-on-Valve
Zn_d	Dissolved Zinc
8-HQ	8-Quinolinol

Chapter 1 Introduction

1.1 Background

Aluminium (Al) is ubiquitous and is the third most abundant element within the earth's crust, accounting for 8.1% of the continental crust (Taylor, 1964; Rudnick & Gao, 2003). The reactivity of Al makes this lithophile element abundant in sparingly soluble oxides and aluminosilicates (Scancar & Milacic, 2006). Aluminosilicate minerals, particularly sodic, potassium, and calcium-bearing feldspars, Na or $K(AlSi_3O_8)$ and $CaAl_2Si_2O_8$, cover 51% of the crustal rocks (Stebbins et al., 1999). Despite the abundance of Al in crustal rocks, the concentration of dissolved Aluminium (Al_d) in seawater ranges from sub-nanomolar (sub nM) to nanomolar concentrations (nM), with the lowest average surface concentration recorded in the Southern Ocean (SO) (0.7-0.8 nM) **(**Middag et al., 2011; Menzel Barraqueta et al., 2020) and the highest within the Mediterranean Sea (65.15-54.90 nM) (Han et al., 2008; Menzel Barraqueta et al., 2020). These low concentrations of Al_d in oxygenated surface seawater, is a combination of Al's particle reactive nature and low solubility. Recently, Al has been classified as a hybrid type metal, which conforms to either a nutrient-type or scavenged-type of configuration, depending on the oceanic basin (Tagliabue, 2019). In the majority of the world's oceans, Al_d shows a scavenged-type distribution (Bruland & Lohan, 2003). This is due to the metal's strong interaction with partial dissolved atmospheric dust particles, which gives a short residence time (2-6 yrs) in surface waters (Orians & Bruland, 1985; Kamer et al., 2004) and a longer residence time of 50-200yrs in deeper waters (Orians & Bruland, 1985). Furthermore, there is a tendency of Al^{3+} to bind to available ligands, forming stable hydroxide complexes (Scancar & Milacic, 2006), which in turn makes amorphous $[Al(OH)_3]$ and the aluminate anion $[Al(OH)_4]^-$ the dominate inorganic species of Al in seawater (Orians & Bruland, 1985, 1986).

Given that atmospheric dust particles are enriched with Al (Mahowald et al., 2018), Al_d concentrations in the surface ocean have been used as a proxy to estimate dust deposition to the open ocean (Measures & Brown, 1996; Measures & Vink, 2000; Measures et al., 2008; Anderson et al., 2016). Aeolian dust is transported to open ocean as predominantly dry deposition, which takes longer to dissociate into the water column (Mahowald et al., 2018). However, with increasing anthropogenic emissions, contributing to low pH environments, the solubility of Al increases, allowing for instantaneous dissolution to surface oceans (Measures

et al., 2010; van Hulten et al., 2013). This could result in a higher concentration of "free Al", known to be hazardous for the environment and living organisms (Gensemer & Playle, 1999; Ma, 2000; Hoekenga et al., 2003).

Accurately quantifying Al_d in seawater is a notoriously difficult task. The concentration of Al_d in seawater has therefore been measured using a wide variety of analytical techniques and apparatus and applied to the majority of the world's oceanic basins (Table 1.1). These analytical techniques can be categorised into Atomic Spectroscopy (AS) (Orians & Bruland, 1985; Measures & Edmond, 1989; Sohrin et al., 2008; Minami et al., 2015), adsorptive Cathodic Stripping Voltammetry (adCSV) (van den Berg et al., 1986) and Fluorometry (Hydes & Liss, 1976; Howard et al., 1986; Ren et al., 2001). Although, these analytical techniques achieved low Limit of detection (LOD), ranging from 0.1-0.7 nM (Table 1.1), the majority of these analytical procedures required an offline preconcentration step to achieve a quantitative Al recovery. Preconcentration involves the separation of the high salt matrix from the existing metal, either by Solid Phase Extraction (SPE) or Liquid-liquid solvent extraction (LLE), which avoids weak spectral signals, high procedural blanks, interferences and contamination. This is especially applicable for popular analytical instruments, such as adCSV or Inductively Coupled Plasma Mass Spectrometry (ICP-MS). By performing such steps the weak spectral and high blanks could be further resolved by incorporating the fluorescent lumogallion (LMG) (Hydes & Liss, 1976), which increased the sensitivity and simplified the analytical procedure, without compromising the LOD, previously achieved by analysing with AS and adCSV. However, ionic interferences from Fluoride (F^-) and Ferric Iron (Fe^{3+}), can reduce the sensitivity of the (Aluminium-Lumogallion) Al-LMG chelate complex. Which lead to the incorporation of a surfactant to enhance the sensitivity and reduce the LOD from 1.9 nM to 0.7-0.4 nM (Ren et al., 2001).

By coupling Fluorometry with Flow Injection Analysis (FIA) studies found that the LOD could be lowered from 1.9 to 0.1 nM and the length of analysis could be decreased from 9 to 3 min per sample (Resing & Measures, 1994; Brown & Bruland, 2008). In doing so, FIA combines the application of preconcentration, fluorometry and spectroscopy in a single manifold. However, in combining these applications the manifold has a number of complications, such as a unidirectional continuous forward flow regime, which consumes approximately 1.5 L of reagent and is significantly higher than both ICP-MS and adCSV, primarily resulting from the use of a peristaltic pump for fluid propulsion. The pulsation nature of the peristaltic pump

further causes stretching of the tubing over time, resulting in measurement drift (McKelvie, 2008). This is especially problematic during long remote maritime expeditions. As a result, such drawbacks led to the development of the second and third generation of FIA, known as Sequential Injection Analysis (SIA) (Ruzicka & Marshall, 1990) and Sequential Injection Lab-on-Valve (SI-LOV) (Ruzicka, 2000), Where both SIA and SI-LOV follow the same principle as FIA. However, instead of a continuous forward flow, SIA and SI-LOV operate using a bidirectional flow, driven by high pressure pumps, which allow for predetermined aspiration and dispensing of sample and reagent. This configuration step results in a reagent consumption of less than 75 mL per 24 hours sample run. Likewise, SI-LOV is a microminiaturization scheme of SIA, which is considerably more compact and robust in design, making it suitable to measuring trace concentrations of target analyte in mobile laboratories such as on a ship, while minimizing background interference.

Trace metal (TM) determination requires analytical instruments, which are selective and sensitive to measuring at nano-picomolar concentrations in high interfering salt matrix solutions (e.g. seawater). Instruments used for multi-element analysis are challenged by polyatomic interferences and contamination, especially for TMs, Fe and Al. These metals are commonly measured on FIA. The aim of this study was to determine the viability of a third-generation modified SI-LOV system known as a miniaturized two-line sequential injection analyser (miniSIA-2) to measure Al_d in seawater. For the instrument and method optimization, the analytical approach follows a three-step procedure, which included Batch method, Stop in Holding coil (SHC) and SHC coupled with a preconcentration step involving SPE to improve the sensitivity and selectivity of the analysis (Hatta et al., 2018). For this project, emphasis was placed on the first part of the method development scheme which involved – the batch method. This thesis presents a detailed batch method development using a miniSIA-2 to determine the Al_d from undiluted seawater, coupled with fluorometric enhancement. In the context of this research, future steps may include method optimization for real-time data analysis for remote marine expeditions, which could be further applied to understanding the seasonal biogeochemistry and distribution of Al_d in remote waters of the SO.

Table 1.1: Analytical methods for the determination of Al_d concentrations in seawater.

Method	Preconcentration/enhancement	Potential Interference	LOD	Precision	Duration	Sample location	Reference
AS							
GF AAS	Solvent extraction (8-HQ)	Spectral interference & systematic errors	0.1 nM	5% at 1 nM	±1 h (Shake)	Pacific Ocean	Orians & Bruland, (1985)
AES							
ICP-MS	SPE Nobias chelate-PA1	Oxide & polyatomic interferences	0.24 nM	<9%	SPE 2 h	North Pacific & Reference seawater	Sohrin et al.,(2008)
HR-ICP-MS	SPE Nobias chelate-PA1	Chelate formation	0.3 nM	<6%	SPE±145 min	Reference seawater & Western North Pacific	Minami et al.,(2015)
Gas chromatography							
Gas chromatography	Solvent extraction $(tfa)_3$	High Blanks & weak spectra	0.6 nM	3.8% at 18.5 nM	±1h (Shake)	Atlantic, Mediterranean & Greenland	Measures & Edmond, (1989)
Voltammetry							
adCSV	Complex ligand DASA		1 nM		10-15 min		van den Berg et al., (1986)
Fluorometry (LMG)							
Fluorometric -LMG	-	Fe^{3+} & F^-	1.9 nM	5% at 37 nM			Hydes & Liss, (1976)
Micelle enhanced fluorescence	Surfactant Triton X-100	Sample manipulation	0.4 nM -0.7 nM	3% at 10 nM or 4% at 5 nM	Max 10h	Bohai sea Yellow Sea	Howard et al., (1986); Ren et al., (2001)
FIA (Fluorescence)							
	SPE(8-HQ), Brij-35, LMG		0.15 nM	1.7% at 2.4 nM	3 min/ 9 min		Resing & Measures, (1994)
	SPE(Toyopearl), Brij-35, LMG		0.1 nM	2.5% at 5 nM	15±30 s	North Pacific	Brown & Bruland, (2008)

1.2 Motivation and approach

Recently, there has been an increased demand for compact, miniaturized instruments to be used on-board ships for TM's measurements. However, there are six parameters which define an instrument as shipboard appropriate. The instrument needs to be selective, sensitive, easy to automate, cost-effective, robust and environmentally friendly. Furthermore, the instrument needs to produce data that is accurate, precise, repeatable and reproductive to make scientific interpretations or any informed decisions for appropriate environmental action. Thus far, FIA has been the most preferred instrument for measuring the concentrations of TM's on shipboard environments. The manifold, however, has a number of drawbacks as well as little improvement in its design and efficiency over years, making it less favourable for onboard TM measurements. Rather, measurements are performed once the samples have returned to land using instruments such as ICP-MS, which require storing samples in Low Density Polyethylene (LDPE) bottles and thereby possibly increasing the chance of contamination.

To eliminate these drawbacks machine design companies have therefore gravitated towards advancing the FIA manifold by designing an instrument which is miniaturized, compact and can measure in-situ data for shipboard analysis (miniSIA-2). The miniSIA-2 can therefore measure in-situ data that can be applied to understanding short-lived phenomena such as Algae blooms, dust influx periods or contaminated metal plumes in remote and highly sensitive environments. In addition, could also be used to test data preparation, sampling strategies and apply the correct procedure (Grand et al., 2011).

As this is a new instrument, the approach would be to work systematically and adjust the method from literature to suit that of the miniSIA-2. By starting with a manual method, the first section is to optimize the instrument to measure high concentrations of Al_d in seawater, followed by applying the method to low concentration (< 10 nM). The lower concentration range is adjusted by applying the three parameters described by Gomes et al., (2019), which are excitation and emission wavelengths, fluorophore concentration and temperature. Using a gradual and systematic approach to method development can eliminate possible uncertainties when working with a fully automated miniSIA-2.

1.3 Aims and objectives

The aim of this thesis was to develop a novel approach for the automation and detection of trace Al_d in seawater by using a newly developed third generation flow analyser (miniSIA-2). Furthermore, the study aims to establish a baseline for future method development schemes to determine the concentration of Al_d and potentially other TM's in seawater at low nanomolar concentrations using the miniSIA-2.

To fulfil the research aim, the study will seek to examine the miniSIA-2 efficiency to measure the signal of Al_d with the sample preparations prepared based on Hydes & Liss, (1976) and Brown & Bruland, (2008). This will require developing and optimizing the batch method by a gradual and systematic approach to produce accurate and precise peak signals to suit the predefined setup of the miniSIA-2. This act's as a means to progress on the method to allow for full automation of the instrument. Once fully automated, the miniSIA-2 could be used on remote shipboard expeditions or even in autonomous robotic gliders to produce in-situ data with an aim to understand seasonal biogeochemical changes experienced by Al within open-ocean waters. Therefore, to achieve the research aim the objectives of this study are summarized below:

1. To prepare a well proposed methodology and instrumental procedure to establish a well-defined Al_d signal at nanomolar concentrations.
2. To study the different parameters to enhance the sensitivity of the analysis and lower the LOD.
3. To investigate the different detection limits for high concentrations and low concentrations.
4. To demonstrate that the sample preparation and design of the instrument is applicable to be automated and to be used on a shipboard environment.

1.4 Project scope and limitations

The scope of this project was to develop a method that could detect Al_d at TM concentrations on a miniSIA-2 for in situ data analysis onboard a ship. Thus reducing contamination from storing samples in LDPE bottles with polypropylene (PP) caps. Developing this method involved finding an appropriate experimental protocol and chemical procedure that would be

able to measure Al_d at low trace concentrations using the miniSIA-2. The developed method would act as a platform for future automation of the miniSIA-2, with the aim of ensuring a sufficient amount of sample analysis in the shortest possible analytical cycle time, whilst keeping reagent and waste to a minimum. Consequently, a systematic methodology was described for using the miniSIA-2, which was based on the literature provided. However, the scope of such a large project presented several limitations. Developing a method on a new instrument required a great deal of trial and error, which was a time consuming process. Furthermore, working on a new instrument required familiarizing oneself with the components, as well as developing a sample preparation tailored to the device. These constraints meant that only the first part of the method development could be accomplished using the batch method, which provides a foundation for automating both the experimental protocols of the SHC and the SHC with SPE in the future. A fully automated and compact manifold scheme would further reduce lab space, whilst limiting spills from vibrations experienced by the ship out at sea.

1.5 Thesis Outline

There are five chapters in this project: Introduction, Literature review, Methodology, Results and Discussion, and Conclusion. The Introduction (Chapter 1) provides a general overview of the research undertaken for the thesis which is followed by the motivation and approach, aims and objectives, the project scope and limitations. The literature review (Chapter 2) covers the general background of the speciation, solubility and distribution of Al_d in seawater, in particular focusing on the hydrolysis of Al in different pH environments and how this affects Al solubility and distribution in oceanic basins. This is followed by the challenges of possible contamination risks associated with poor sample handling and the potential risks of contamination when storing samples in LDPE plastic containers. Following the sampling section, the preconcentration section describes the three types of chelating resins that can be used to preconcentrate Al from seawater, along with the corresponding matrix removal procedures (Solvent extraction or SPE). Thereafter, a brief description is given of alternative detection methods and their corresponding preconcentration procedure and drawbacks for measuring Al_d in seawater. These include Atomic absorption spectrometry (AAS), (ICP-MS & HR-ICP-MS), Voltammetry, and Fluorometry. The descriptions of the three generations of FIA with emphasis on their advancement in manifold components and experimental protocols over the years to detect low trace concentrations, as well as their relevance to this project is covered. The

Methodology (Chapter 3) describes three distinct assay protocols, each with their own parameters, which require optimization before being able to fully automate the method on the miniSIA-2. A brief description of the sampling method employed, the reagents prepared and used, and the calibration standards applied is presented. Finally, the miniSIA-2 hardware and software are described along with a step-by-step method preparation procedure, applied to the miniSIA-2. The Results and Discussion (Chapter 4) describes and discusses the development of the analytical protocol using a systematic approach, by first establishing a signal under the proposed conditions for high concentrations (800 – 100 nM), followed by adjusting parameters further used for the lower concentration range (< 10 nM) to establish a suitable protocol sequence for the lower concentrations and achieve the lowest detection limit. The Conclusion (Chapter 5) gives the concluding findings of the thesis, followed by the future recommendations.

Chapter 2 Literature review

2.1 Speciation and Distribution

Quantification techniques depend on the speciation of Al (Tria et al., 2007). Al^{3+} cation is a hard lewis acid (small, compact and reduced polarisation) or within geochemical terms referred to as a lithophile element which are elements typically found as silicates (aluminosilicates). Hard acids react preferentially with hard bases (H_2O, OH^-, O^{2-}, F^-) (Smith & Nordberg, 2015). Within the solution, regardless of the anion present, Al^{3+} cations are solvated by six water molecules (Fratiello et al., 1968), giving mononuclear $[Al(H_2O)_6]^{3+}$ an octahedral configuration (Figure 2.1).

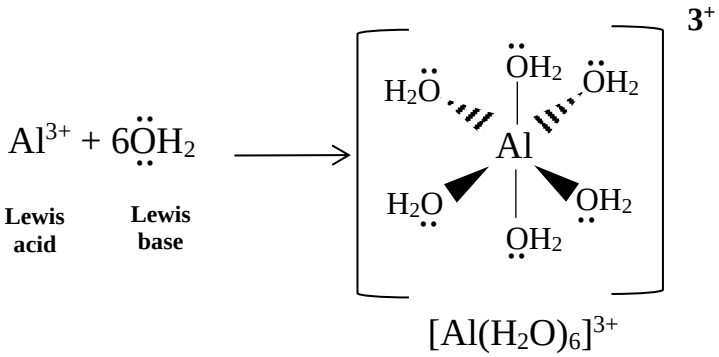

Figure 2.1: Solvated Al^{3+} within an aqueous solution.

Al speciation is predominantly pH dependent (Figure 2.2). However, factors such as the concentration of Al, availability of inorganic and organic ligands and temperature of the aqueous solution play a role in the speciation (Scancar & Milacic, 2006). In essence, how these ions participate in dynamic equilibrium, which is how the interaction of one species, affects the rearrangement of another (Pyrzynska, 2000). The Al^{3+} species are labile (Pyrzynska, 2000) within biological functional waters and it's assumed that Al^{3+} hydrolytic tendency is preferably towards Al-ligand-hydroxide complexes in alkaline conditions (Wesley et al., 1996), giving rise to monomeric $[Al(OH)_2]^+$, $Al(OH)_3$, $[Al(OH)_4]^-$ species. Under normal conditions, Al is insoluble, however, under either acidic (< 6) or alkaline conditions (> 6), solubility increases. Within aqueous solutions, preferably within an acidic solution of a pH < 3, the dominant species of Al is the prevalent mononuclear $[Al(H_2O)_6]^{3+}$ simply expressed as Al^{3+}. Mononuclear $[Al(H_2O)_6]^{3+}$ hydrolyses to $[Al(H_2O)_5OH]^{2+}$, expressed as $[Al(OH)]^{2+}$ and hydrolysis of $[Al(OH)]^{2+}$, yields $[Al(H_2O)_4(OH)_2]^+$, abbreviated as $[Al(OH)_2]^{+,}$ all within a

slightly less acidic solution of a pH 4-5 **(**Scancar & Milacic, 2006). These three species of Al (Al^{3+}, $[Al(OH)]^{2+}$ and $[Al(OH)_2]^{+}$) also referred to as "free Al" are detrimental towards the environment and are toxic to living organisms (Gensemer & Playle, 1999; Ma, 2000; Hoekenga et al., 2003). Within neutral solutions, pH 6.2 -7, the dominant species is amorphous $Al(OH)_3$, of which aluminate anion $[Al(OH)_4]^-$ is the existing species at pH ≥ 8 (Wesley et al., 1996; Scancar & Milacic, 2006).

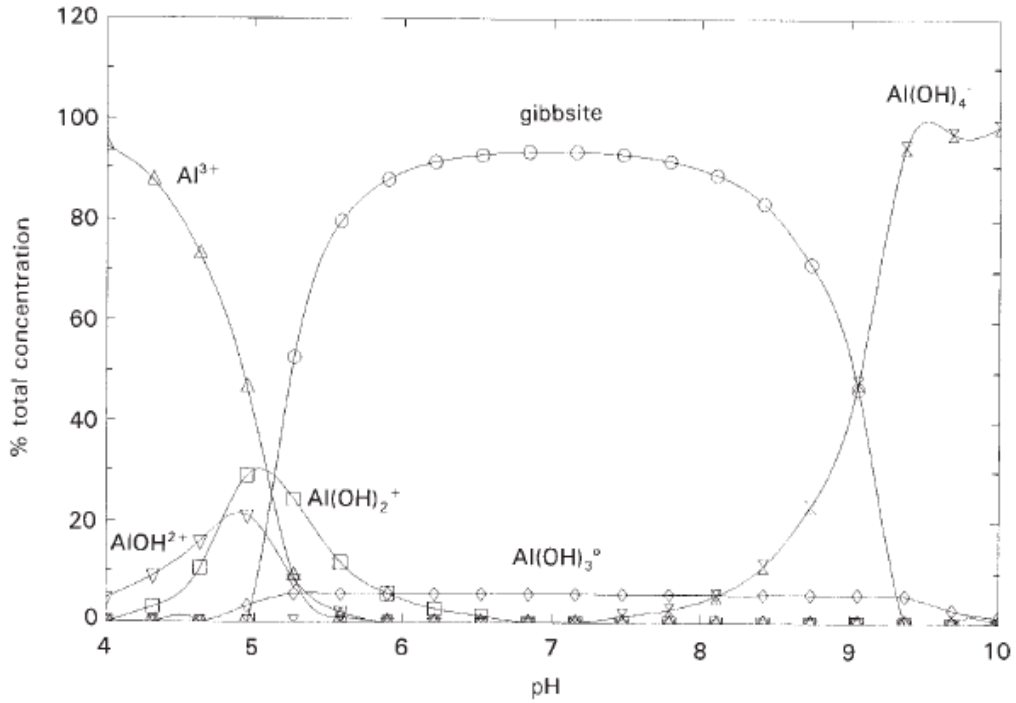

Figure 2.2: Al's speciation as a function of solution pH (Gensemer & Playle, 1999).

2.1.1 Al solubility in seawater

Al has a low solubility in oxygenated seawater (Orians & Bruland, 1985), however, increased acidic precipitation due to industrialized emissions, can influence the solubility of Al in seawater. The current pH of seawater is 8.08 to 8.33 for waters of t = 25ºC, P = 1.0 atm, fCO_2 = 3.33E-4 atm and salinity (S_A) = 35.17 g/kg (Marion et al., 2011). Figure 2.2 indicates that the two major hydrolysis species of Al in seawater are $Al(OH)_3$ (Equation 3) and $[Al(OH)_4]^-$ (Equation 4) (Orians & Bruland, 1985, 1986).

Equation 1	$[Al(H_2O)_6]^{3+}+H_2O \rightleftharpoons [Al(H_2O)_5OH]^{2+}+H^+$	pH 4-5
Equation 2	$[Al(H_2O)_5OH]^{2+}+H_2O \rightleftharpoons [Al(H_2O)_4(OH)_2]^{+}+H^+$	pH 4-5
Equation 3	$[Al(H_2O)_4(OH)_2]^{+}+H_2O \rightleftharpoons [Al(H_2O)_3(OH)_3]+H^+$	pH 6.2-7
Equation 4	$[Al(H_2O)_3(OH)_3]+H_2O \rightleftharpoons [Al(OH)_4]^-+H^+$	pH ≥8

2.1.2 Al distribution across Oceanic basins

Multi-biochemical processes affect the distribution of Al_d in oceanic basins. The concentration of Al_d increases from the sources such as Aeolian dust (Menzel Barraqueta et al., 2019), hydrothermal vents (Resing et al., 2015), ice melts (Giesbrecht et al., 2013) and continental shelves (Menzel Barraqueta et al., 2019), with Aeolian dust contributing to majority of Al_d introduced into the surface waters of the oceans (Tria et al., 2007). A characterising feature of Al is the relatively short residence time (2-6yr) in surface waters (Orians & Bruland, 1985; Kamer et al., 2004). The short residence time of Al_d in seawater is due to the particle-reactive nature of Al_d in seawater. Figure 2.3, illustrates typical distribution configurations of Al_d in seawater. Majority of the oceanic basins (Indian, Pacific and SO) show a scavenged type distribution (2), with a high surface concentration, mid-depth minimum and an increased concentration at the base of the water column (Bruland & Lohan, 2003). However, oceanic basins of the Mediterranean Sea, North Atlantic and the Arctic Ocean have vertical profiles which resemble that of a nutrient-type distribution (1) (low surface concentrations and increases with depth) and show a partial correlation with Si. Despite the correlation observed, Al plays little role in active biological uptake and instead the result is either preferential scavenging or Al replacing the Si in biogenic silica.

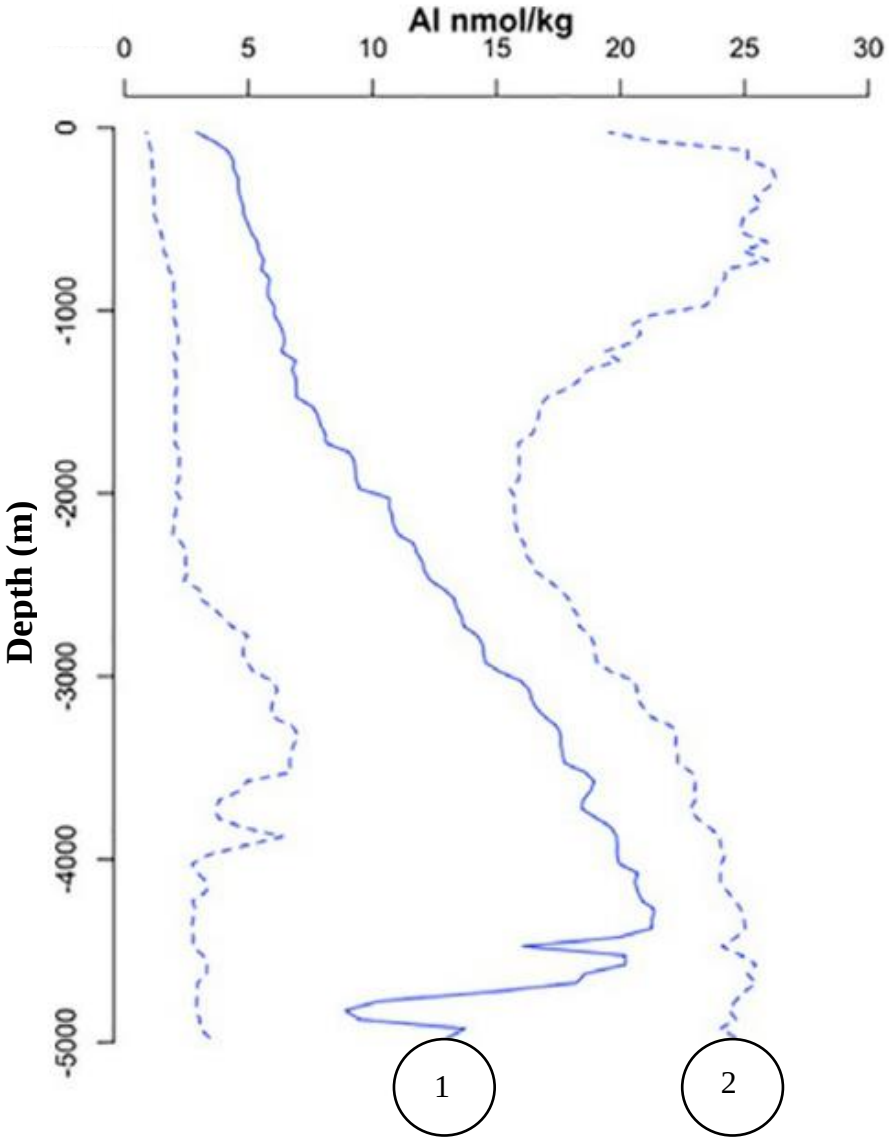

Figure 2.3: The distribution of Al_d in seawater: 1) nutrient-type distribution and 2) a scavenged-type distribution (Tagliabue, 2019).

2.2 Sampling

2.2.1 Contamination risks

The sampling and analytical methods must eliminate the risk of contamination in order to ensure precise and accurate measurements, which represent the actual concentration, activity and chemical speciation of Al (Cutter et al., 2017). Sampling and analysing Al_d within oceanic seawater comes as a challenge. Al_d exist in nM concentrations in seawater and is ubiquitous in the atmosphere, manufactured sampling material, research vessel and produced by human activity (Tria et al., 2007). Improvements in sampling handling procedures which limit cross contamination, can further lower the LOD of the desired analytical method. Cross contamination can be eliminated if sampling material is made of either LDPE, High Density Polyethylene (HDPE) or Perfluoro Alkoxy (PFA) fluorocarbon polymers (Tria et al., 2007; Cutter et al., 2017). However, for dissolved Trace metals (TM_d) it is recommended to sample with thoroughly acid cleaned LDPE and HDPE bottles, of which Al and Titanium must be sampled in bottles and caps made entirely of LDPE (Cutter et al., 2017).

2.2.2 Sample storage

Brown & Bruland, (2008), recognised Al contamination when they stored acidified seawater samples in either HDPE or PFA bottles, which they believed is linked to manufacturing procedures involving an Al co-catalyst during the manufacturing of the polyolefin. They concluded that LDPE sample bottles were best suited for long-term storage of seawater at pH 1.7-1.8. Precautions taken with the type of cap, as some distributors supply LDPE bottles with PP caps, which contribute to a significant amount of Al contamination. To limit cross contamination, it is essential to store samples upright during transportation and in a dark and cool place prior to analysis in a class 100 lab or laminar bench, to limit air borne Al from getting introduced into the samples.

2.3 Preconcentration

The high salt matrix associated with the low Al_d concentrations in seawater results in a considerable amount of interferences when analysing with a variety of instruments. Therefore, isolating the desired analyte and enhancing the signal, increases the instrumental precision and subsequently improves the LOD.

2.3.1 Chelating resins

Preconcentration is a prerequisite for measuring trace Al_d in seawater by majority of analytical instruments. The low concentrations of Al_d and the contrasting salt matrix in open ocean samples compromise instrumental detection limits. Primarily due to matrix interferences and Al concentrations below detection limit. Therefore, by implementing a preconcentration step can the Al concentration be enriched and the matrix interference either minimized or suppressed. The preconcentration step is carried out by applying a chelating resin which has a high affinity for the Al metal, while allowing the matrix to pass through. Three chelating resins have been used for on-line preconcentration of Al (Figure 2.4).

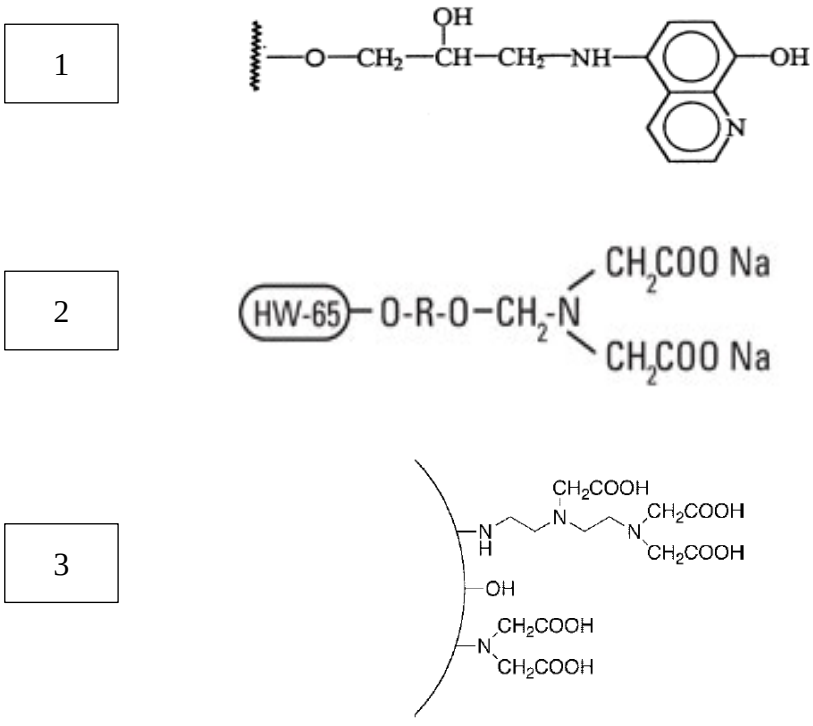

Figure 2.4: The three chelating resins used for Al. Chelating resin 1) is 8-HQ immobilized onto a vinyl polymer gel (Dierssen et al., 2001) with 2) the Toyopearl AF Chelate 650M and 3) is Nobias Chelate-PA1 (Wang et al., 2014).

Chelating resin, 8-Quinolinol (8-HQ) is an oxine (1), is more selective and efficient in separating transition metals then chelating resins carrying a 2,2'-Iminodiacetic acid (IDA) functional groups (Sohrin & Bruland, 2011). However, lacks in commercial availability and requires covalent immobilization onto a stable, hydrophilic, organic resin beads, which can be difficult to replicate and time-consuming (< 7 Hours) (Landing et al., 1986; Dierssen, Balzer & Landing, 2001).

Toyopearl AF Chelate 650M (2) is a commercially available, polymetric non-swelling chelating resins, with a spacer arm of IDA functional groups (Sohrin & Bruland, 2011), with a microporous methacrylate backbone. The lack of selectivity, due to the weak functional group, can make this resin more prone to retention by Ca^{2+} and Mg^{2+}, instead Al^{3+} (Camel, 2003). However, the main choice for FIA detection is that this produces a 100% Al retention, with the use of a CH_3COONH_4 column conditioning buffer and a weak hydrochloric acid eluent (Table 2.1) (Brown & Bruland, 2008).

Nobias Chelate-PA1 has dual functionality, as it has an 2,2',2",2"'-(1,2-Ethanediyldinitrilo)tetraacetic acid (EDTA) and IDA functional group. Nobias Chelate-PA1 been applied to the preconcentration scheme of analysing Al_d by HR-ICP-MS and ICP-MS, producing an Al% retention of 101-104%, with a HAcO-NH_4AcO column conditioning buffer and a nitric acid eluent (Table 2.1) (Sohrin et al., 2008; Minami et al., 2015).

Table 2.1, gives a brief summary illustrating the preconcentration conditions of each chelating resin, with its corresponding Al% retention and the instrument used for detection.

2.3.2 Solvent extraction

Liquid-Liquid solvent extraction (LLE) is the partitioning of two immiscible solvents, generally water (polar) and an organic solvent (nonpolar), for the extraction of a desirable substance/metal from an analyte (Harris, 2006; Houck & Siegel, 2015). Figure 2.5, shows the extraction of Al from seawater by LLE. Extracting Al from seawater, requires adding a suitable chelating ligand to the seawater in a separatory funnel (Orians & Bruland, 1985; Measures & Edmond, 1989). As previously mentioned, the speciation of Al is dependent on the solution's pH (Scancar & Milacic, 2006). With the optimal chelate complexation forming when the metal exhibit's a neutral net charge ($Al(H_2O)_3(OH)_3^0$) (Sohrin & Bruland, 2011). Amorphous Al is

the dominant species at a pH of 6.2 -7 (Scancar & Milacic, 2006), therefore buffering the solution to that exact pH range is critical for achieving precise and accurate concentrations and ensuring complex formation. Once the Al complexes to the chelating ligand, a small portion of organic solvent is added (Orians & Bruland, 1985). The Al-chelate is insoluble in seawater (polar) and soluble in the organic solvent (nonpolar) (Houck & Siegel, 2015). Therefore, is able to separate from the aqueous phase to the organic phase. LLE chelating ligands for the preconcentration of trace Al has been 8-HQ (Orians & Bruland, 1985; Alonso et al., 2001) and 1,1,1-trifluoro-2-4-pentanedione (Measures & Edmond, 1989), coupled to a variety of detection methods (AAS, FIA and gas chromatography). Although, Measures & Edmond (1989), excluded the step of evaporation of the organic phase, proposed by Orains and Bruland (1986), they still achieved a low LOD. In addition, Orains and Bruland (1986), numerously evaporated the organic phase to residual and dissolved this with strong to dilute acid before analysing for Al_d by Graphite Tube Furnace Atomic Absorption Spectrometry (GF AAS). Over the decades, popularity declined, primarily due to hazardous nature of chloroform and the labour-intensive separation procedures (Sohrin & Bruland, 2011). Likewise, Al is prone to cross contamination and the large amount of reagent consumption is not economical.

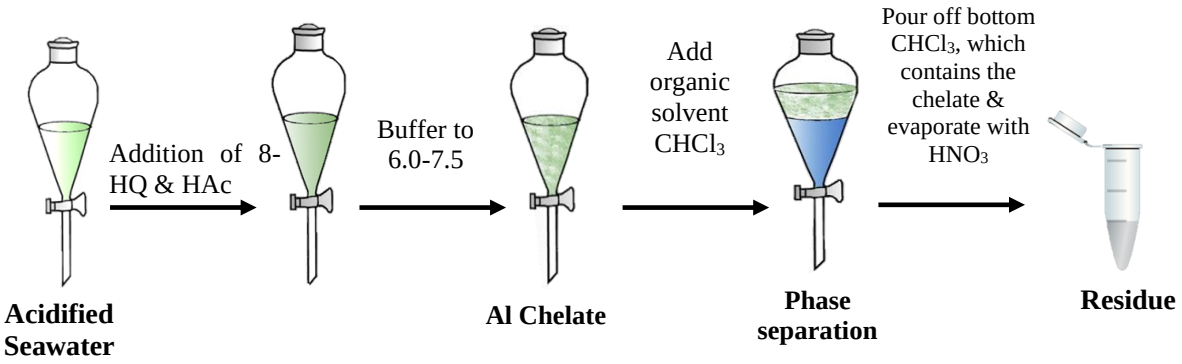

Figure 2.5: LLE for Al using an 8-HQ chelating resin. Showing a step-by-step procedure of extracting the Al chelate complex from acidified seawater using the separatory funnel technique. Theory by Orians & Bruland (1985); Measures & Edmond (1989).

2.3.3 Solid-phase extraction (SPE)

A simplified, environmentally friendly alternative to LLE is SPE, which is driven by sorbent phase adsorption, instead of liquid partitioning (Houck & Siegel, 2015). Within ultra-trace metal determination, SPE is either carried out by batch or mini column manifold (Wells & Bruland, 1998). The column manifold is more favourable and presently the most sought after for preconcentrating trace Al in seawater. The advantage is the set-up, which consists of a mini column, packed with a suitable solid adsorbing chelating resin, held together by porous polyethylene frits, forming part of a closed manifold (Figure 2.6) (Grand et al., 2016). The polyethylene frits are comprised of fine pores, which can compensate for a high backpressure, due to the contrasting pore size of the chelating resin, if the flow is not monitored (Horstkotte et al., 2016).

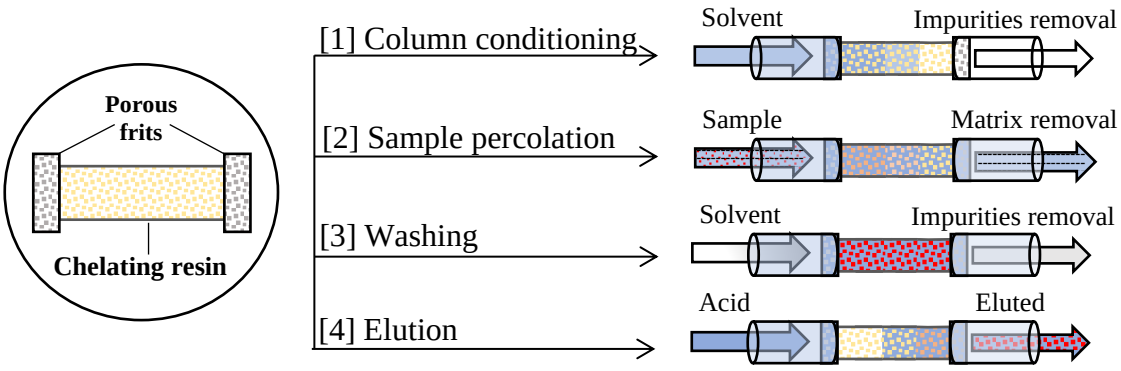

Figure 2.6: Column manifold and the four successive steps for SPE, theory by Camel, (2003).

SPE is associated with four successive steps for achieving selective, chromatographic, quantitate and efficient retention of the analyte to the sorbent (Figure 2.6). In essence, choosing the appropriate solid sorbent (8-HQ, IDA or EDTA) for retaining the desired metal is crucial for selective retention of the desired analyte and detection analysis. Prior to sample loading, the column needs to be conditioned with a solvent (1), to ensure solvation of resins functional groups, removal of impurities and air and saturate the sorbent to the optimal pH. Optimization of the sorbent pH stabilizes the chelation of the metal complexes formed with the resin. Therefore, the column conditioning solvent should be of similar nature to that of the sample (Camel, 2003). Column conditioning generally requires additional steps prior to sample loading, initiating with acid elution, followed by a wash step (deionised water and air) and then a buffer solvent of an optimal pH as sample (Sohrin et al., 2008; Minami et al., 2015). Table

2.1, illustrates the increased Al retention percentage of 97.5% to 100%, by simply incorporating a column conditioning step, prior to sample percolation. This ensures that binding sites are deprotonated to effectively allow for Al retention (Brown & Bruland, 2008).

Sample percolation (2) requires a predetermined filtered volume of seawater, at a specific pH, flowing at an optimized flow rate (Camel, 2003). The sample flows through the chelating column, the analyte adheres to the high affinity binding sites, thus forming a chelate on the surface of the resin (Sohrin & Bruland, 2011; Houck & Siegel, 2015). While the matrix passes through to waste. The flow rate should be kept slow, which reduces back pressure, while effectively retaining the analyte, however, fast enough to avoid chelation of undesired metals, such as alkaline and alkaline earth metals (Camel, 2003).

Chelating trace Al functions on the principle of Lewis acid-base interactions. The trace Al is the Lewis acid, of which the chelating resin functional groups (O-, N-) act as the Lewis base, thus forming weak outer sphere complexes with the O and N (Camel, 2003). Low pH solutions protonate the atoms, which limits adsorption. Therefore, solutions of higher pH, deprotonate the functional groups for achieving effective complex formation and sorption possible. However, if the solution becomes too basic, the solution can lead to complex formation and precipitation of metals, which can lead to decrease in sorption effectivity. Therefore, an optimal Al recovery % is achieved at a sample pH of 5.5-6.0 for Toyopearl and Nobias-chelate (Table 2.1) (Brown & Bruland, 2008; Minami et al., 2015).

Sample loading to the column is generally accompanied by a wash step (3) (Minami et al., 2015; Grand et al., 2016), which washes away inferencing metals or remaining matrix. The wash solvent could be a buffer solvent, followed by air (Minami et al., 2015) or simply deionised water (Grand et al., 2016). The column capacity of ±80µM allows for segregated sample loading, to ensure adequate analyte retention. Elution (4) with a compatible acid for a distinctive chelating resin, ensures efficient recovery of the analyte from the column (Brown & Bruland, 2008). The lower the acid concentration, the lower the instrumental blanks, which can cause TMs to be left behind during elution. If the acid solution is too strong, it could damage or extract the coated sorbent of the chelating resin.

Table 2.1: 1) 8-HQ (Resing & Measures, 1994), 2) Toyopearl AF Chelate 650M (Brown & Bruland, 2008), 3) Nobias chelate-PA1 (Sohrin et al., 2008) & 4) Nobias chelate-PA1 (Minami et al., 2015) for Al_d in seawater.

Solid sorbent	**Conditioning solvent**		**Sample percolation**			**Elution acid**		**Al %**	**Detection**	**Reference**
Resin	M	pH	ml	ml/min	pH	M	ml/ min		Manifold	
8-HQ	-	-	126	2.5	5.5	0.05 M HCl	0.60	97.5	FIA	1
Toyopearl	0.1M CH_3COONH_4	5.5	±10	2.5	5.75	0.1 M HCl	0.60	100	FIA	2
Nobias Chelate	0.05 M HAcO-NH_4AcO	6.0	120	3.0	6.0	1M HNO_3	1.0	101-104	HR&ICP-MS	3&4

2.4 Detection methods

Described below are alternative detection methods used for measuring Al_d in seawater, which include AAS, ICP-MS & HR-ICP-MS, Voltammetry, Fluorometry and FlA. However, many of these detection methods are considered outdated as the analysis for Al_d has mostly been performed using fluorometry and FIA.

2.4.1 Atomic absorption spectrometry (AAS)

AAS is an inexpensive and element specific detection method used to measure a wide variety of TM's (Michalke & Nischwitz, 2013). AAS functions on the basis of changing the state of a liquid sample to that of gas, through applying heat to a cell (atomizer). When light is emitted through these "nonionized gas clouds", will the gas absorb electromagnetic radiation at a specific wavelength, in exchange, producing a measurable absorption signal, which is proportional to the concentration of the absorb atoms (Sperling, 2006; Fernández et al., 2018).

Therefore this type of analytical technique depends entirely on the type of atomizer used. With Flame Atomic Absorption Spectrometry (F AAS) and Electrothermal Atomic Absorption Spectrometry (ET AAS), e.g GF AAS, being the most popular for TM determination. However, with regards to measuring Al_d in seawater, F AAS lacks in sensitivity and further encounters interference, primarily due to ionization of refractory oxides when analysing for Al, as a hotter flame is required to break the oxygen bond (Sperling, 2006).

In essence, GF AAS is more applicable for measuring Al_d in seawater (Orians & Bruland, 1985; Salomon et al., 2000), as these have an increased sensitivity and require small sample volumes of 1µl (Harris, 2006). Concentrations of Al_d were determined in seawater of the Pacific, and achieved LOD of 0.1 nM and a precision of 5% at 1 nM (Orians & Bruland, 1985). However, GF AAS, are prone to non-atomic absorption (sodium chloride and phosphates), which interfere with the analyte wavelength (Smith & Nordberg, 2015). Therefore a labour extensive preconcentration by solvent extraction using 8-HQ, at a pH of 6.0-7.5 is required (Orians & Bruland, 1985). The solvent extraction step requires matrix separation/preconcentration extraction with nitric acid digestion for GF AAS, which is dangerous when implementing GF AAS on an shipboard environment. Therefore not appropriate for shipboard environment (de Jong, 2000).

2.4.2 Inductively coupled plasma mass spectrometry (ICP-MS) & High resolution Inductively coupled plasma mass spectrometry (HR-ICP-MS)

In terms of the current analytical techniques available, ICP-MS is the most favoured method for detecting TM's in seawater. This is primarily due to ICP-MS's ability to allow multiple and simultaneous TM detections of Al, Mn, Fe, Co, Ni, Cu, Zn and Cd at high precision and low detection limits (Sohrin et al., 2008; Sohrin & Bruland, 2011; Minami et al., 2015). Directly measuring TM's in seawater by ICP-MS is, however, exceptionally difficult primarily due to the high salt matrix and the low concentrations of the target metals. In order to achieve these low detection limits, ICP-MS relies on an offline preconcentration step which poses a significant risk of cross-contamination, in addition to being time consuming. The most commonly used preconcentration method used to measure Al_d is by SPE with a Nobias Chelate-PA1 chelating resin column (Sohrin et al., 2008; Minami et al., 2015). The result is a Al recovery of 101-104% (Table 2.1) with a low detection limit of 0.24 nM for Al_d (Sohrin et al., 2008; Sohrin & Bruland, 2011; Minami et al., 2015).

Even though measuring Al_d by using both ICP-MS and HR-ICP-MS is possible, Sohrin et al., (2008) and Minami et al., (2015) highlighted the high susceptibility of cross contamination for metals Al and Fe seen by the high procedural blanks. This is believed to be due to a consequence of either contamination or airborne particles introduced into the sample. However, with both experiments following clean procedures: deionised water, ultra clean purity reagents, thoroughly cleaned LDPE bottles and analysed either within a class 1000 clean room or class 100 laminar flow bench. Further disadvantages of measuring Al_d by ICP-MS is the complex sample pre-treatment, resource demanding nature and requirement of a large space and skilled personal to operate, therefore not suitable for in situ deployment (Grand et al., 2019).

2.4.3 Voltammetry

2.4.3.1 Adsorptive Cathodic Stripping Voltammetry (adCSV)

AdCSV with a hanging mercury drop electrode is a single element electrochemical instrument (Grand et al., 2019). Measuring Al in seawater by adCSV requires a preconcentration step that involves Al to complex with 1,2-Dihydroxyanthraquinone-3-sulfonic acid (DASA), followed by polarographic determination. A detection limit of 1 nM Al in a seawater matrix has been achieved (van den Berg et al., 1986). The adsorption step is sensitive to the adsorption potential of the metal and the high negative potential of Al (-175V) can make analysis difficult without preconcentration. Further difficulties are caused by sodium (Na), Potassium (K) and Barium (Ba) which are ions present in the seawater matrix and exhibit similar adsorption potentials to Al. (Tria et al., 2007). The adCSV manifold is compact and portable, however, is less favourable due to the need for a stable mercury drop, where mercury is hazardous and dangerous for application on ship-board environments (Grand et al., 2019).

2.4.4 Fluorometry

2.4.4.1 Lumogallion (LMG)

Fluorometry is a highly sensitive and selective technique, which involves reacting a non-fluorescent analyte of interest with a fluorescent reagent. These than react to produce a fluorescing complex which emits a fluoresce that is entirely unique to that metal. A favourable fluorescent reagent used for the determination of Al in seawater is LMG (Tria et al., 2007). LMG (4-chloro-6-[(2,4-dihydroxyphenyl) azo]-1-hydroxybenzene-2-sulfonic acid) is a tetradentate ligand, that complexes with soluble Al^{3+}, forming a fluorescent Al-LMG chelate complex (Al-LMG) (Nishikawa et al., 1967 & 1968; Wu et al., 1995) at a stoichiometric ratio of 1:1 (Ren et al., 2001) (Figure 2.7).

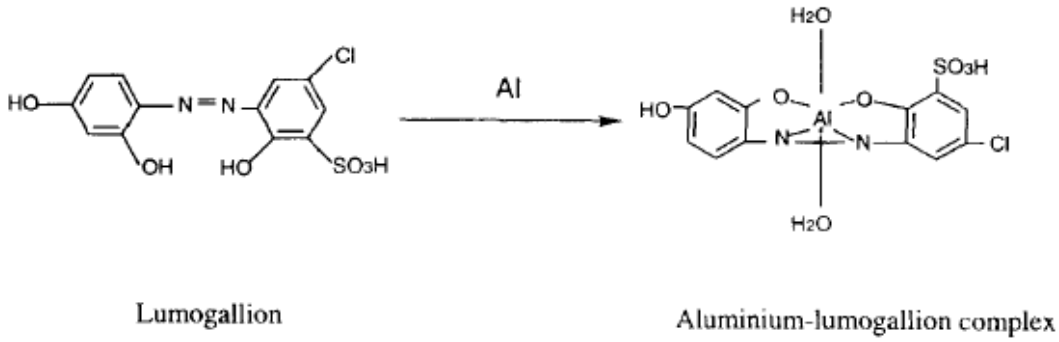

Figure 2.7: Synthesis of Al-LMG chelate complex (Wu et al., 1995).

The excitation wavelength (λ_{ex}) of the fluorescent Al-LMG chelate complex is at 500 nm and it emits a reddish/yellow fluorescence at a emission wavelength (λ_{em}) of 590 nm (Zhou, 1995; Mendecki et al., 2020). Elements of iron (Fe^{3+}) and fluoride (F^-), interfere with the fluorescence of the Al-LMG complex. The interference of F^- in seawater is more pronounced than that of Fe^{3+} primarily due to the availability of F^- in seawater and the tendency of Al to form series of compounds with F^-, which limits the accessibility of Al to form the Al-LMG chelate complex. Adding Be^{2+} reduces F^- in solution by forming stable complexes. Fluorescence is a short-lived phenomenon, with a glow time of 10^{-9} to 10^{-7} and immediately stops once the light source is eliminated (Singh, 2016), with the Al-LMG chelate complex only being stable for 10 hours (Ren et al., 2001).

Several methods have been reported for enhancing the selectivity and sensitivity of the fluorimetric Al-LMG chelate complex which involves the addition of a non-ionic surfactant (Howard et al., 1986; Resing & Measures, 1994; Ren et al., 2001; Brown & Bruland, 2008). The addition of the surfactant creates a Micellar with the chelate complex, e.g Al-LMG-Triton X-100 ternary complex (Howard et al.,1986). A Micellar system can protect the fluorescence from experiencing quenching, enhances the fluorescent intensity and further minimizes ionic interferences (Abdeldaim & Mansour, 2018).

2.4.5 The three generations of Flow injection Analysis

There are three generations of flow injection techniques for sample manipulation. The first generation is known as a Flow injection Analysis (FIA) which implements a unidirectional (forward) and laminar flow regime. The second generation, an alternative to FIA, implements a bidirectional and turbulent flow regime and is known as Sequential Injection Analysis (SIA).

The third generation is a modified version of SIA, which runs on the same flow regime, however, at a miniaturized scale and is known as Sequential Injection Lab-on-Valve (SI-LOV). The SI-LOV further advanced to a micro-Sequential Injection Lab-on-Valve system (μSI-LOV) to reduce reagent consumption and waste (Table 2.2).

Table 2.2: The differences between the three generation of flow injection instruments.

Generation	Injection analysis	Flow	Flow profile	Mixing	Re	Cycle length min/sample	Reagent consumption in 24Hr
First	FIA	Unidirectional	FIA gram	Confluence point	Laminar	15±30 s	>1.5 l
Second	SIA	Bidirectional	Gaussian peak	Zone penetration	Not laminar	1	<75ml
Third	SI-LOV	Bidirectional	Gaussian peak	Zone penetration	Not laminar	13	<75ml

2.4.5.1 Flow injection Analysis (FIA)

FIA was first described by Ruzicka and Hansen in 1975, as a new concept of a continuous forward flow analyser, an advancement from the monotonous batch analysis. This analytical technique involves the injection of a known volume of sample into a continuously, unidirectional flowing carrier stream of reagent. The sample merges into a reagent stream, causing a reaction, while simultaneously flowing downstream towards a detector (Ruzicka & Hansen, 1975). In 1994, Resing and Measures, incorporated the fluorometric LMG (Hydes & Liss, 1976), micellar-enhanced fluorescence (Howard et al., 1986) and the solvent extraction (8-HQ) (Orians & Bruland, 1985) methods for the determination of Al by an automated FIA scheme. The method allowed for a detection limit of 0.15 nM, with a precision of 1.7% at 2.4 nM and sample analysis within a 3 min duration. This method was later modified by Brown & Bruland (2008), which involved three major changes; (1) 8-HQ was replaced with commercially available Toyopearl AF-Chelate 650M resin, (2) introduced a column conditioning step, (3) adjusted the pH of the 2M ammonium acetate buffer from 6.0±0.1 to 9.0±0.1. These modifications improved the method for determining Al_d to a detection limit of 0.1 nM with a precision of 2.5% at 5 nM. Today, FIA combines preconcentration, matrix extraction, fluorescence, surfactant enhancement and spectrophotometry for the detection of individual TMs (Al, Fe, Cu, Co, Mn, Zn) (Brown & Bruland, 2008; Grand et al., 2019). The modern FIA system incorporates a low-cost design, robust (shock and vibration), shipboard (portable) and easily operative manifold (Tria et al., 2007).

The manifold for Al-FIA shown in Figure 2.8 can be subdivided into six sections (1) Propulsion, (2) Injection, (3) Mixing /Separation, (4) Reaction, (5) Detection and (6) Data analysis (McKelvie, 2008). Fluid propulsion requires a peristaltic pump (8-channel) (Resing & Measures, 1994; de Jong et al., 2000; Brown & Bruland, 2008), which transports carrier and reagent solution at a flow rate of 0.2 – 4 mL/min (McKelvie, 2008) through chemically inert narrow bore tubing. The injection system consists of two rotary valves, each with a six-port configuration. These valves are known as Valco 6 Port valves (Brown & Bruland, 2008) and are positioned on an electrical actuator (Aldstadt et al., 2006). The two valve configurations, allows Valve 1 and Valve 2 to interchange, depending on the predetermined analyte/reagent injected. The Mixing/Separation components are two mixing coils (< 4 m) and one reaction coil (8 m). The Teflon mixing and reaction coils are "French knitted" (Brown & Bruland, 2008). This configuration increases radial mixing and limits dispersion, which is experienced with coiled tubular reactors. Turbulent mixing is encouraged for flow techniques to efficiently transform the species into a detectable species. The reaction components include a dry bath incubator heating block and a Toyopearl AF-chelate 650M preconcentration resin column. The 8 m reaction coil lies within the 50ºC dry bath incubator. For the measurement of Al, the detector (Hitachi F-1050 fluorescence spectrophotometer with xenon light supply) is used at set λ_{ex} = 489 nm and λ_{em} = 559 nm wavelengths (Brown & Bruland, 2008).

Due to the laminar flow of FIA, the Al-LMG chelate complex does not undergo complete complexation. As a result, FIA is considered an incomplete reaction, which refers to the Al-LMG chelate complex not having reached equilibrium before being detected. Achieving analytical precision is therefore based on the repeatability (Harris, 2006). Injecting a sample into a reagent stream, causes dilution and dispersion (Zagatto & Worsfold, 2005). Dispersion dilutes the product zone on the sides and concentrates the product in the centre stream (Kradtap Hardwell, 2012) because the flow within the centre of the tube runs twice as fast compared to the sides of the tubing. The flow characteristics thus result in the detector first detecting low concentrations followed by detection of the concentrated product zone and then again low concentrations. This gives rise to a peak signal known as FIA gram (Figure 2.9). The FIA gram (peak height or peak area) is used to precisely relate the signal to the quantity of analyte (Kradtap Hardwell, 2012).

FIA has a number of drawbacks, which compromise the efficiency of measuring TM's. In essence, running at a constant flow rate requires continuous consumption of reagents and generation of waste (Ruzicka, 2016). The consumption of reagents per 24 hour duration, consuming approximately 1.5 L, can be costly, as the LMG solution is expensive. Overuse of this manifold during long remote expeditions can also result in pulsation of tubing (McKelvie, 2008), which can cause variation in flow rate and furthermore increase drift and uncertainty of measurements.

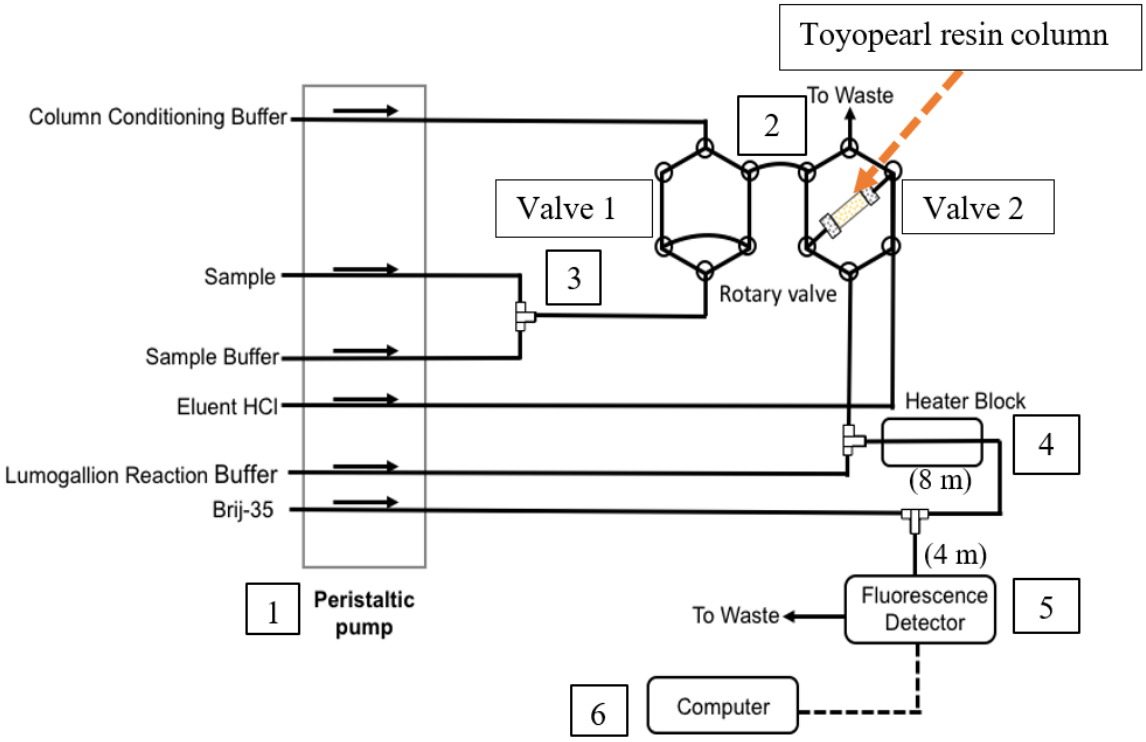

Figure 2.8: The Al-FIA setup of Brown & Bruland, (2008), indicating the six sections of the manifold design, 1- The peristaltic pump for propulsion, 2- injection of sample using electrical actuator, 3- reaction/separation driven by reaction coils, 4- reaction by a heater block, 5- detection and 6- computer for data analysis.

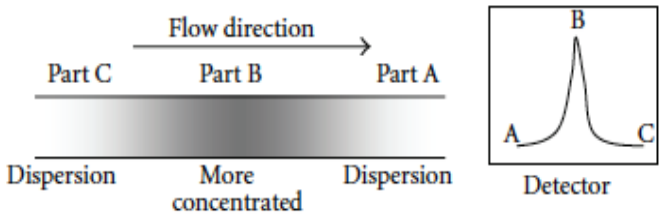

Figure 2.9: Diagram showing the product and dilution zones of a FIA gram. Detection zones for samples are indicated by A (low concentration) – B (concentrated product zone) -C (low concentration) (Kradtap Hartwell, 2012).

2.4.5.2 Sequential Injection Analysis (SIA)

In order to eliminate the impact of measurement drift associated with the peristaltic pumps, the modifications to the manifold design led to the second generation of flow injection analysers, known as SIA (Ruzicka & Marshall, 1990). The basic principles for analysis are similar to that of FIA, however, instead of a peristaltic pump a syringe pump is utilized to achieve a consistent flow rate. Figure 2.10 represents the basic configuration of a single channel SIA manifold. In the modified system, the injection valve is substituted by a multiposition valve which comprises of six ports where each port is connected to different sample streams/reagents or components. The valve enables automated sequential aspiration and dispensation of precisely measured aliquots of sample and reagent into a Holding coil (HC) (Aldstadt et al., 2006). As a result, a partial reaction occurs in the HC until the flow in the manifold gets reversed, resulting in a complete reaction by propelling the analyte to the reaction coil and finally to the detector. This type of manifold improved the scheme design by incorporating the detector in the manifold itself (Grand et al., 2011). Such an arrangement reduces chances of cross contamination (Aldstadt et al., 2006). Further modifications to the manifold were made to incorporate a compact design and to facilitate a lower amount of reagent consumption.

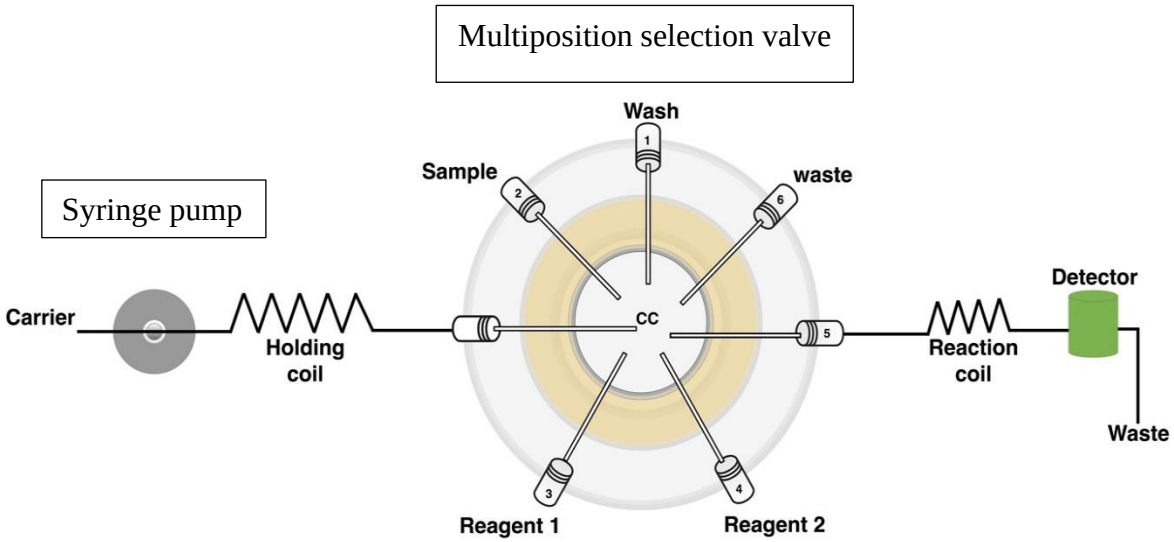

Figure 2.10: The basic manifold design of the first SIA with a single pump, holding and reaction coils and a 6-port multiposition selection valve, following the single line scheme of FIA. Diagram adjusted from Aldstadt et al., (2006).

2.4.5.3 Sequential Injection Lab-on-Valve (SI-LOV & µSI-LOV)

In 2000, Ruzicka introduced the third generation of injection analyser. The ultimate goal was to simply reduce the reagent consumption from a micro- to sub microliter volume. This was done by incorporating the detector as a build-in Photomultiplier Tube (PMT) holder within the multiposition selection valve (Figure 2.11), instead of an external detector seen previously in SIA (Figure 2.10). The built-in detector reduced the travel distance for the analyte to reach the detector for analysis. This lowered the reagent consumption and further contributed to a lower waste generation, while resulting in a miniaturized manifold. This design scheme is also known as a µSI-LOV (Figure 2.11). The scheme of microminiaturization further contributed to a compact and robust instrument capable of measuring TMs, while minimizing background interferences (Grand et al., 2011).

The first single line µSI-LOV manifold for the automated fluorescence determination of TM's in seawater, incorporated an opaque lab-on-valve with a six-port multiposition valve and a PMT. A Tungsten-Halogen lamp was placed perpendicular to the detector and used to excite the fluorescent samples. The manifold further included a 500 µL HC connected by 0.8 mm PTFE tubing to a 1000 µL glass barrel syringe pump. A buffer carrier connected to port 6 of the manifold interacts with the sample and carries it to the PMT for detecting the fluorescent emitted light (Figure 2.11; Grand et al., 2011). The µSI-LOV manifold was first used to determine dissolved Zn (Zn_d) in filtered unacidified seawater by a fluorometric detection (Figure 2.11). Matrix elimination or preconcentration of Zn was neglected for the defined protocol sequences. The increased sensitivity for measuring low Zn concentrations, without preconcentration or matrix elimination, was achieved by optimization of the reagent/sample aspiration sequence (Grand et al., 2011).

The experimental protocol sequence used by Grand et al., (2011) to measure dissolved Zn in seawater using µSI-LOV is outlined in Figure 2.12 and is known as the SHC procedure. That is, the reaction between the sample and reagents occurs within the HC to form the chelate complex which is then transferred to the flow-cell for detection **(**Hatta et al., 2018). In summary, the fluorescence determination of Zn_d required the aspiration of the reagent, followed by the sample (volumetric reagent/sample ratio of 2:3) into a HC with help of the syringe pump (Figure 2.12). Injecting the sample last minimizes the dispersion experienced by the sample, and in turn increases the contact the sample has with the reagent. Once the reaction

is complete the flow direction is reversed, and the reaction mixture is sent to the flow cell for detection. The method of Grand et al., (2011) yielded a LOD of 0.3 nM for Zn at an analytical cycle of 1 min per sample.

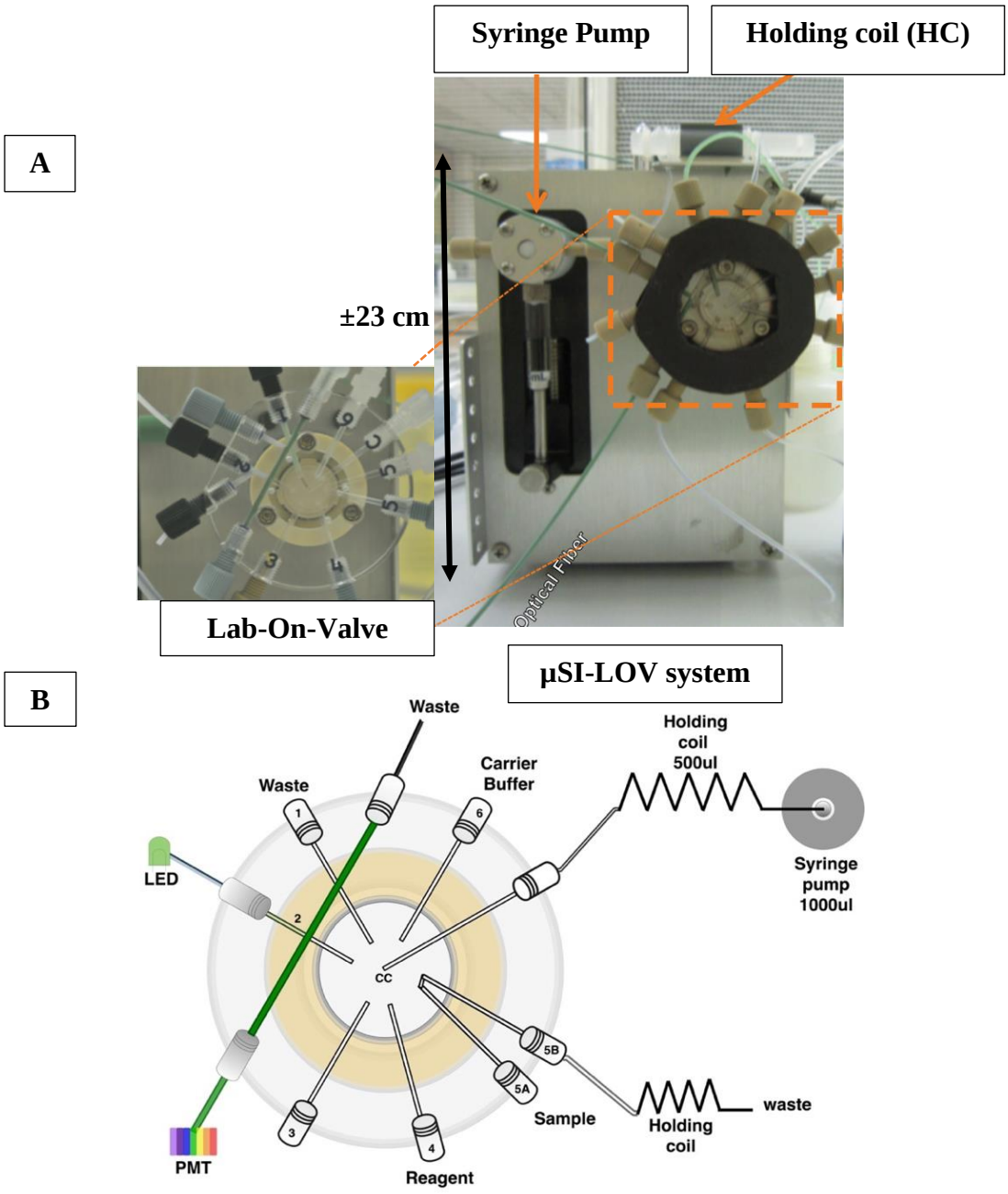

Figure 2.11: The µSI-LOV manifold for fluorescence determination in seawater for Zn_d. Panel A: indicates the graphical diagram, showing the 6 port multiposition valve, the syringe pump and the HC. Panel B: indicates the schematic diagram of the µSI-LOV and allocated ports for the samples and reagents with the customized flow channels (Grand et al., 2011).

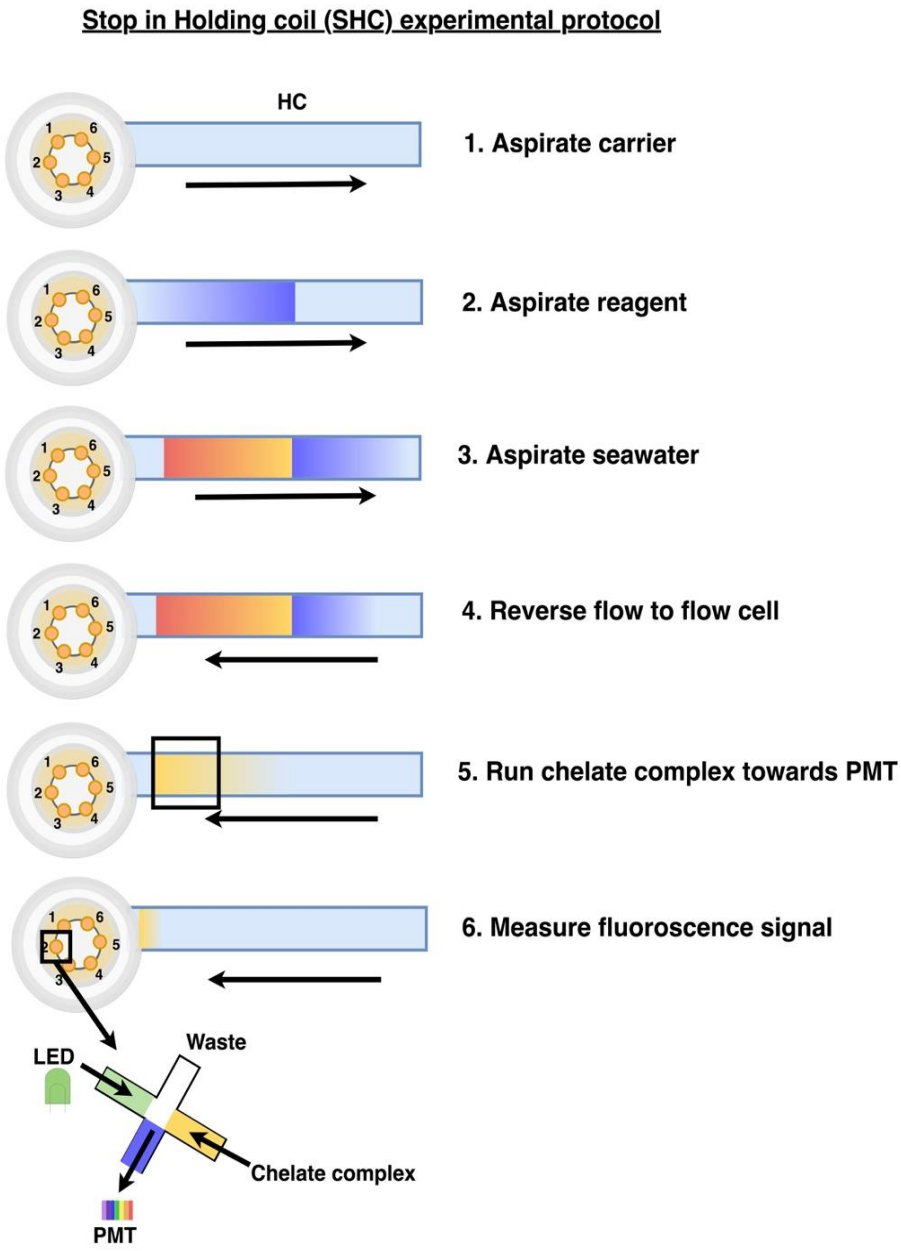

Figure 2.12: The analytical sequence for the fluorometric determination of Zn_d in seawater, using SHC protocol. The method uses one HC. Diagram modified from Grand et al., (2011).

2.4.5.4 SI-LOV with three holding coils

Even though the SHC protocol sequence achieved a LOD of 0.3 nM for Zn_d in seawater, the sequence neglected preconcentration of the desired metal and the removal of the high

interfering salt matrix. That is, there was room for further modification to measure even lower Zn concentrations. Thus, the design scheme of the µSI-LOV was further modified to incorporate two HCs and a mini column packed with the chelating resin, Toyopearl-AF Chelate 650M for the preconcentration of Zn and the removal of the high interfering salt matrix. The result was a µSI-LOV manifold that incorporated both a SPE and a SHC step to improve the LOD from 0.3 to 0.02 nM for Zn_d in seawater at an analytical cycle of 13 min per sample (Grand et al., 2016).

To achieve a LOD of 0.02 nM for filtered Zn_d in seawater, the protocol sequence required modifying two aspects of the manifold. The first modification was the incorporation of a SPE step to eliminate the high salt matrix and isolate the target Zn by incorporating the chelating column directly into the manifold design. This minimized the chances of cross contamination compared to using a separate offline SPE step. The second modification was optimizing the SHC protocol sequence by using two HCs instead of one and incorporating a central merging centre within the LOV to increase the sample and reagent contact surface for complexation. The manifold design incorporates similar components as that of SIA, however, the manifold was more compact and robust in design to suite measurement of TM's on a shipboard environment.

The improved manifold scheme of Grand et al., (2016), is shown in Figure 2.13, and incorporates three HCs (HC1, HC2 and HC3). Two high flow bidirectional syringe pumps that connect to HC1 & HC2 are further connected to a six-port multiposition selection valve, equipped with a central merging channel (CC). The CC allows for simultaneous merging of the reagent and the sample for mixing and are driven by the syringe pumps. The six-port multiposition valve has a custom-made, transparent LOV positioned to the front in a vertical position, with each port allocated to a specific reagent, sample or component. Port 1 is allocated to HC3, port 2 to the fluorescence flow cell, which is comprised of two optical fibers and PMT positioned perpendicular to the blue Cree XLamp LED set to 100% light intensity, port 3 the inlet to the Toyopearl AF-Chelate column, port 4 includes the 0.1 M HCl eluting acid, port 5 the buffered seawater and port 6 the fluorescent reagent. The entire system utilizes deionised water as a carrier solution (Grand et al., 2016).

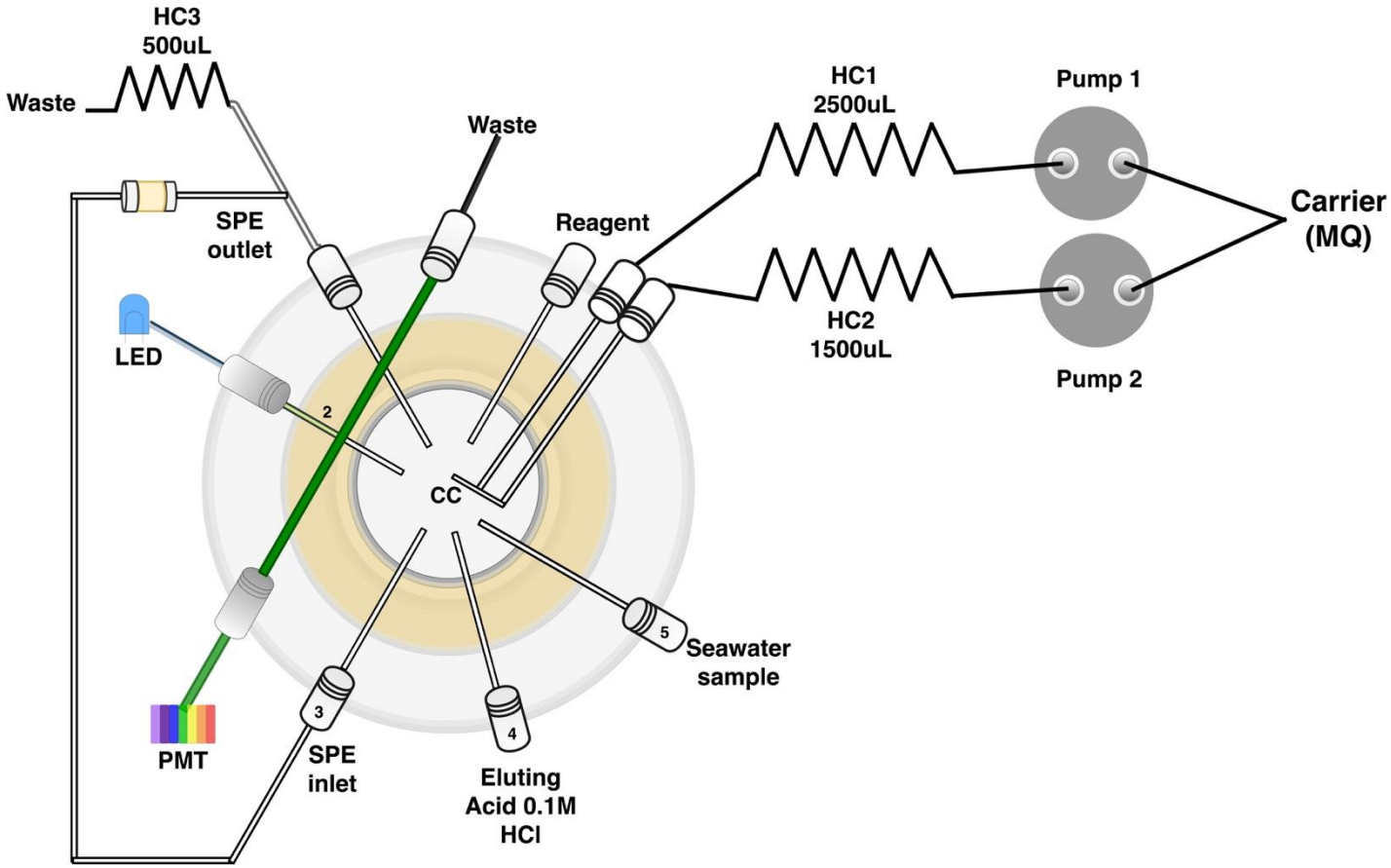

Figure 2.13: The miniSIA-2 manifold setup for Grand et al., (2016). Comprised of three Holding coils (HC1, HC2 and HC3), a six-port selection valve (LOV) with their corresponding reagent/sample ports. A merging central channel (CC), connecting the HC1 and HC2, connected to twin high flow bidirectional syringe pumps which connect to a carrier (MQ). An external Toyopearl AF-Chelate 650M column, with the inlet at port 3 and the outlet port connected to a tee-piece at HC3. Two optical fibers connect the XLamp XP-E2 blue LED, perpendicular to the photomultiplier tube (PMT) (λ_{ex} 494 nm and λ_{em} 516 nm) at port 2.

2.4.5.5 The SHC and SPE experimental protocol

The experiment protocol sequence used by Grand et al., (2016) involved a SPE and SHC step incorporating three HCs. The protocol sequence is shown by Figure 2.14 (Preconcentration step) & 2.15 (Analytical step). Prior to starting the analysis, the system goes through a wash step in which eluting acid and deionised water are pumped through the system. The wash step primes the system by removing air bubbles and simultaneously cleaning the SPE column. Following the wash step, preconcentration of TM is performed using the SPE column (Figure 2.14). Buffered seawater is aspirated into HC1 and then dispensed towards the SPE (Toyopearl) column. This process is repeated 4-8 times to ensure sufficient Zn is chelated onto the Toyopearl resin, while the seawater matrix runs towards waste through HC3 (Grand et al., 2016).

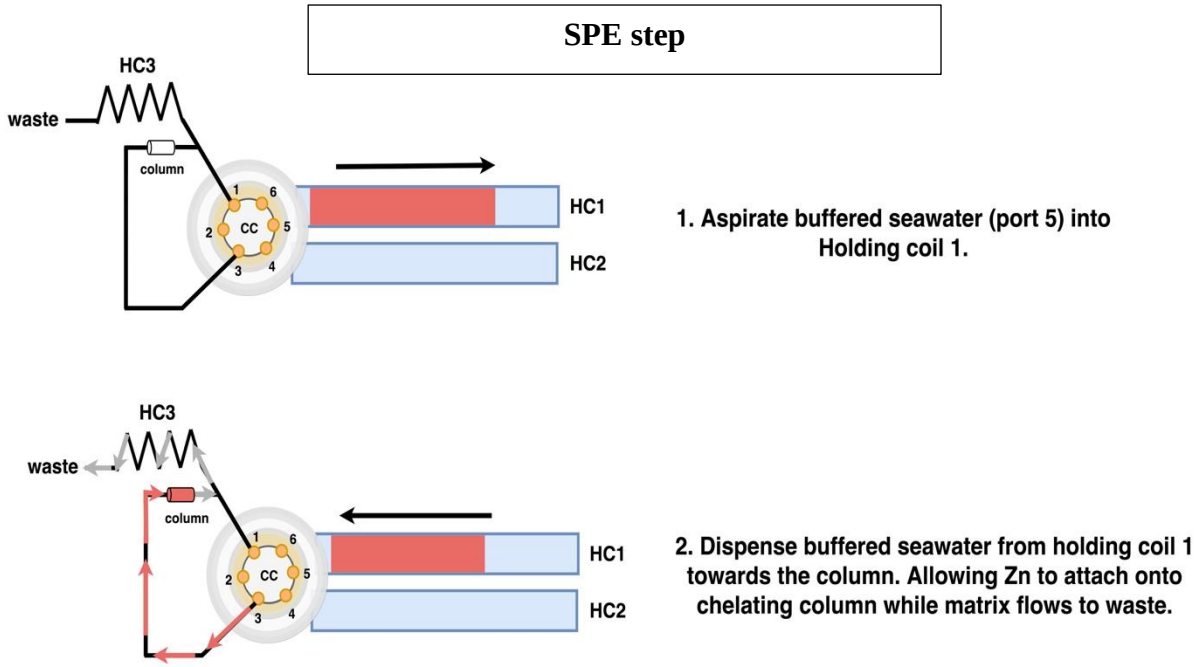

Figure 2.14: The SPE step used for the experimental protocol sequence, involving preconcentration of the buffered seawater sample. Diagram modified from Grand et al., (2016).

The preconcentration step is then followed by the SHC step (Figure 2.15), which involves aspirating the eluting acid into HC1 and dispensing this towards the SPE column to extract the adsorbed Zn. The eluted Zn is then stored in HC3. While the elute remains in HC3, the fluorescent reagent is aspirated into HC2. The reaction between the reagent and Zn in eluting acid is done by aspirating the eluting acid stored in HC3 towards HC1, while simultaneously

dispensing the reagent kept in HC2, towards HC1. As the fluorescent and the elute meet within the CC of the multiselection valve, the chelate complexation starts forming before being aspirated into HC1. The chelate complex is held within HC1 until being dispensed towards the fluorescent detector for analysis (Grand et al., 2016).

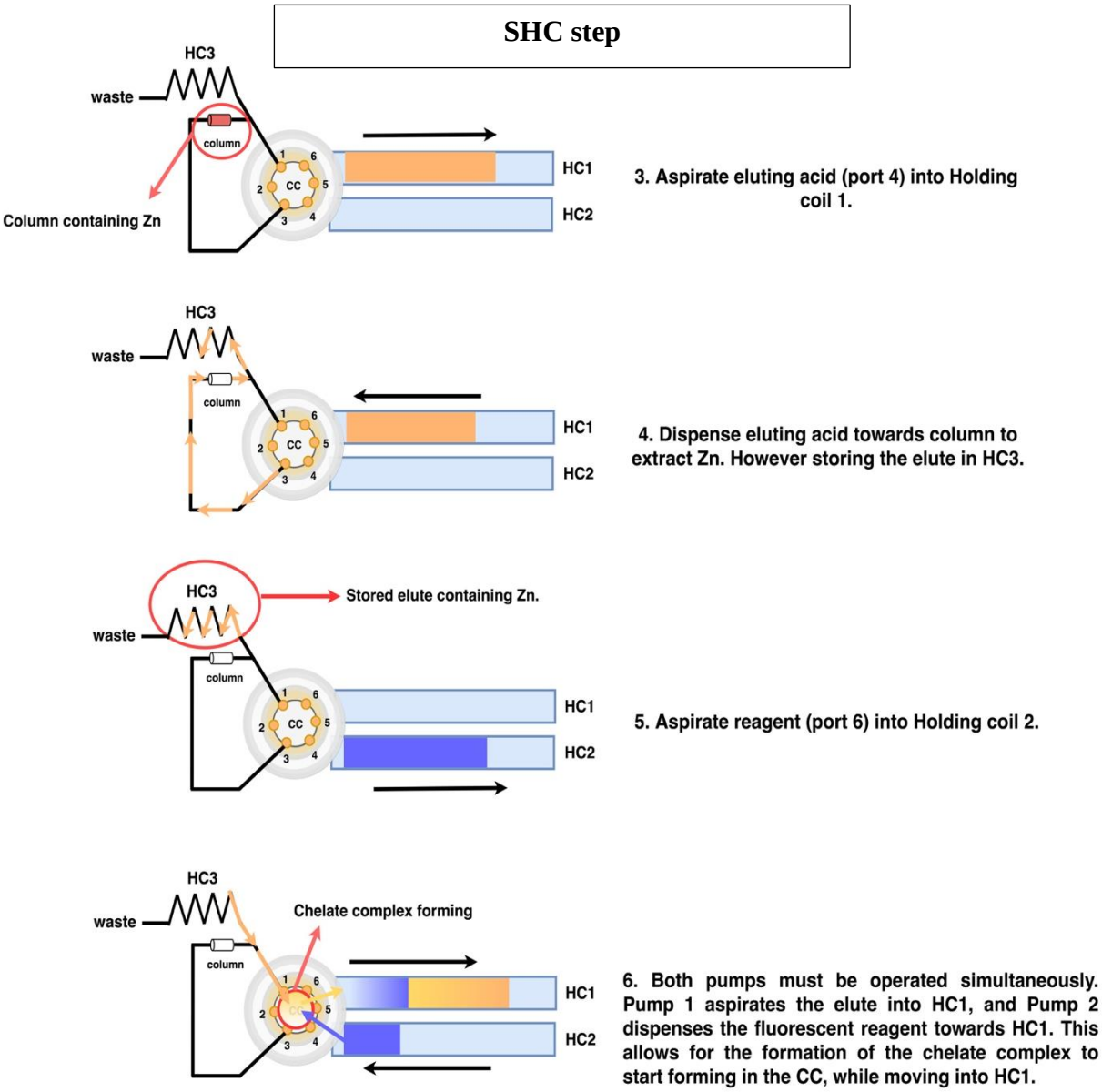

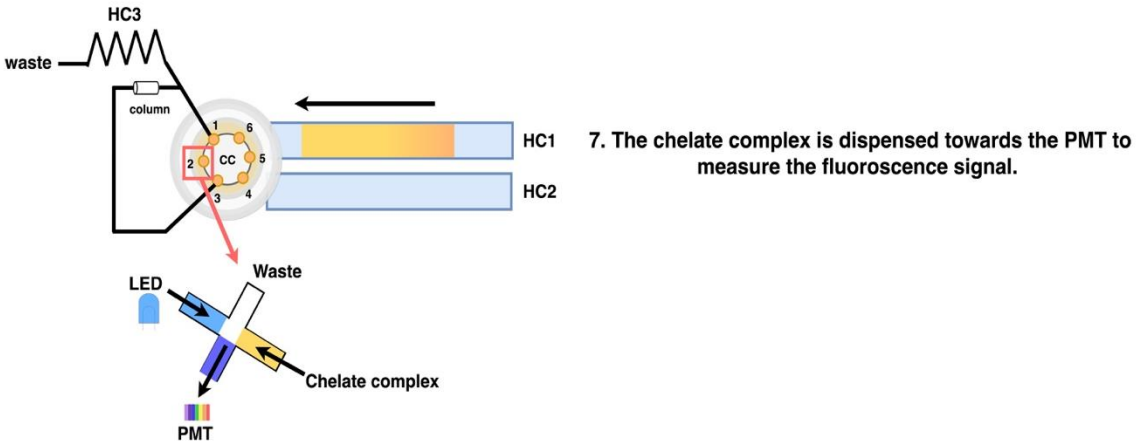

Figure 2.15: The second step (SHC) in the experimental protocol sequence, which utilizes two HCs to complete the reaction and determine dissolved Zn at a LOD of 0.02 nM Zn and analytical cycle of 13 min. Diagram modified from Grand et al., (2016).

Despite the low LOD (0.02 nM Zn_d) achieved by the manifold, the scheme design has several limitations. As a result of the long distance between the multiposition port and the column, the sample or elute will undergo greater dispersion. This results in an increased analytical cycle time. Another limitation is the lack of ports on the multiposition valve. This prevents the incorporation of additional steps such as incorporating a Brij-35 for increasing the sensitivity or an online buffering step to reduce the contamination risk. With the addition of additional ports to the multiposition valve, any offline steps will be eliminated, and the entire system will be fully automated. As a result, the system will be more compact and robust.

Chapter 3 Methodology

The method was modelled to that outlined by Hatta et al., (2018) for measuring Fe. This is a newly designed instrument and therefore, there is not yet a prescribed methodology. The focus was placed on optimizing the Batch method by considering important fluorescent parameters described by Gomes et al., (2019). The method focuses on measuring Al_d in seawater by a modified SI-LOV system equipped with a SPE column and a build-in Fluorescence module (miniSIA-2). The miniSIA-2 was developed by GlobalFIA, Fox Island, WA, USA. Figure 3.1, gives the systematic steps with the corresponding parameters to develop a fully automated scheme to measure Al_d in seawater. These steps are as follows: 1) Batch method, 2) SHC and 3) SHC with SPE.

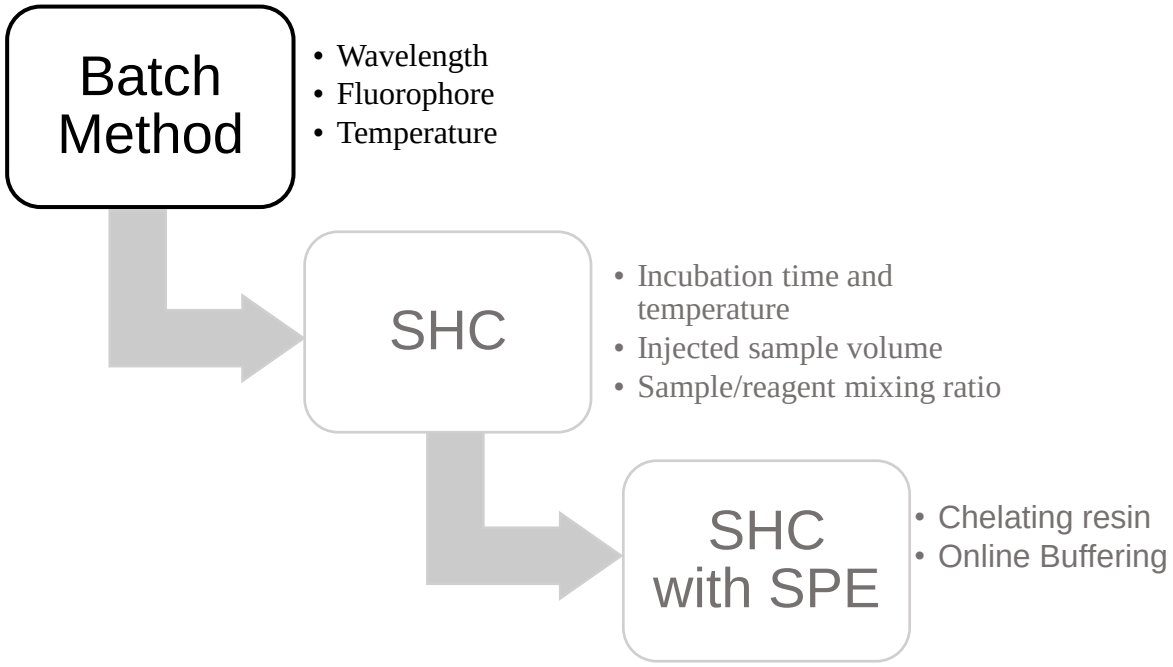

Figure 3.1: The systematic method approach with their corresponding parameters. The methodology can be subdivided into three distinct protocol assays, each with their own distinct parameters, which require optimization before progressing to the next step. For this project only the batch method was optimized.

3.1 Stock seawater

Stock seawater was collected from the spring SCALE (Southern oCean seAsonal Experiment) expedition aboard the research vessel SA Agulhas II during the year of 2019. During the expedition, vertical seawater samples were collected using a Seabird, trace metal clean, Titan all-titanium conductivity-temperature-depth (CTD) rosette. Attached to the rosette were 24 internally Teflon-coated PVC 12 litre, acid cleaned, GO-FLO bottles (GeneralOceanics). The rosette was connected to a non-metallic Kevlar hydrowire, which allows the CTD to simultaneously measures salinity, density and temperature, once submerged into the sea. The GO-FLO bottles have trigger switches, which closed at predetermined depths. Following collection, the GO-FLO bottles were packed into clean liners and transported to a class 100 (ISO) container for filtration and sub sampling. Stock seawater samples were filtered through a 0.2 µm filter (Acropak 500 Supor Membrane) under pressurized trace clean, filtered nitrogen gas, which was pumped into the Teflon-coated, acid cleaned GO-FLO bottles. Following the ship-board procedures, samples were stored in a class-100 clean laboratory at Stellenbosch University.

3.2 Reagents

All reagents and standards were prepared in a class 100 clean laboratory, of which all samples and reagents were stored and analysed in either Teflon or LDPE bottles/vials and kept upright. The bottles/vials were washed and cleaned by a 3-step protocol procedure (Cutter et al., 2017) or kept overnight in a 6M HCl bath on a heating plate at 50°C. Deionised water from a 18.2 M-Ω Milli-Q analytical reagent-grade water purification system was used for various analytical processes (cleaning, preparing standards etc). Two Al standard stock solutions (5000 nM and 360 nM) were prepared by diluting 1002±5 µg/mL Al (Inorganic ventures®) in 0.1% HNO_3 (Merck® ultrapur). A 2 M ammonium acetate buffer was prepared by diluting Acetic acid (HAc, 100%, Merck®, suprapur), with deionised water and Ammonium hydroxide (NH_4OH 25%, Merck® suprapur) and adjusting the pH to 6.0±0.1. A 0.5 M HCl wash solution was prepared by diluting 30% UpA Hydrochloric acid (HCl) in deionised water. LMG stock solutions (0.02% and 0.2%) were prepared by diluting 2 mg and 20 mg of >98.0% LMG (Industrial Analytical (Pty) Ltd) in 10 ml of deionised water. The LMG stock solution was then ultrasonicated and placed in a refrigerated and dark storage. A LMG work solution was then prepared afresh every day by diluting the LMG stock solution in 2M ammonium acetate buffer (6.0±0.1). A 5% brij-

35 solution was prepared by adding 84 ml of brij-35 (Sigma-Aldrich) to 500 ml of deionised water.

3.3 Calibration

Standard solutions used in the experiments were prepared by weight by diluting the 5000 nM and the 360 nM Al stock solutions in 0.01M HCl acidified deionised water and filtered seawater. The deionised water matrix was used as a control to distinguish between interferences from the high salt matrix of the seawater. Two sets of bulk standards were prepared. The first set of Al standard solutions were (800-100 nM Al) to establish the basic analytical setup, whereas the second set of standards solutions (10-2 nM Al) were used for determining the instrumental detection limits.

3.4 Method evaluation

Method evaluation was performed on a Tecan Spark 10M multimode microplate reader, set to the following conditions: Temperature = 22°C / 25ºC, λex = 470 nm, with an excitation bandwidth = 20 nm, λ_{em} = 570 nm, with an emission bandwidth of 20 nm. Samples were prepared by the batch method described by Hydes and Liss, (1976). However, buffering samples either with a 0.2% or 0.02% LMG work solution (pH of 6.0±0.1) to a pH of 5.4±0.1 for deionised water or pH of 5.0±0.1 for seawater samples. Samples were heated at 80ºC for 90 min in a water bath and allowed to cool to Room Temperature (RT) (18-19°C) before being analysed.

3.5 Hardware

3.5.1 Miniaturized two-line sequential injection analyser (miniSIA-2)

Experimental analysis was performed on a miniSIA-2, developed by GlobalFIA, Fox Island, WA, USA (Figure 3.2). The unit is composed of an 8-port, cheminert, multi-position selection valve (Valco valves). This selection valve is furnished with a 8-port, transparent, customized flow channelled, monolithic LOV manifold, assembled vertically, with a preferred rotational orientation to the selected port by command from the commercially available software (FloZF, GlobalFIA, Seattle, USA). To facilitate simultaneous fluid merging and sample manipulation, the central channel (CC) of the LOV acts as the confluence point, connecting the

polytetrafluoroethylene (PTFE) 0.8mm tubing of the two thermostat HCs, HC1 (2875 µL) and HC2 (1280 µL). Connecting the corresponding HCs are the two bi-directional positive displacement milliGAT high flow (HF) pumps (P1 and P2), which attach to a 1.6mm PTFE tube of the carrier reservoir (Figure 3.2 and 3.3).

The SPE column, packed with Toyopearl AF- Chelate -650 M resin (length = 0.28 mm, Internal volume = 0.10 µm) was held in place by two 20 µm porous polyethylene frits. The mini column was attached to a short external PTFE tubing, with the inlet connected to port 6 and the outlet connecting to port 5A and HC3 (460 µl). A bolt-on fluorescence 10cm light path absorbance flow cell, mounted to port 2 of the LOV, connects to a blue LED (CREE XLAMP XP-E2) excitation beam via fiber optic cables. The blue LED, positioned within a custom-made manually adjustable fine-tune rotational knob, which allows for controlling light intensity manually from 0 - 100%. This is located on the central platform of the miniSIA-2. Two diffraction grating monochromators (λ_{ex} 470 nm) and (λ_{em} 560 nm) (Chroma), connect to a photon counter (photomultiplier tube, PMT). Background light is reduced by placing the PMT perpendicular to the excitation beam (Houck & Siegel, 2010) (Figure 3.3). The PMT amplifies the electrical signal and generates an output current, which is proportional to the measured emitted intensity of the fluorescence. The fluorescence sample peaks and protocol assays were measured using a commercial available software FloZF.

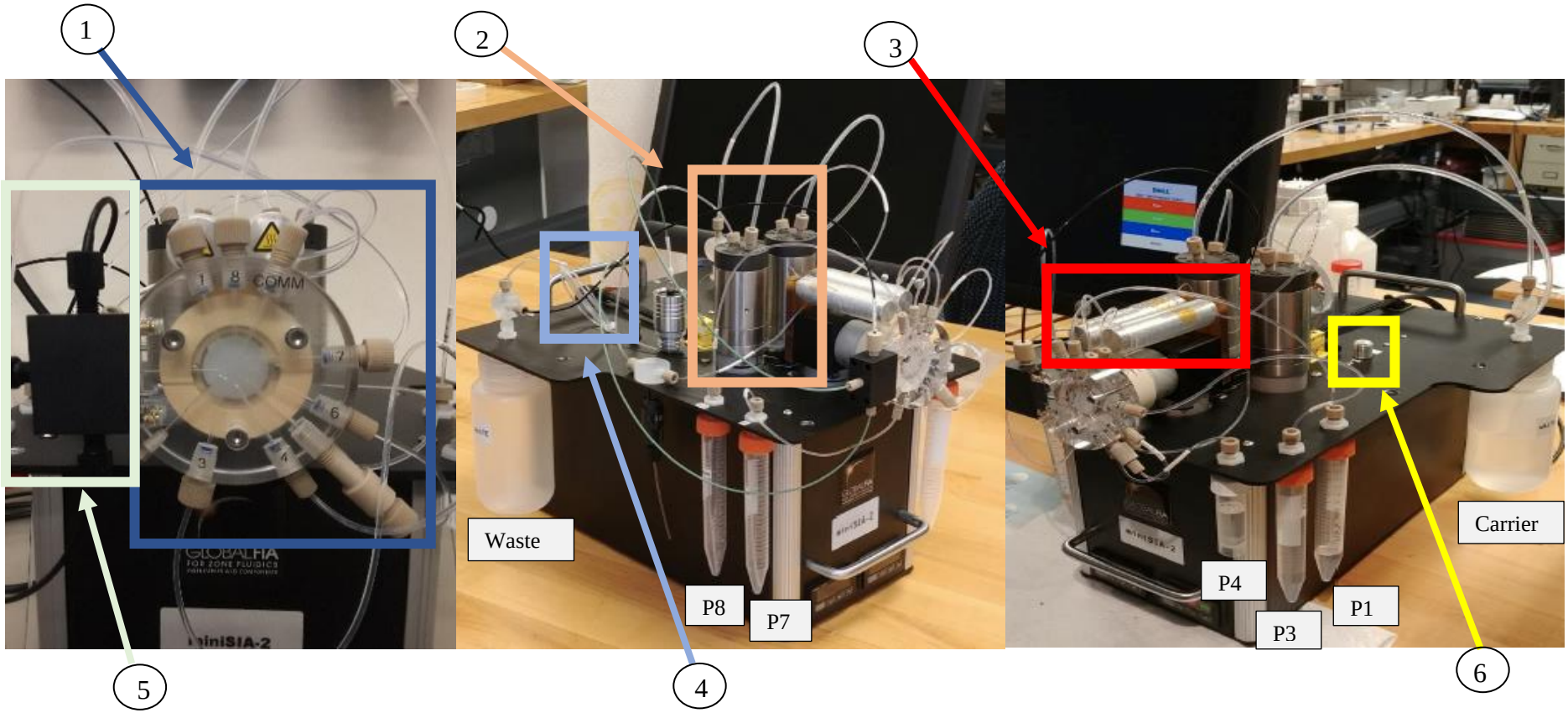

Figure 3.2: The miniSIA-2 setup. Sample and reagents are connected to 1) 8-port LOV multiposition cheminert selection valve, labelled as P1-P8, with fluid propulsion driven by 2) twin high flow bidirectional milliGAT pumps, which connect to 3) two thermostat s, which connect in the central channel (CC) of the LOV. The CC allows for simultaneous mixing of the reagent and sample by reversing the flow from 4) holding coil 3 towards 5) the sample chamber connected through the optical fiber to the photomultiplier tube and the blue LED light. The light intensity can be manually controlled by 6) the light knob.

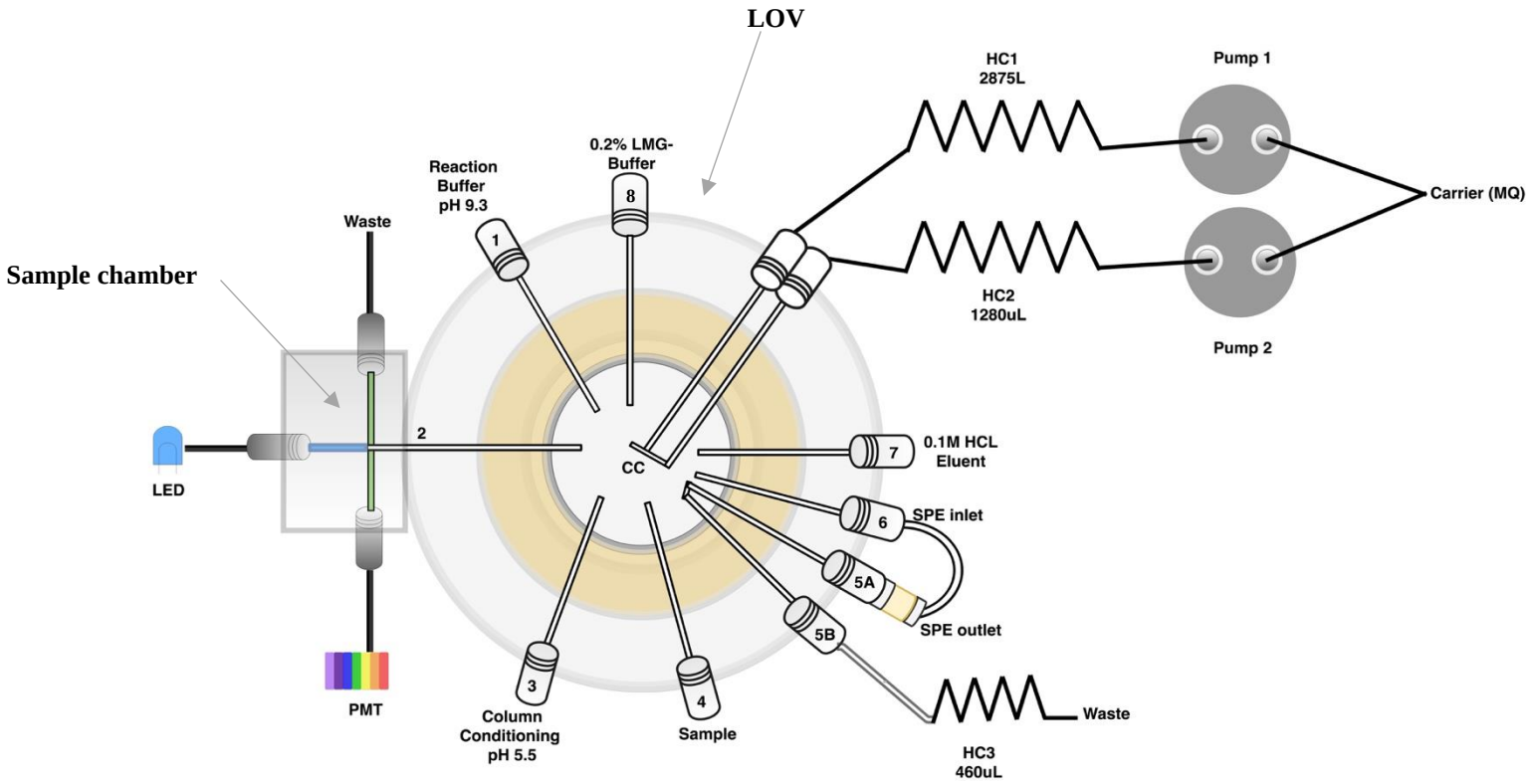

Figure 3.3: A schematic diagram of the miniSIA-2 with the reagents and sample allocated to the appropriate ports of the LOV. The total volume of each holding coil (HC1 (2875 µL), HC2 (1280 µL) and HC3 (460 µL)) is shown. This is the maximum fluid capacity of each HC, before reagent/sample runs into the corresponding bidirectional pump (HC1 and HC2) or towards waste (HC3). Illustrated is the sample chamber, with the PMT placed perpendicular to the blue LED as this reduces background light. The merging central channel (CC), connected to the two thermostat holding coils allows for reagent/sample mixing.

3.6 Software

The system was controlled by a FloZF 5.2 software, which was installed and run from a 6.4-bit Dell laptop. The FloZF 5.2 program runs statistics, data acquisition and peak height calculations using Matlab R2014a (MathWorks,USA). The program allowed the user to define and build their own protocol sequence, based on the commands available within the software. Figure 3.4, shows the first protocol sequence used, labelled as Al-Fluorescein Final (Al-F), with Figure 3.5 showing the second protocol sequence used, labelled as Al-Fluorescein Original (Al-O). The input parameters for example 140,7,1 are defined as the volume (µL) aspirated, the flow rate (µL/s) and the holding time. The volume (µL) parameter was the only parameter adjusted. Reducing the volume (µL) allows the analysis to be performed at the fastest speed while limiting the amount of dispersion experienced by the sample. In this thesis, the flow rate (µL/s) was not adjusted to a faster speed, since this could lead to back-pressure build-up in the manifold, although this remains a possible opportunity for future research.

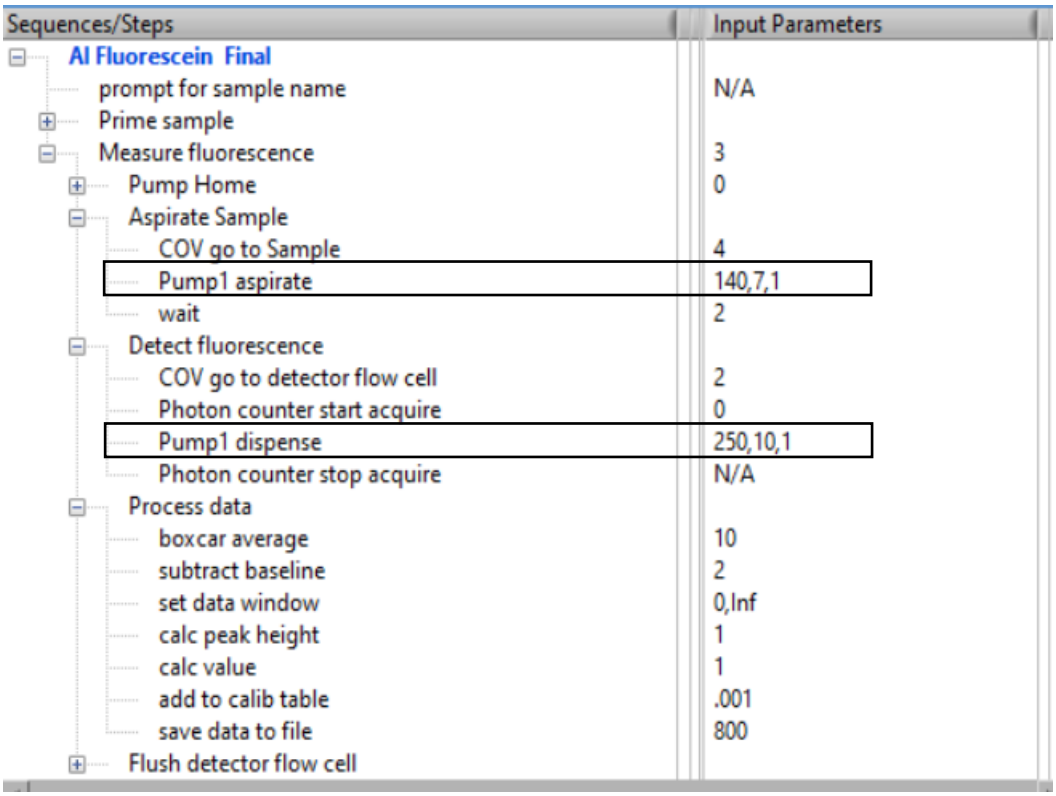

Figure 3.4: The protocol sequence for Al Fluorescein Final (Al-F). Pump 1 aspirates 140 µL of the sample to HC1, which then holds it for 2 seconds before dispensing 250 µL of the sample to the detector (port 2). The LED is kept at 100%.

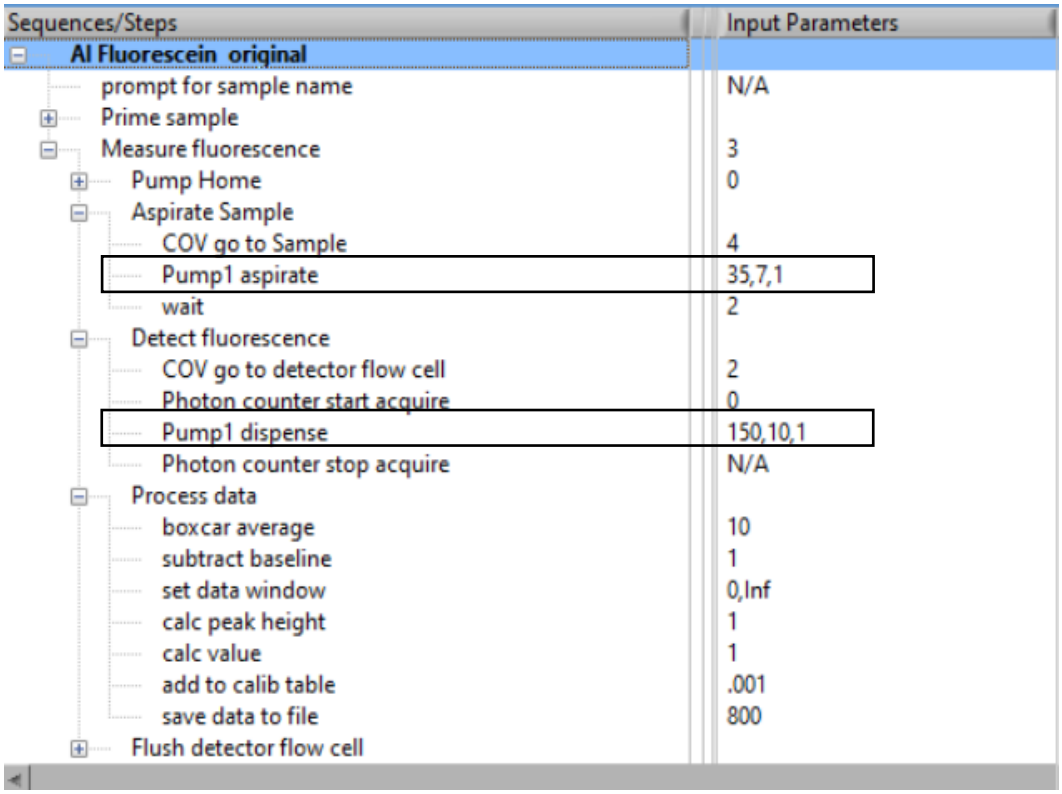

Figure 3.5: The protocol sequence Al Fluorescein original (Al-O). Pump1 aspirates 35 µL of the sample to HC1, which then holds it for 2 seconds before dispensing 150 µL of the sample to the detector (port 2). The LED is kept at 100%.

3.7 Sample Preparation

Samples were prepared by the batch method (Hydes & Liss, 1976), refer to the summarized procedure (3.7.1) below. The standard additions were buffered either with a 0.2% or 0.02% LMG work solution (6.0±0.1), for which the deionised water samples were buffered to a pH of 5.3±0.1 and the seawater samples to a pH of 5.0±0.1, respectively. Once buffered, the samples were placed in a water batch set to 80°C for 90 min before allowed to cool to room temperature in the dark. Samples were vigorously shaken before connected to sample port 4 and either analysed by protocol sequence, Al-F or Al-O. The miniSIA-2 monochromators are set to excite the samples at λ_{ex} 470 nm and emit a signal at λ_{em} 560 nm, with the blue LED light source set to 100%.

3.7.1 Summarized procedure

1. Add a 100 µL of the 0.2% or 0.02% LMG stock solution to 10 ml of 2 M ammonium acetate (pH 6.0±0.1), which makes the LMG work solution.
2. Add 500 µl of LMG work solution (0.2% or 0.02% LMG work solution, buffered to a pH 6.0±0.1) to test tube.
3. Add 10 ml of the acidified sample into the test tube.
4. Shake the solution vigorously and wait for 3 min.
5. Place solution in a water bath at 80°C for 90 min in the dark.
6. Allow samples to cool to room temperature in the dark.
7. Prior to aspiration to detector, shake sample vigorously and connect to port 4.
8. Aspirate 140 or 35 µL of reaction mixture directly into a 10 cm long light path flow cell with the wavelength set to λ_{ex} = 470 nm and λ_{em} 560 nm, respectively.
9. Fluorescence measurement should be seen at 24 or 16 seconds.

3.8 Calculating the LOD

Using the blank technique, the LOD was calculated. Defined as the lowest concentration of a compound that can be detected with reasonable certainty by an analytical procedure (Shrivastava & Gupta, 2011; Gomes et al., 2019). The LOD was calculated using Equation 5:

Equation 4 $$LOD = \frac{F \times SDdev}{b}$$

where,

b = slope of the regression line or taken from the calibration graph (Equation 7)

Equation 5 $$b = \frac{y^2 - y^1}{x^2 - x^1}$$

SDdev is the average standard deviation of the blank, and F is the factor of 3.3.

Chapter 4 Results & Discussion

Measurement of Al_d at low (< 10 nM) concentration levels in aqueous phases can be accomplished by a number of methods (van den Berg et al., 1986; Sohrin et al., 2008; Minami et al., 2015). However, many of the available methods are error prone when measuring Al_d in seawater. This is primarily due to the high contrast between the salt matrix and the ultra-low Al concentrations observed in oceans such as those of the (SO) (0.9 nM), Pacific (3.3 nM), and Indian (5.5 nM) (Menzel Barraqueta et al., 2020). For a period, methods based on the use of ICP-MS were the only ones that could reliably produce data at the required low concentration of Al. However, these methods suffer from contamination issues at the time of sample collection and storage. Since manufacturers no longer produce LDPE bottles with LDPE caps and instead replaced them with PP caps, resulting with PP caps contaminating samples during storage. This makes it necessary that samples be analysed on-board the ship as soon as they are collected. Thus, methods such as FIA (Resing & Measures, 1994), need further development to improve sensitivity and stability to be used on-board a ship.

The miniSIA-2, chosen here to measure Al_d, is a third generation of FIA known as a μSI-LOV and the manifold scheme for it was developed through adjustment of a previously described miniSIA based method to measure Zn at trace concentrations in seawater (Grand et al., 2016). However, due to a number of drawbacks discussed in Section 2.4.5.5 (increased dispersion of sample due to distance of column and lack of ports), the manifold required adjustments and an slightly advanced μSI-LOV was developed. A significant change in the scheme is the incorporation of two-addition ports, so instead of a 6 port multi-position selection valve, the miniSIA-2 is comprised of an 8 port multi-position selection valve. The additional ports on the manifold allowed the direct inclusion of a build-on preconcentration column located on the manifold itself. In Grand et al., (2016), the preconcentration column was incorporated as an attachment and connected by a long PTFE tube via a tee-piece to HC3 (Figure 2.13). As a result, the design is less compact and the analytical cycle increased as the buffered seawater and the elute have to travel a longer duration and therefore are more likely to anticipate dispersion. Furthermore, with the addition of two extra ports, a sample buffering and brij-35 addition can be carried out online, resulting in an fully automated online analysis that limits human error and excludes offline steps that may contribute to contamination.

For the development of the analytical protocol, a systematic approach was selected. Given the time constrains and the lack of availability of laboratory access during COVID period, only the initial steps have been optimised and described here and further developments are required before this miniSIA-2 based method can be successfully used. In addition to this a similar manifold of the miniSIA has been used previously to measure Fe_d and Zn_d at TM concentrations in seawater, the system is yet to be configured to measure Al_d. That is, both instrument configuration and chemical protocol require development. For the chemical development of the method and to simplify the method and identify the source of variability in measured parameters, an adjustment to the batch method described by Hydes & Liss, (1976) was chosen. This step allows for solutions to be precisely measured, mixed, incubated, heated and monitored in a reproducible way. This act's as a foundational step for method optimization to measure Al_d for further development and automation on the miniSIA-2.

In this chapter the systematic route towards method optimization, using the outlined methods from Brown & Bruland, (2008) and Hydes & Liss, (1976) are described. First the findings of the analytical method developed and used to determine the concentration of Al_d in deionised water and seawater by a miniSIA-2 is described and discussed. This includes establishing a signal under the proposed conditions for high concentrations (800 – 100 nM), followed by adjusting these parameters to obtain a suitable detection limit. This is then further used for the lower concentration range (< 10 nM) to establish a suitable protocol sequence for the lower concentrations.

4.1 Formation and detection of the Al-LMG chelate complex in deionized water

Al_d is determined from a fluorescent signal given out by an Al-LMG chelate complex. The preliminary step was to determine the viability of sample treatment for forming the complex, as well as the ideal instrument parameters while determining the signal.

Therefore, the first step was taken toward the establishment of the window within which the Al-LMG peak can ideally be identified. The optimal known pH window for the formation of the Al-LMG chelate complex lies between 5.0-5.5 (Hydes & Liss, 1976). Thus, the samples were prepared with the addition of a 0.2% LMG solution as discussed in section 3.7 and 3.7.1

with the analyte pH buffered between 5.0 to 5.4. To verify that the Al-LMG chelate complex forms and that the PMT can detect the emitted fluorescence signal, without possible interferences from Fe, F- or Gallium (Ga), a blank (Al_d = 0 nM) and a high Al_d (992 nM) sample in deionized water was run. The two samples were run consecutively using the Al-F sequence (see Figure 3.4) and the obtained peaks are shown in Figure 4.1.

The average peak height count for the blank and the 992 nM sample was 12400 and 26500 counts, respectively. The extension of the peak confirms that the Al-LMG chelate complex signal window is between 6 and 24 seconds with the highest peak obtained at around 12 seconds.

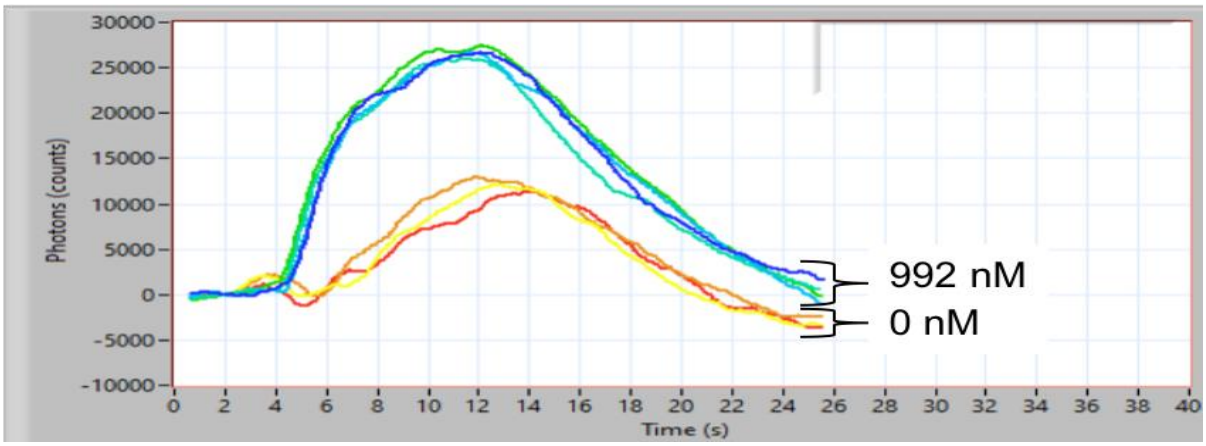

Figure 4.1: The peak shape profiles for blank (0 nM) and 992 nM Al standard samples measured in deionized water. The peak window of the Al-LMG chelate complex formed between 6 to 24 seconds, with the maximum peak forming at 12 seconds when using a 0.2% LMG solution.

Furthermore, the contrasting peak heights between the blank and 992 nM Al standard sample support the formation of the Al-LMG chelate complex. Further supporting this finding is the baseline value that remains stable throughout the experiment with well-defined peak heights and a RSD of less than 10% for both blank and 992 nM Al samples (Table 4.1).

Table 4.1: The results indicate a stable background, well-defined peak heights and a low RSD for both blank and 992 nM standard samples.

Al-LMG chelate complex						
Conc nM	Peak Height (counts)	Baseline value	STDEV	%RSD	Replicate	Sequence Name
992	26500	483000	1790	6.77	11	Al-F
0	12400	477000	1070	8.68	11	Al-F

The results show a stable background (baseline value, Table 4.1) throughout the experiment with well-defined peak heights (RSD, less than 10%) for both blank and 992 nM Al solution. The increased peak height for the 992 nM Al solution compared to the blank supports the formation of the Al-LMG chelate complex and its impact on the signal detected by the PMT detector. The fact that there is a visible peak observed for the blank, may suggest interferences from impurities in the blank, or interference from other ions (Ga, Fe, F^-) resulting in the possibility of minor formations of additional chelate complexes with LMG. However, the possibilities of interference are relatively insignificant as observed by the low RSD (<10%) for both blank and 992 nM Al.

4.2 Determination of Al_d at high concentrations (100-800 nM)

In order to confirm the validity of measurement using fluorescence signal for high-range Al_d samples, standard solutions (800, 600, 400, 200, 100 and 0 nM) made from adding appropriate amount of Al standard stock solution (5000 nM) to deionized water and were treated in the same manner as described in the above section.

The obtained peaks (Figure 4.2) for the standard solutions show a broad bell shape between 6-20 seconds with peak heights for low range standards (< 184 nM) unnoticeably different from the blank. However, a clear distinction in the signal was observed for higher end samples (400-800 nM).

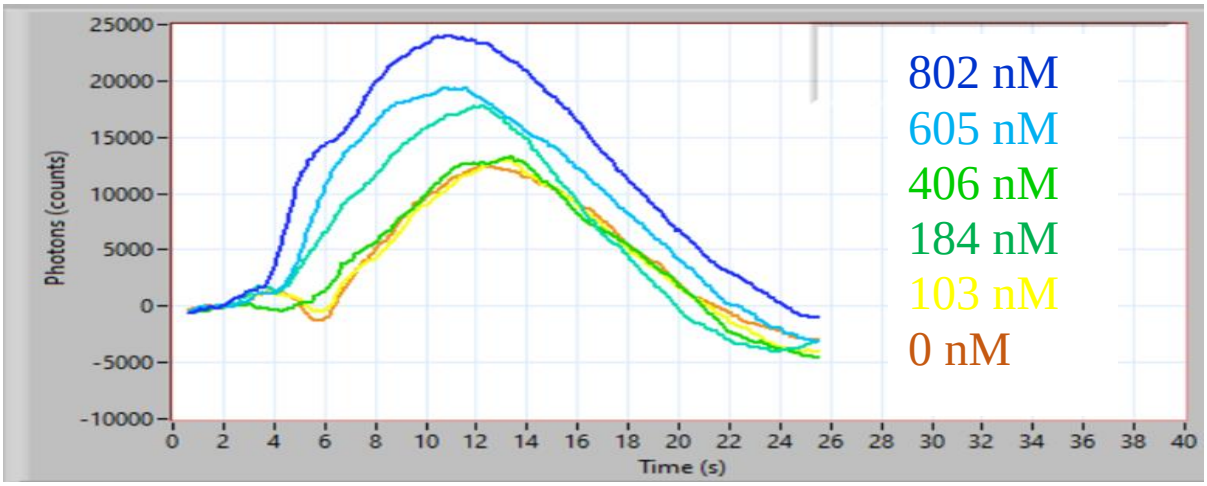

Figure 4.2: The broad bell shape profile for six standard Al additions (800-0 nM Al) in deionized water. The higher end concentration range (800-400 nM) indicated a good peak height discrepancy, with a minor or no peak height discrepancy for the lower end concentration range (184-0 nM).

The response in the form of peak height was analysed to create a calibration curve (Figure 4.3). The average peak height (counts, n = >5) was plotted on the y-axis and standard addition concentrations on the x-axis. Regression analysis of the data produced an R^2 = 0.97 (Figure 4.3) with a low RSD (<15%) (Table 4.2). The analyses further provided a, LOD to be 242 nM.

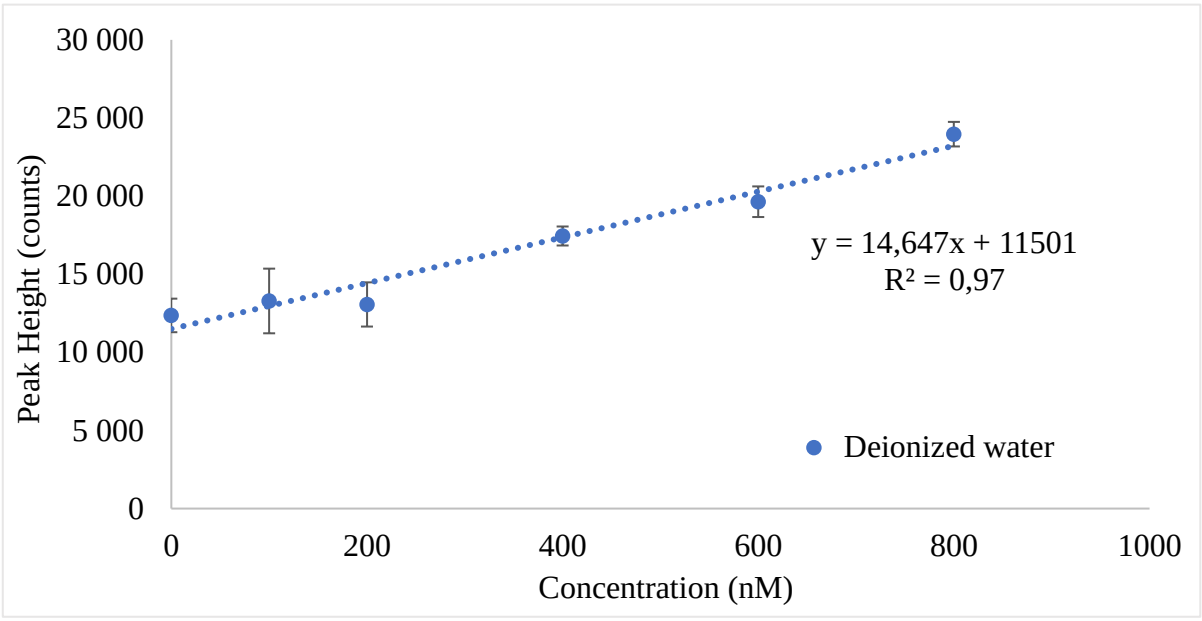

Figure 4.3: The calibration curve (R^2 = 0.97) for standard Al samples (800-0 nM) in deionized water using a 0.2% LMG work solution, and analysed by Al-F sequence.

There was a lack of discrepancy in the peak height counts for 184 nM (average peak height = 13100 counts) and 103 nM (average peak height = 13300 counts) Al standard sample which have concentrations below the LOD. The signal at lower concentration range is vital in understanding the detection limit of the analytical setup and for the assessment of the sample preparation procedure to fully understand the limitations of the analytical method. Clearly the variability of replicates at the lower end of the range need further improvement. Moreover, the determined LOD seem to be high and more efforts are required to increase the sensitivity of the method. For now, the success of such optimization is clear from the linearity of data within the measured range (Figure 4.3 and Table 4.2) and confirms that the proposed set-up and sample preparations is applicable for measuring the concentration of Al_d on a miniSIA-2 instrument.

Table 4.2: The results indicate a low RSD for Al standard samples with a lack of discrepancy among the lower end concentrations (184-103 nM).

Al standard additions in deionised water						
Conc nM	Peak Height (counts)	Baseline value	STDEV	%rsd	Replicate	Sequence Name
802	24000	464000	786	3.28	12	Al-F
605	19600	467000	980	4.99	13	Al-F
406	17400	476000	608	3.48	7	Al-F
184	13100	474000	1415	10.83	5	Al-F
103	13300	475000	2070	15.58	6	Al-F
0	12400	477000	1073	8.68	11	Al-F

Even though Figure 4.3, achieved an $R^2 = 0.97$, the lack of separation of signal among the lower concentrations suggests that the exterior conditions such as the protocol sequence need adjusting before adjusting the sample treatment. By adjusting the run-protocol sequence one can limit dispersion experienced by the sample while the sample moves towards the detector for analysis. Furthermore, this will improve the analytical sensitivity and reduce the waste generated and the amount of fluorescent consumed in the process. Therefore further tests were run where the protocol sequence was adjusted from Al-F to Al-O sequence by the use of a lower amount of sample protocol sequence.

4.3 Adjusting the protocol sequence: Method validation for deionized water using the Al-O sequence

To overcome poor detection at low concentration range following Al-F protocol sequence described above (Figure 3.4), the run-setup was modified to the Al-O protocol sequence (Figure 3.5). In the Al-O protocol sequence the volume of the aspirated sample was reduced from 140 µL to 35 µL and the injected sample pumped to the detector was reduced from 250 µL to 150 µL. This resulted in reduced dispersion and dilution of the sample during analysis. Here again six Al standards were prepared in deionized water (800, 600, 400, 200, 100 and 0 nM) and analysed following the Al-O sequence (Figure 4.4).

The peaks occurred between 4 and 9 seconds (Figure 4.4) and represent a gaussian-type peak shape. The shape of the peaks depicted in Figure 4.2 and Figure 4.4 clearly show a difference in peak heights obtained when analysing either with the AL-F or the Al-O sequence, where the Al-F sequence exhibits a wider peak window (6-24 seconds, Figure 4.2) compared to the Al-O sequence (4-9 seconds, Figure 4.4). Additionally, the Al-O sequence produced a smoother curve and a more defined peak shape profile, potentially indicating a better baseline and lower interference from matrix.

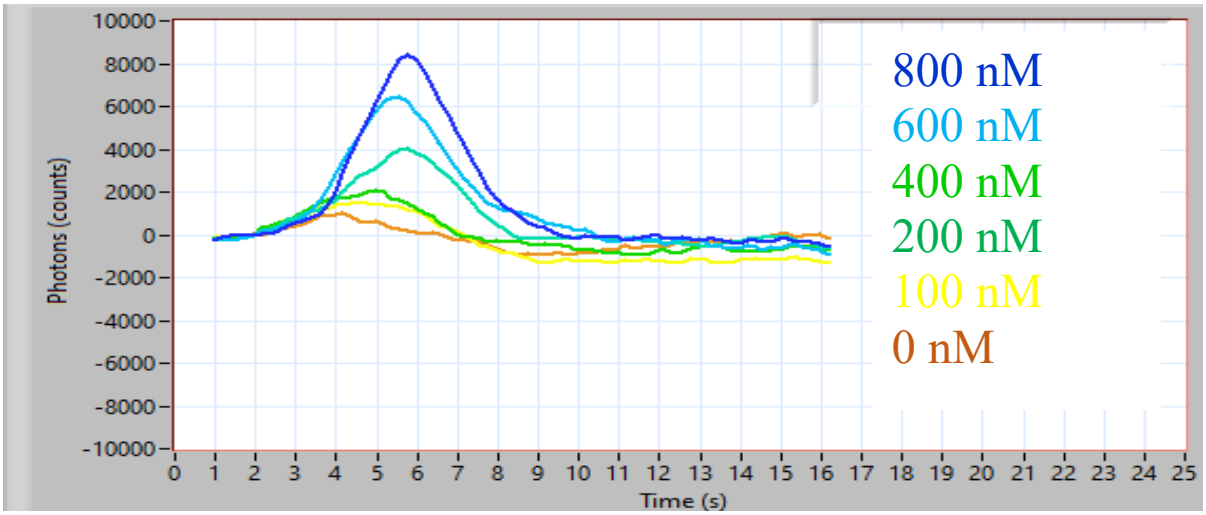

Figure 4.4: The gaussian peak shape for Al standard additions (800-0 nM) in deionized water prepared by a 0.2% LMG work solution and analysed by the Al-O. Indicating a clear discrepancies among all concentrations.

According to Figure 4.2 and Figure 4.4, the peak shape profile of the Al-F and Al-O protocol sequences are clearly differ as follows: The low-end concentration Al samples between 200-0 nM, showed a clear separation of signal from the blank peak which was not apparent for Al-F sequence. The Al-O sequences produced peak heights, ranging from 910 to 1900 counts (range of 990 counts) for the concentration range between 200-0 nM (Table 4.3) which allowed measurable differences in peak heights, which was not the case for the Al-F sequence where the difference in peak height between the blank and 200 nM sample was only 90 counts (Table 4.2) making measurements impractical. Despite a better resolution in the Al-O sequence the measurements at low concentration range were still error prone with RSD, more than 19 (Table 4.3) because of poorly defined peak profiles.

The calibration curve for the Al-O protocol sequence (Figure 4.5) was plotted by taking the average peak height (counts, n > 8; see Table 4.3) for respective standard concentration and a linear trend line was fitted. An improved coefficient of regression (R^2) of 0.99 was obtained for Al-O sequence protocol and resulted in improved sensitivity. Due, in part, to the larger count range of the Al-O sequence, the LOD of the Al-O sequence (115 nM) was also substantially lower than that of Al-F (242 nM). Thus, the Al-O protocol sequence for measuring Al_d was found to be better for the measurement and detection of Al_d. As such, all further method development was conducted following the Al-O sequence.

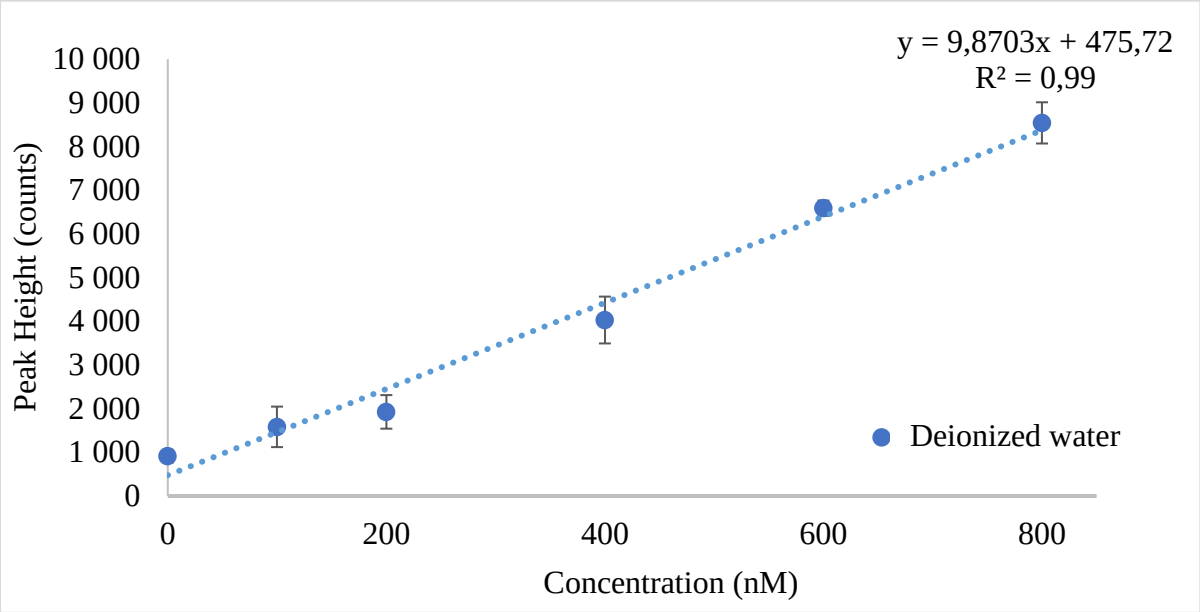

Figure 4.5: The calibration curve for six Al standard additions (800-0 nM), the coefficient of regression indicating an (R^2 = 0.99) when using the Al-O protocol sequence.

Table 4.3: Results indicating clearer discrepancies in peak heights when analysing with Al-F (Table 4.2), however, exhibiting a higher RSD of more than 10 for Al-O.

Deionised water						
Conc nM	Peak Height (counts)	Baseline value	STDEV	%rsd	Replicate	Sequence name
800	8500	248000	453	5	8	Al-O
600	6600	250000	260	4	12	Al-O
400	4000	254000	325	8	10	Al-O
200	1900	252000	370	19	10	Al-O
100	1600	249000	355	22	10	Al-O
0	910	255000	344	38	11	Al-O

4.4 Matrix effect: Method validation for seawater using the Al-O sequence

Compared to fresh water, seawater contains high salt and ionic matrix, which can have a profound impact on the reaction chemistry, such as the formation of the Al-LMG complex as well as fluorescence signal from additional metals that could form a complex with LMG. In order to assess possibility of direct analysis of seawater using the miniSIA-2, the batch method was used to give a clear representation of how ionic interferences within a high salt matrix can impact peak configurations.

As in previous sections, Al_d standards of known concentration (800, 600, 400, 200, 100, and 0 nM) were prepared in seawater from the spring SCALE expedition (see section 3.1) and analysed by the Al-O sequence (Figure 4.6). The peaks occurred between 4 and 9 seconds, as was the case for deionised water (Figure 4.5; Table 4.3). However, the peak shape was that of a sharp peak (6-7 seconds), with somewhat fluctuating background values on either side of the peak. Furthermore, a small offset “peak” is observed at 3-4 seconds and also peaks forming below the instrumental background value for samples having concentration of 100 nM and the Blank. Given that below baseline signal is only evident at concentrations below 100 nM, interference from matrix or complexation of Al other than forming Al-LMG complex cannot be ruled out.

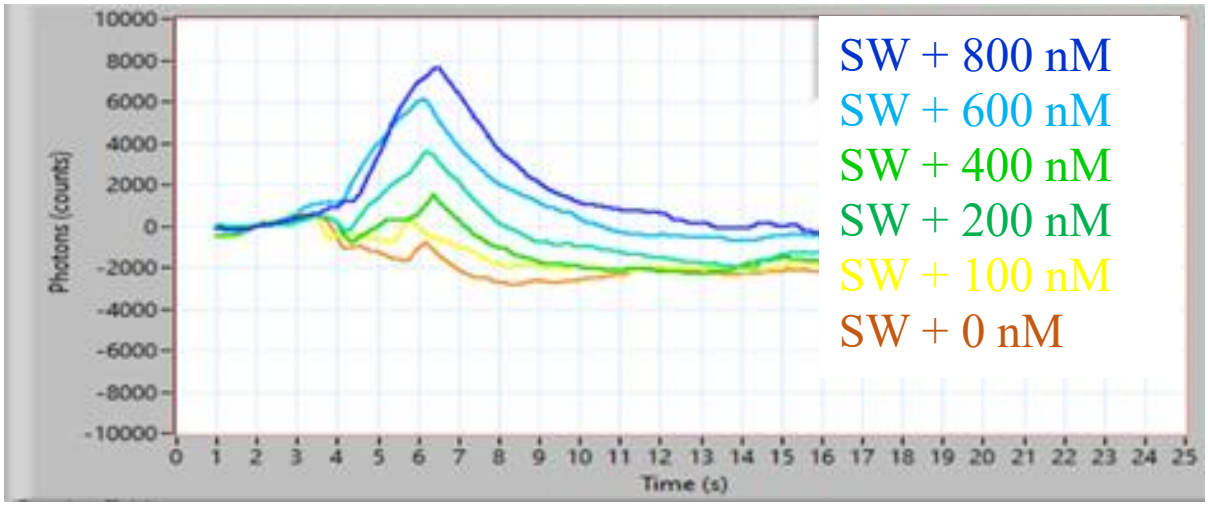

Figure 4.6: The sharp pointed tailing peak shape for Al standard additions nM (800-0) in a seawater matrix, with an offset peak at 3-4 seconds.

The tailing peak shape with a fluctuating background (Figure 4.6), is a clear indication of ionic interference with Al which is caused by partial dissociation of the chelate complex and in turn distorting the fluctuating background signal of the descending peak. In addition to this, the small offset "peak, observed at the 3-4 seconds interval" likely represents ions (eg Fe, Ga, F^-) other than Al that can form a chelate complex with LMG (Nishikawa et al., 1967; Ren et al., 2001). Although, the interfering chelate emitted only a weak fluorescence signal. Furthermore, given that the "actual" peaks form at a retention time of 6-7 seconds, it is possible that the additional "peak" could be giving a false peak height value for the lower concentration range (100 and 0 nM), as the "actual" peak falls below the instrumental background**.** This would also explain, in part, the high RSD value (>20) for the 100 and 0 nM samples (Table 4.4).

Despite the artifacts, the calibration curve shows a better linear fit (R^2 = 0.97) even with the seawater matrix (Figure 4.7). The curve also displays the method to be better sensitive thereby further improving the LOD to be at 51 nM.

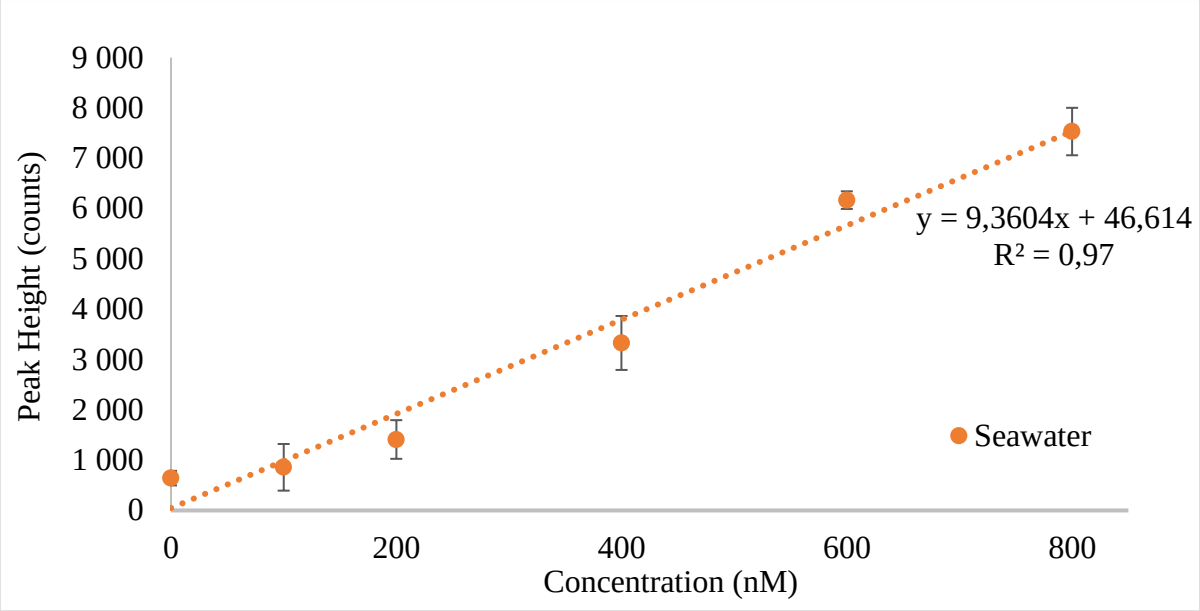

Figure 4.7: The calibration curve (R^2 = 0.97) of Al standard additions (800-0) in seawater using a 0.2% LMG work solution and run by the Al-O protocol sequence.

Table 4.4: Results indicating stable baseline values with a clear discrepancy in peak heights, however, with an relatively high RSD for the lower concentration range.

Seawater						
Conc nM	Peak Height (counts)	Baseline value	STDEV	%rsd	Replicate	Sequence name
800	7530	215000	471	6	9	Al-O
600	6170	207000	175	3	9	Al-O
400	3330	214000	536	16	10	Al-O
200	1410	213000	384	27	15	Al-O
100	858	212000	464	54	12	Al-O
0	643	219000	145	23	8	Al-O

When comparing the seawater (Figure 4.7) and the deionised water (Figure 4.5) profiles, no significant difference between the two matrices could be ascertained except for the y-intercept for seawater curve showing a 10 times lower peak height compared to the deionised water. Furthermore, some matrix effect in seawater cannot be ruled out. In a similar study using a similar manifold design to that of the miniSIA-2, while measuring the concentration of Fe in seawater, Hatta et al., (2018) concluded that salinity contributes to a minor offset of the calibration slopes. However, we find this offset to be more pronounced in the peak shape profile for seawater when measuring Al_d (Figure 4.7). This further highlights the importance of

studying both the calibration slope and the peak configuration, to ensure that no false peak values are measured from weak interfering chelates complexes.

4.5 Improving method sensitivity: Addition of Brij-35 solution to seawater

Even though, the measurements in seawater matrix gave a significantly lower LOD (51 nM) (Figure 4.7) than that for the deionised water (115 nM) (Figure 4.5), further improvements are necessary in order to measure Al_d in seawater where average global seawater concentration is in the order of 15 nM (Barraqueta et al., 2020). Thus, a further experiment was conducted for improving the sensitivity of the fluorescent chelate through the addition of a brij-35 solution.

A 50 µL of a 5% non-ionic brij-35 solution was added to the Al standards (800, 600, 400, 200, 100 and 0 nM) prepared as before in a seawater matrix. The brij-35 was added to the standards heated at 80°C in a water bath after the formation of the Al-LMG chelate complex.The addition of the brij-35 after the Al-LMG chelate formation changed the previously observed sharp pointed peak shape profile of seawater (Figure 4.6) to a smooth Gaussian curve, especially for the higher concentration range (800-400 nM) (Figure 4.8). However, like with other cases above, the lower concentration range (200-0 nM) indicated smaller peaks with a fluctuating background signal, with the peak signals forming below the instrumental background and a small offset peak at 3-4 seconds.

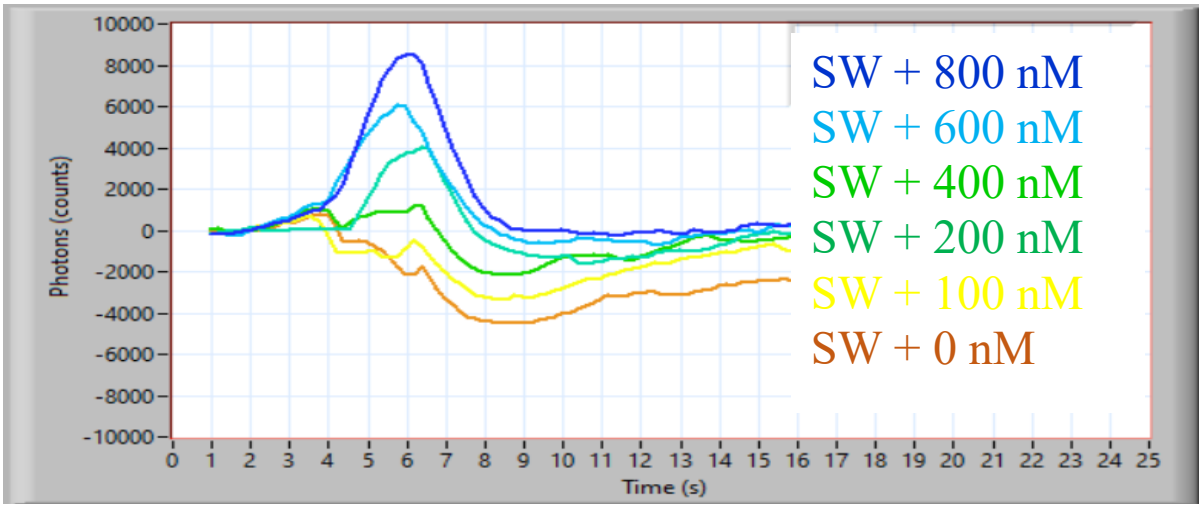

Figure 4.8: The partially gaussian peak shape profile for the addition of a brij-35 solution to Al standard additions in seawater using a 0.2% LMG work solution. A small offset peak can be seen at 3-4 seconds.

These gaussian peaks indicate a stable matrix and minimal interference from ions such as Fe, Ga and F- in the formation of the Al-LMG chelate complex and that the addition of brij-35 did not have an adverse impact (Abdeldaim & Mansour, 2018). The peak configuration descended back to the background level for the higher concentration range (800-200 nM) further indicating the formation of stable chelate complexes and that any interferences from ions within the seawater matrix, which was evident in Figure 4.6, have mostly been eliminated.

The data obtained from the curves (Table 4.5) was once again used to plot a calibration curve with a linear fit (Figure 4.9). The average peak height is the average of 6 peak height replicates, except for the blank which was derived from 5 peaks. The RSD for the higher range (>400 nM) was less than 16 but for the lower range (200 – 100 nM) the RSD was 20-28. The baseline values were stable throughout the experiment and ranged between 208000-215000 (Table 4.5).

Table 4.5: Results showing a stable baseline value with a clear discrepancy in peak height values and a lower RSD then without the addition of the brij-35 (Table 4.4).

Brij-35 addition to Al standard additions in seawater						
Conc nM	Peak Height (counts)	Baseline value	STDEV	%rsd	Replicate	Sequence Name
800	8780	209000	929	11	6	Al-O
600	6360	208000	494	8	6	Al-O
400	4250	209000	667	16	6	Al-O
200	1340	211000	270	20	7	Al-O
100	630	209000	176	28	7	Al-O
0	778	215000	28	4	5	Al-O

Figure 4.9 below shows the linearity plot of the Al standards additions with brij-35 addition. It is clear that the addition of the brij-35 contributed to an increased sensitivity (Abdeldaim & Mansour, 2018), which allowed for lowering of the LOD from 51 nM (Figure 4.6) to 9 nM (Figure 4.8).

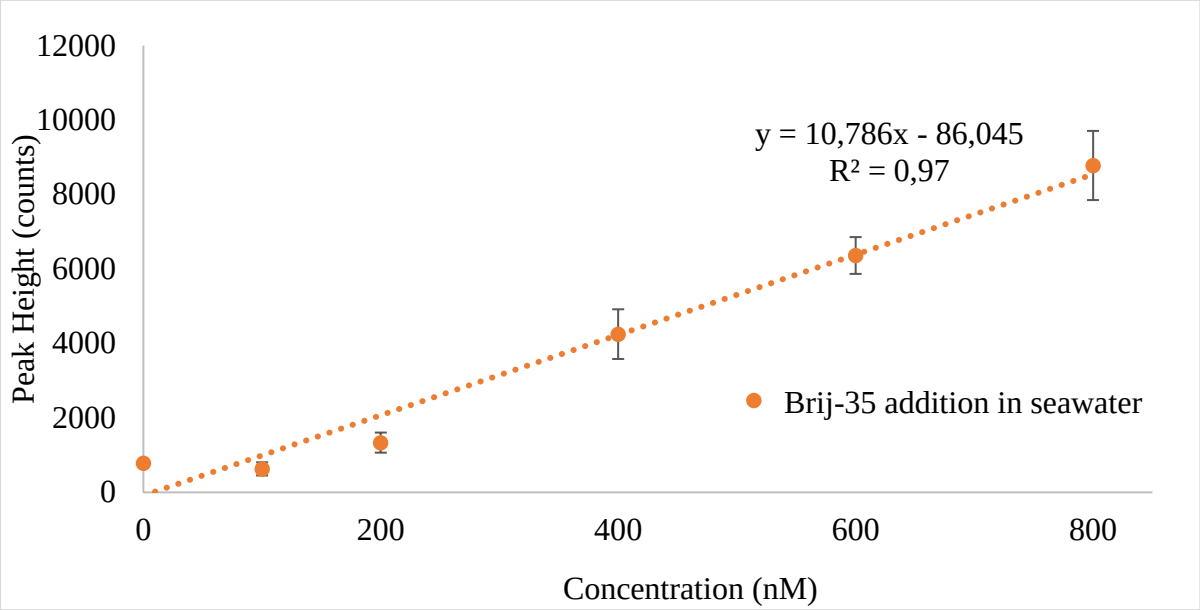

Figure 4.9: A linearity study (R^2 = 0.97) of the addition of a brij-35 to Al standard additions in a seawater matrix using a 0.2% LMG solution and analysed by the Al-O sequence.

Although the obtained LOD was well below the average seawater concentration, the peak configurations at low concentrations were still problematic. Smaller peaks were partially removed for the higher concentration range (800-400 nM). The smaller peaks observed around 3 to 4 seconds still persisted at the lower concentration range (200-0 nM) and the fluorescence signal was below the background. This suggests that brij-35 addition was not sufficient to optimize the proposed methodology for low-range Al concentrations. In order to get a better understanding of why Al_d was difficult to measure in this range, further method optimization focused on low-range Al standards (10 – 0 nM) and determining optimal conditions for relevant parameters e.g., excitation and emission wavelengths, fluorophore concentration and temperature to gain a better understanding.

Measurement of Al_d at low concentrations

The aim of the batch experiments involving lower concentrations of Al standards (10-0 nM) was to optimize relevant parameters in order to obtain a better and consistent peak shape profile and further improve the sensitivity. A further decrease in the LOD would support the idea of using this method in future for measuring in-situ Al_d in open ocean seawater onboard a ship. As seen by the previous experiments, the miniSIA-2 was able to measure Al_d at a LOD of 9 nM for higher Al standard concentrations (800-400 nM). In oceans such as the Atlantic, Mediterranean and Arctic, the Al_d concentrations ranges between 54.9-12.3 nM making measurement applicable using this LOD. However, for oceans such as the SO, Pacific and the Indian required an instrumental LOD of 0.7 nM for Al_d. However, measurements in the lower concentration ranges 200-0 nM indicated minor contrast of peak heights and generally exhibited high RSD (Figures 4.7 & 4.9). These low discrepancies in the lower concentration range could be a result of possible fluorescence error.

Results from a study conducted by Gomes et al., (2018), focussed on possible fluorescence measurement errors and determined these to be caused by either the excitation wavelength being out of range, concentration of the fluorophore, temperature, the solvent or contamination. Parameters such as contamination and solvent errors could be eliminated for these experiments. This is because the experiments were performed in a class 100 laboratory using deionised water or seawater as a solvent, and vials/containers were thoroughly acid washed to prevent contamination.

Therefore to understand the possible sources of error and to enhance the signal intensity, especially when working with the lower end concentrations. Required analysing the three remaining experimental parameters relevant when optimizing the Al method on a new instrument, these parameters are 1) excitation and emission wavelength's, 2) Fluorophore concentration and 3) temperature. Focusing on the lower concentration of Al standards, the aim of the batch experiments was to optimize relevant parameters to obtain a better and consistent peak for Al solutions <20 nM. This subsequently results in a low LOD, which would support the idea of using the method for measuring Al concentrations on a shipboard environment during remote maritime expeditions to the SO.

This section will highlight the drawbacks and possible difficulties while analysing at a lower concentration range, which would further help identify possible factors that need to be accounted, such as placing an opaque box over the manifold and regulating the temperature of the miniSIA-2.

4.6 Excitation and emission wavelengths

4.6.1 Tecan Spark 10M multimode microplate reader

The first possible source of error for the low signal intensity when measuring within the lower fluorescent range (<200 nM), could be attributed to the excitation and emission wavelength's being out of range. As prior measurements on the miniSIA-2 indicated a fluctuation of the baseline values and a high RSD for concentrations less than 200 nM in seawater (Figures 4.2, 4.6 & 4.8).

The miniSIA-2 comes with a custom build-on module with predetermined wavelengths (λ_{ex} = 470 nm & λ_{em} = 560 nm). For wavelength adjustments, the entire module must be replaced with a new one with a new set of wavelengths. Therefore, instead of adjusting the module of the miniSIA-2 rather determine if indeed the fluorescence of the Al-LMG complex is being read at the optimal wavelength setting for the lower concentration range using a 0.2% LMG work solution. Thus, in a separate batch experiment an extensive λ_{ex} and λ_{em} scan was performed using a different equipment (Tecan Spark 10M multimode microplate reader) for 89 nM Al sample and a blank. The blank and 89 nM standard was prepared in deionised water matrix by adding a 0.2% LMG working solution and buffering the samples to a pH of 5.48. Figure 4.10, represents the scanned λ_{ex} and λ_{em} for 1) deionised water and a 2) 89.10 nM Al. The λ_{ex} and the λ_{em} wavelengths to which the miniSIA-2 are currently set are highlighted in red and outlined by a black box.

The λ_{ex} scan starting from 440 nm and ending at 500 nm and the λ_{em} scan from 540 nm to 600 nm, respectively (Figure 4.10). The λ_{ex} and λ_{em} to which the miniSIA-2 monochromators are set gave a peak height of 375 for deionised water and 15699 for the 89.10 nM Al sample at an λ_{ex} of 470 nm. The λ_{em} of 560 nm gave a peak height of 628 for deionised water and 14947 for the 89.10 nM Al sample. The λ_{yield} (Column 3) was calculated by subtracting the 89.10 nM Al sample (Column 2) from the deionised (Column 1). The λ_{yield} indicates the optimal λ, at which

the Al-LMG should be measured under the predefined conditions, and after eliminating the matrix. The λ_{yield} for the 89.10 nM standard was 15324 at λ_{ex} (470 nm) and 14319 at λ_{em} (560 nm). The highest λ_{yield} during the scan; however, was observed at λ_{ex} of 492 nm (20855) and λ_{em} of 596 nm (24362) (indicated in bold and outlined by a black box).

λex	1	2	3	λem	1	2	3
440	70	6352	6282	540	514	5705	5191
442	78	6765	6687	542	578	6646	6068
444	74	7255	7181	544	618	7416	6798
446	75	7814	7739	546	660	8425	7765
448	71	8244	8173	548	666	9253	8587
450	72	8612	8540	550	715	10258	9543
452	82	9233	9151	552	691	10950	10259
454	93	9829	9736	554	686	12080	11394
456	109	10291	10182	556	691	13014	12323
458	120	11016	10896	558	653	13878	13225
460	151	11433	11282	560	628	14947	14319
462	191	12268	12077	562	614	15820	15206
464	223	13191	12968	564	571	16639	16068
466	278	13798	13520	566	522	17653	17131
468	332	14699	14367	568	477	18416	17939
470	375	**15699**	15324	**570**	432	19084	18652
472	434	16609	16175	572	384	20002	19618
474	424	17199	16775	574	343	20586	20243
476	483	18252	17769	576	303	21001	20698
478	456	18945	18489	578	258	21711	21453
480	476	19187	18711	580	226	22162	21936
482	475	19809	19334	582	176	22792	22616
484	479	20211	19732	584	153	23047	22894
486	416	20468	20052	586	129	23571	23442
488	394	21058	20664	588	106	23503	23397
490	365	20981	20616	590	85	24100	24015
492	**295**	**21150**	**20855**	592	75	24107	24032
494	299	21097	20798	594	62	24039	23977
496	220	20581	20361	596	**51**	**24413**	**24362**
498	173	20864	20691	598	49	24305	24256
500	162	20851	20689	600	38	24069	24031

Figure 4.10: The λ_{ex} and λ_{em} scan of a (1) blank, an (2) 89.10 nM and (3) calculated λ_{yield} of Al standard samples analysed using a Tecan Spark 10M multimode microplate reader. The Al standard samples were buffered to a pH = 5.28 with a 0.2% LMG work solution. The fixed λ_{ex} and λ_{em} to which the miniSIA-2 is set (λ_{ex} = 470 & λ_{em} = 560 nm) is highlighted in red and outlined by a black box. The optimal λ_{ex} and λ_{em} is indicated by the highest λ_{yield} at an λ_{ex} of 492 nm and an λ_{em} of 596 nm (highlighted bold and outlined by a black box).

These wavelengths (λ_{ex} = 492 nm & λ_{em} = 596 nm) fall within the optimal range (λ_{ex} 500 nm and λ_{em} 590) at which LMG forms a fluorescent chelate complex with Al (Mendecki et al., 2020). In contrast the λ_{ex} and λ_{em} of the miniSIA-2 are set to a λ_{ex} = 470 nm and λ_{em} = 560 nm respectively, where the λ_{yield} for the proposed sample procedure are not within the optimal wavelength range for detecting the fluorescence of the Al-LMG chelate complex. Clearly, there is a need for adjustment of set wavelengths on miniSIA-2. However, this would require customizing a new set module with a new set of predetermined wavelengths. Instead further experiments were conducted for adjustment of other parameters (fluorophore concentration and temperature) and adjust the sample preparation to investigate alternative means to maximize the Al yield to suit the set wavelengths (470 nm and 560 nm) of the miniSIA-2.

4.7 Impact of Fluorophore concentration

The second possible source of error is the fluorophore concentration. Therefore, the first adjustment to the method was testing for the correct LMG concentration. Initially low concentration standards (50-0 nM) with usual 0.2% LMG working solution in deionized water matrix were run at room temperature (18-19°C) on the miniSIA-2. The average peak height was calculated for more than 10 repetitive samples. The RSD were below 6%, with the exception of the blank, which had a RSD of 22% (Table 4.6).

Table 4.6: Results showing saturated peak height values for the concentration range 50-5 nM, accompanied by a low RSD and stable baseline value.

Al standard concentrations in deionised water						
Conc nM	Peak Height (counts)	Baseline value	STDEV	%rsd	Replicate samples	Sequence Name
50	26000	586000	836	3	14	Al-O
35	26800	582000	547	2	14	Al-O
25	26500	601000	772	3	17	Al-O
10	27700	607000	1507	5	16	Al-O
5	28900	609000	778	3	19	Al-O
0	4960	600000	1108	22	11	Al-O

There was a clear separation in the peak height for the blank to the peak heights for the remainder of the standard samples. For the standards containing Al (50-5 nM), the separation in signal was not so evident among themselves resulting in a small variation in average peak height (Table 4.6, Figure 4.11). The baseline value was relatively constant (± 600000 counts),

exhibiting a slight fluctuation of ±0.14 for the 35 nM and 50 nM standard (Table 4.6). Overall, the peak shape profile (Figure 4.11) suggests that the fluorescence signal is saturated at all tested Al_d concentration.

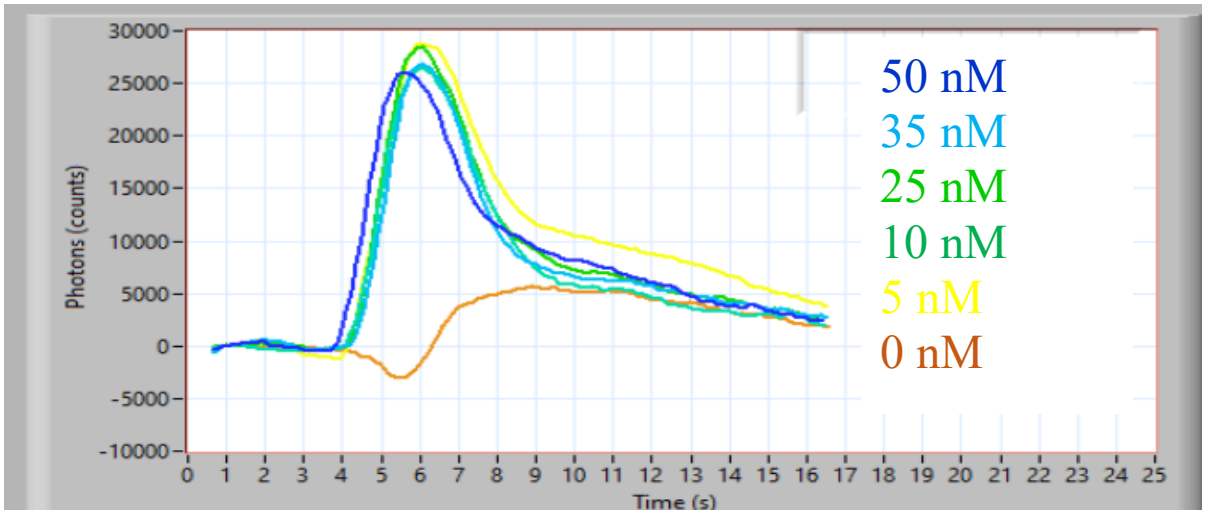

Figure 4.11: The peak shape profile of running a 0.2% LMG work solution using the miniSIA-2 as a detector for the lower end concentrations (50-0 nM). The peak shape indicates a saturated peak height, with the exception of the blank.

Given the lack of a difference in peak heights, there was no significant correlation ($R^2 = 0.17$) (Figure 4.12). The lack of a difference in peak height also suggests that the signal is saturated. It is possible that the added fluorophore concentration is in excess to the Al_d present in the standards. In other words, the fluorescence from uncomplexed lumogalliun is overpowering the signal from Al-LMG complex.

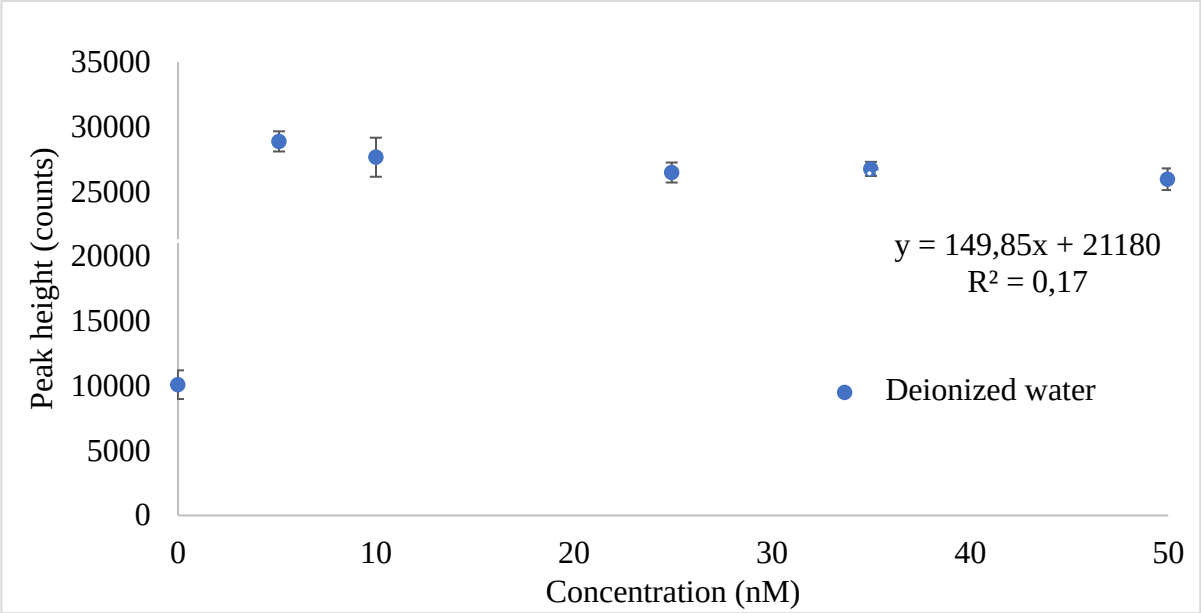

Figure 4.12: The saturated linearity study of low Al standard additions (50-0 nM) in deionized water with a 0.2% LMG work solution. The average peak height values indicated a relatively constant values for the concentration range of 50 nM to 0 nM, however, with the exception of the blank which showed a lower peak height of 4960 counts.

According to Gomes et al., (2019), this type of saturation could also be a form of quenching experienced by the fluorescent in the excited state, which in turn could explain the low RSD values. In other words the high fluorescence concentration is masking the lower concentrations from being detected. Thus, another experiment was conducted using the Tecan Spark 10M multimode microplate reader to test if the concentration of LMG indeed impacts the fluorescence signal at low Al_d concentrations.

Low-range Al standards (10-0 nM) in seawater were treated separately with two LMG working solutions (0.2% and 0.02%) and tested using the Tecan Spark 10M multimode microplate reader. The experiment was run by setting the instrument to the same wavelengths to that of the miniSIA-2. The experimental conditions were as follows: Temperature = 25ºC, λ_{ex} = 470 nm, with an excitation bandwidth = 20 nm, λ_{em} = 570 nm, and an excitation bandwidth of 20 nm. Observed peak heights were used to plot the calibration curves for the two sets (Figure 4.13). A better fit (R^2 = 0.96) was obtained at lower fluorophore concentration (0.02%) compared to when standard solutions were treated with 0.2% LMG solution (R^2 = 0.72).

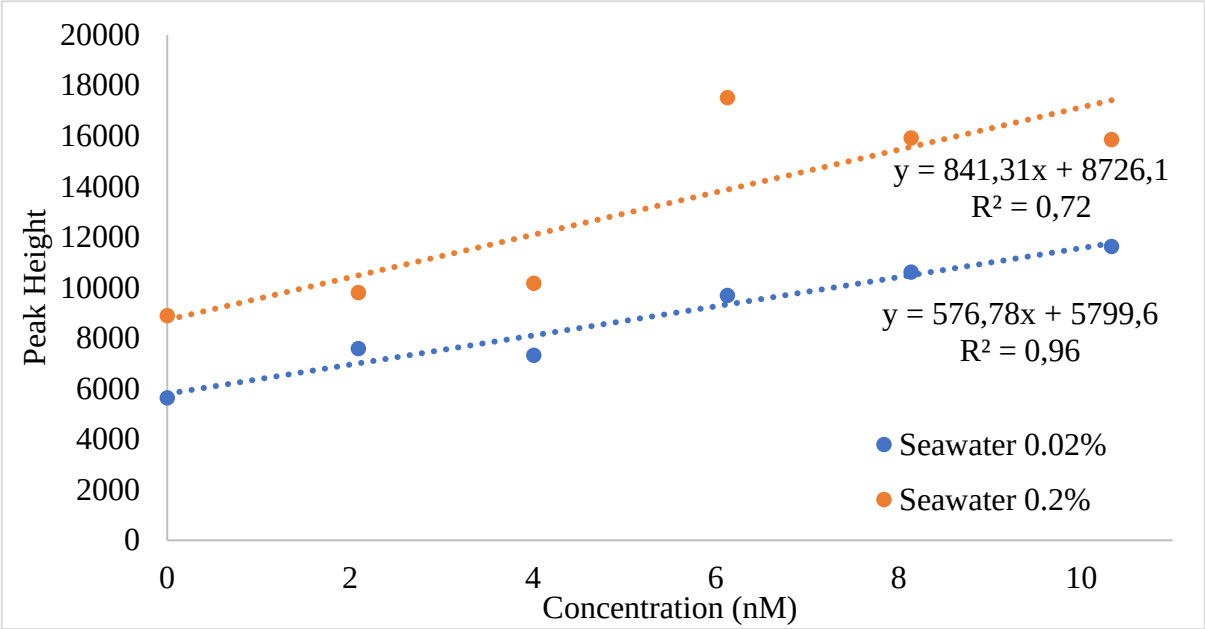

Figure 4.13: The calibration curves of low concentration (10-0 nM) Al standard additions in seawater (with 0.02% (blue dot) and 0.2% (orange dot) LMG work solution. The experiment was analysed by a Tecan Spark 10M multimode microplate reader. The wavelength's were set to an λ_{ex} = 470 nm & λ_{em} = 570 nm, with a bandwidth of 20 nm and the temperature set to 25ºC.

A possible reason for the substantial increase in R^2 from 0.72 to 0.96 is due to the fact that LMG is in excess (0.2% LMG work solution) in comparison to the lower Al concentration (10-0 nM). Therefore making the uncomplexed LMG more prone to absorption than the chelate complex itself (Hydes and Liss., 1976). Thus making measurement of lower concentrations more favourable with a LMG work solution of 0.02%.

By lowering the LMG concentration to 0.02%, and running the experiment in deionized water with a low concentration (10-0 nM) at room temperature (18-19°C) and using the miniSIA-2 as the detector. Indicated a subtle increase in peak height values, with the exception of 8 nM (outlier) and a stable baseline value. The RSD ranged from 16 and 17 for the concentrations 0 to 2 nM and less than 11 for the remaining concentrations (Table 4.7).

Table 4.7: Results showing stable baseline with high RSD values (>10) and a subtle increase in peak height values.

Al standard concentration in deionised water						
Conc nM	Peak Height (counts)	Baseline value	STDEV	%RSD	Replicate samples	Sequence name
9.85	5380	546000	548	10	16	Al-O
7.92	**4890**	**544000**	**584**	**12**	**16**	**Al-O**
6.05	5310	545000	561	11	16	Al-O
3.95	5270	538000	402	8	15	Al-O
2.16	5160	544000	899	17	18	Al-O
0	4810	542000	756	16	17	Al-O

A calibration curve was plotted from the peak height values (Table 4.7) and an coefficient regression of $R^2 = 0.75$ was obtained. Suggesting that the 0.2% LMG was indeed masking the lower signal from being detected (Figure 4.12).

However, when focused represented a curvilinear profile (Figure 4.15). The curvilinear profile suggests a stable chelate complex, indicating that the lower concentrations can be measured with the sample preparations employed. However, that the samples were susceptible to experiencing a form of quenching during the analysis.

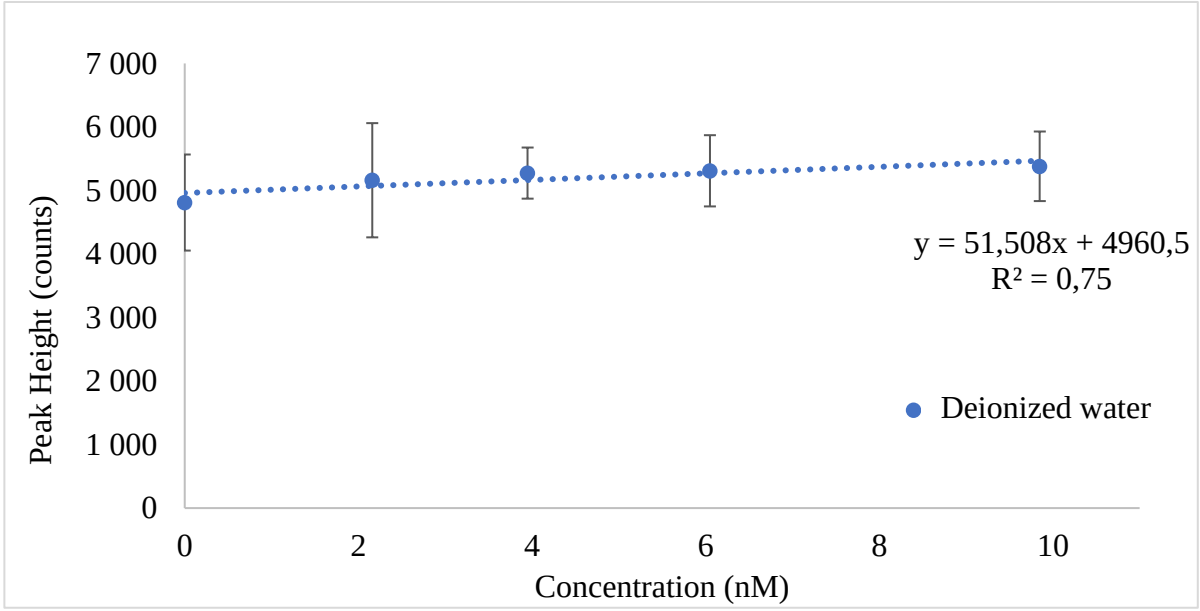

Figure 4.14: The linear plot showing a partially linear standard addition for low concentration samples (10-0 nM) in deionized water using a 0.02% LMG work solution.

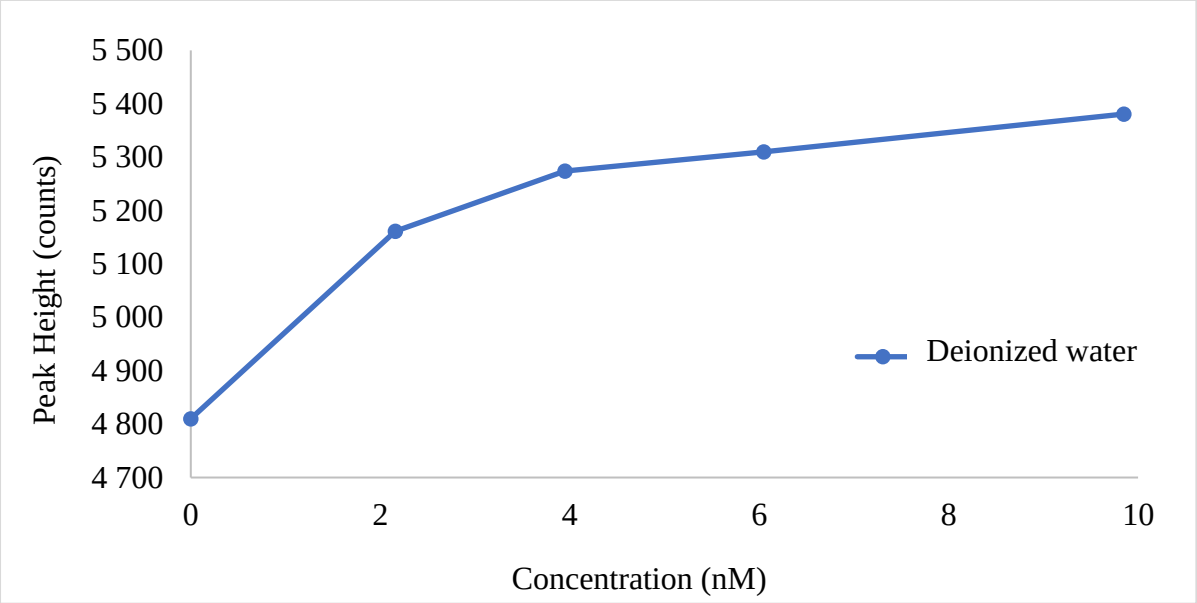

Figure 4.15: The focused linear plot of Figure 4.14. The figure indicates a curvilinear configuration, which may indicate a form of quenching.

Further evidence of quenching can be seen by the peak profile (Figure 4.16). As the peak height represents a weak shape profile with a dip at 4 to 6 seconds. Suggesting that the weak shape profile indicates a weak chelate complex (high RSD value of more than 10) that underwent rapid dissociation. Another explanation could be that the curvilinear profile and the weak peak shape profile could be caused by a short-term light exposure from the surrounding lab or internal temperature fluctuations within the sample chamber of the miniSIA-2.

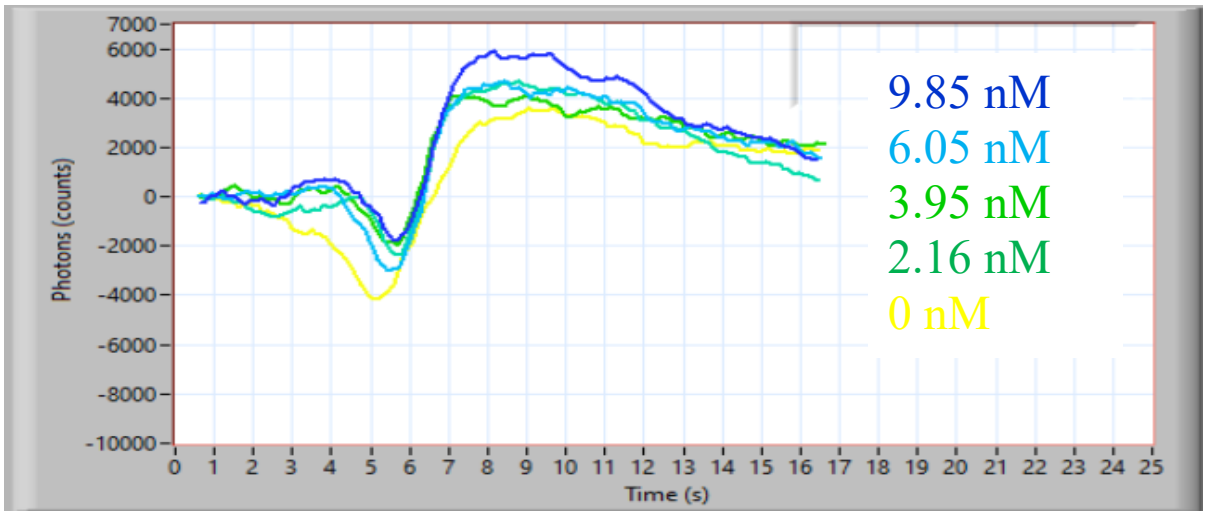

Figure 4.16: The weak peak shape profile of deionized water, indicating a dip at 4 to 6 seconds. This type of configuration is an indication of quenching experienced for the samples during the analysis.

By running the samples in a seawater matrix will further determine whether the short-term exposure to light from the laboratory environment or the fluctuations in temperature inside the miniSIA-2 sample chamber affect the standard samples. As before, the experiment was conducted at room temperature (18-19°C), with a 0.02% LMG solution and replicated more than 18 times. The average peak height was calculated for more than 10 repetitive samples. The RSD were below 7% for all the samples. (Table 4.8).

Table 4.8: Results showing fluctuating baseline baseline values with low RSD and an inverse concentration gradient.

Al standard concentrations in seawater						
Conc nM	Peak Height (counts)	Baseline Value	STDEV	%rsd	Replicate samples	Sequence Name
10.38	73700	495000	5230	7	15	Al-O
8.14	84900	514000	4370	5	17	Al-O
6.13	86400	497000	3562	4	15	Al-O
4.11	93000	502000	4163	4	15	Al-O
2.09	94900	491000	5227	6	18	Al-O
0	98600	507000	4846	5	16	Al-O

The data obtained (Table 4.8) was used to plot a calibration curve with a linear fit (Figure 4.17) The calibration plot indicated an inverse concentration gradient (R^2 = -0.93) with the highest peak representing the blank (98600 counts) and the lowest peak the 10.38 nM (73700 counts). The inverse concentration gradient could possibly be caused by a phenomena called photobleaching. Photobleaching is believed to occur when the fluorescent signal “fades” due to chemical changes of the fluorescent when exposed to excess light (Gomes et al., 2019). Although the samples were allowed to cool down in the dark, the analysis on the miniSIA-2 were performed while uncovered in the laboratory making samples susceptible to excess light exposure during analysis.

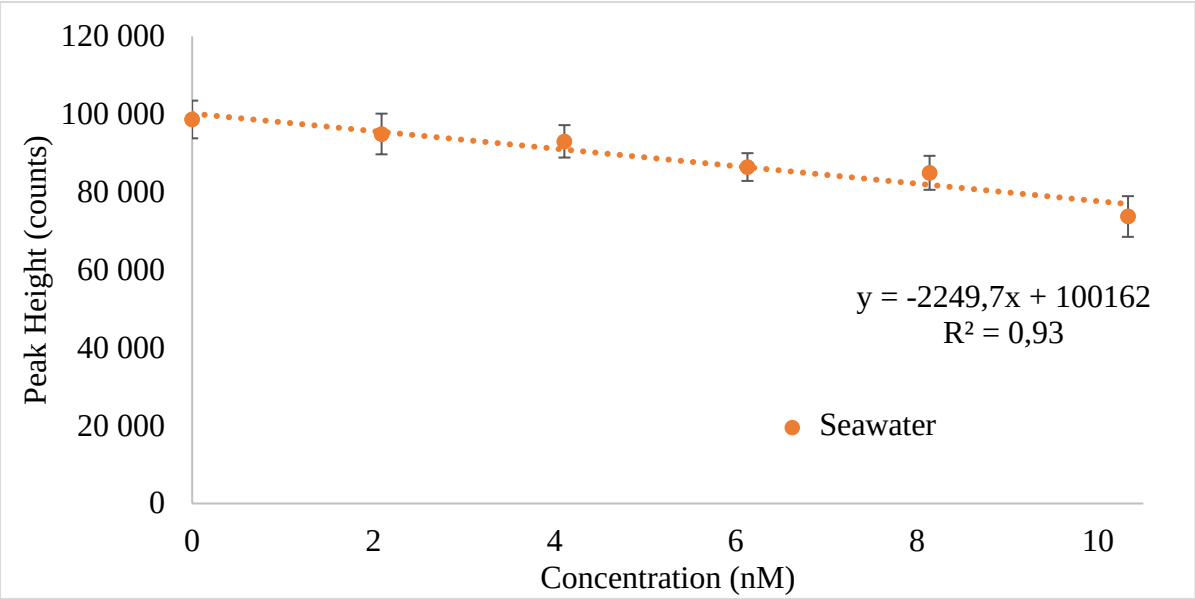

Figure 4.17: The calibration curve of low Al standard concentrations (10-0 nM) in seawater with the addition of a 0.02% LMG work solution at a manifold temperature of 18-19°C. The concentration gradient indicates an inverse gradient, with blank being the highest peak and 10.38 nM the lowest.

However, when looking at the peak shape profile of seawater (Figure 4.18) showed a stronger shape profile than the weak shape profile of deionized water (Figure 4.16). This indicates that the Al-LMG chelate complex in seawater are less susceptible to dissociation from excess light than those in deionized water, and that photobleaching contributes relatively little to the inverse concentration gradient of the seawater standard samples.

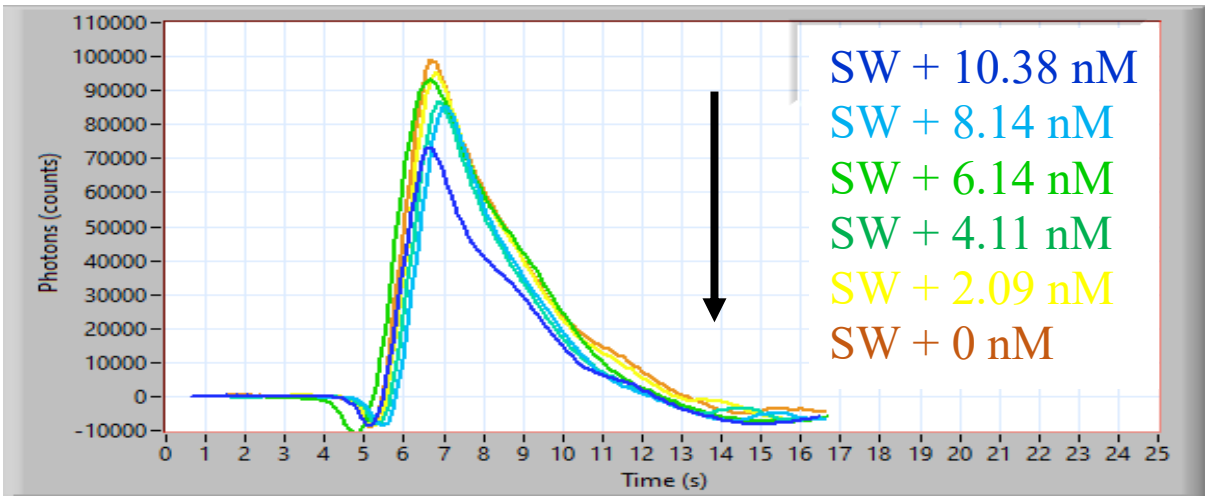

Figure 4.18: The peak shape profile in seawater. Indicating an inverse concentration gradient, with highest being the blank and the lowest concentration the 10.38 nM.

Instead the inverse concentration gradient can be associated to the fluctuations in temperature experienced inside the miniSIA-2 sample chamber during analysis. This is evident when comparing the baseline values and the RSD of the deionised (Table 4.7) and seawater matrix experiments (Figure 4.19 & Table 4.8). The baseline values for the seawater experiment (Figure 4.19), repetitively fluctuated from ±507000 to ±491000 throughout the experiment, although unnoticeable on the peak height profile (Figure 4.18). A contrasting observation is the high RSD (more than 16) and stable baseline value for the deionized water (Table 4.7) and the low RSD (less than 7), but fluctuating baseline value for the seawater (Table 4.8).

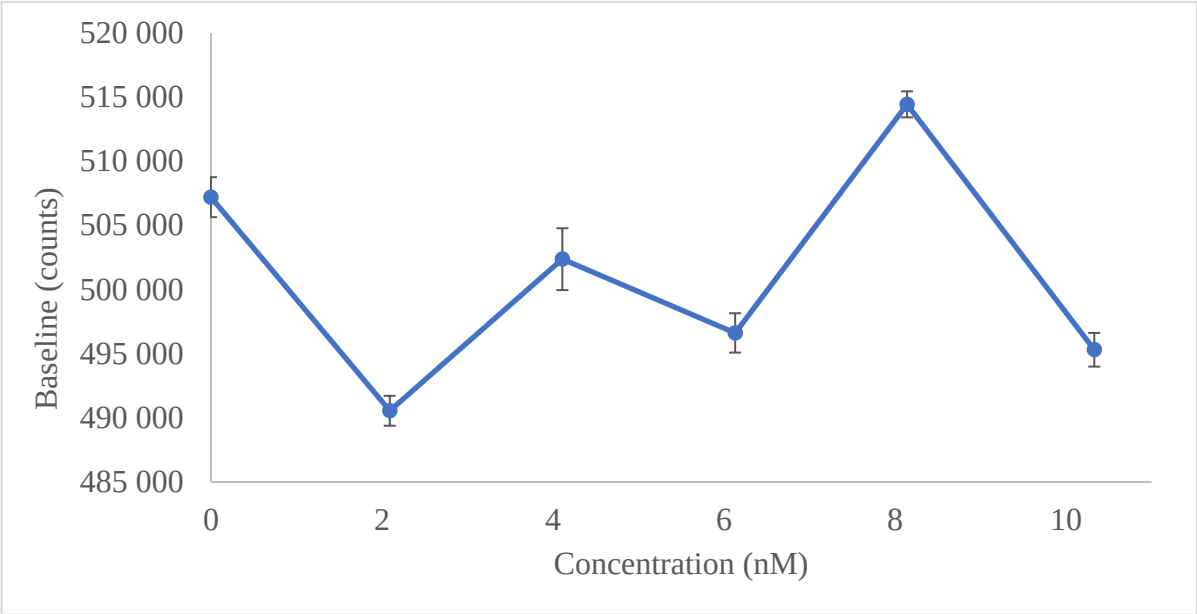

Figure 4.19: A graphical representation of the average baseline value at room temperature (18-19°C) indicating a fluctuated baseline value which is responding to changing internal temperatures.

The changing baseline values could also be an indication of fluctuations in temperature experienced within the miniSIA-2 during the analysis which the PMT voltage tries to regulate. This irregular temperature shows up in the graph through the fluctuating baseline values (Figure 4.19). This indicates that the experiment is temperature sensitive. The following two experiments were therefore conducted to confirm the temperature sensitivity of the measurement procedure. To determine the effect of temperature on the experiment, an opaque box was used over the miniSIA-2 for the remaining experiments to eliminate the effects of light exposure to the samples.

4.8 The effect of Temperature

As shown by the previous experiments (Figure 4.17, 4.18 and 4.19) temperature and light intensity are important aspects to consider when analysing Al_d in the lower end concentration range (10-0 nM). By increasing the temperature of the miniSIA-2 from room temperature (18-19°C) (Figure 4.18) to 25°C (Figure 4.20) ensures that the manifold is less susceptible to fluctuations in temperature experienced during the analysis. Therefore potentially minimizing temperature fluctuations which the PMT voltage tries to regulate.

This can be seen by running standard samples (10, 6, 4, 2, 0 nM), with the exception of 8 nM prepared in seawater as before. However, with the miniSIA-2 set to 25°C (Figure 4.20). By increasing the temperature of the manifold from 18-19°C to 25°C, changed the previously inverse concentration gradient (Figure 4.18) to that of a broad bell-shaped peak profile (Figure 4.20). However, with the peak height decreasing by more than 90% from that of room temperature. The profile further indicates a pronounced dip at a signal window between 3-7 seconds. Not previously as apparent with regards to room temperature. Therefore potentially indicating a slight dissociation of the Al-LMG chelate complex in response to increasing the temperature of the manifold.

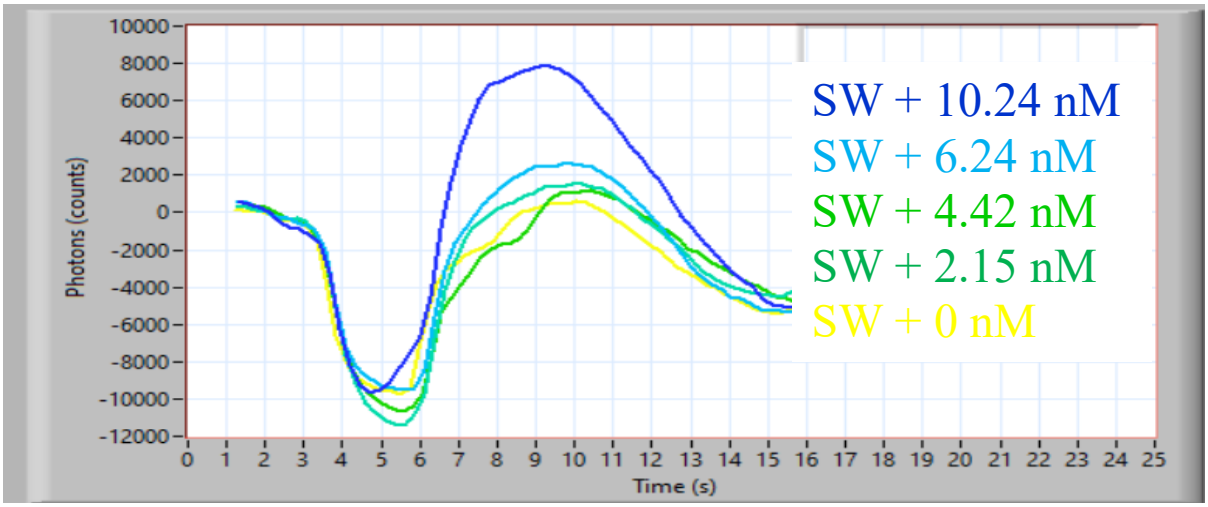

Figure 4.20: A broad-bell shaped peak profile and reduced peak height values, with a pronounced dip at 3-7 seconds were obtained for the analysis at a concentration range (10-0 nM) with the miniSIA-2 set to 25°C.

The slight dissociation of the Al-LMG chelate complex can be furthered explained by the high RSD (>45) values. With the RSD ranging between 45-85 due to increasing the temperature of the manifold (Table 4.9). The reason being is that the Al-LMG chelate complex has already

completed complexation and when slightly heated again, will encourage dissociation. Despite this, the average peak height (replicated > 10) indicates that only slight dissociation was observed. As the average peak height counts increased from 1260 counts (blank) to 5550 counts (10 nM). With the baseline value increasing steadily from 479000-503000 throughout the analysis time (Table 4.9).

Table 4.9: Results indicating an increase in peak height values, accompanied by a steady increase in baseline values with a high RSD (>45).

Al standard concentrations in seawater						
Conc nM	Peak Height (counts)	Baseline Value	STDEV	%rsd	Replicate samples	Sequence Name
10,24	5550	503000	4584	83	15	Al-O
8,35	**2560**	**501000**	**1833**	**85**	**17**	**Al-O**
6,24	2700	492000	1307	48	14	Al-O
4,42	1680	497000	998	59	15	Al-O
2,15	1480	484000	1005	68	15	Al-O
0	1260	479000	566	45	10	Al-O

Based on the average peak height values (Table 4.9) a calibration curve (Figure 4.21) with a linear fit was plotted (Figure 4.21). Despite, the partial dissociation of the complex (high RSD), the calibration curve shows an significant improvement in the analysis at 25°C. The coefficient of regression (R^2) improved from a negative R^2 = -0.93 (Figure 4.17) to a R^2 = 0.86, with a LOD of 4.45 nM for that of 25°C. Thus, indicating that stable manifold temperatures are crucial if Al_d is to be measured at such low concentrations.

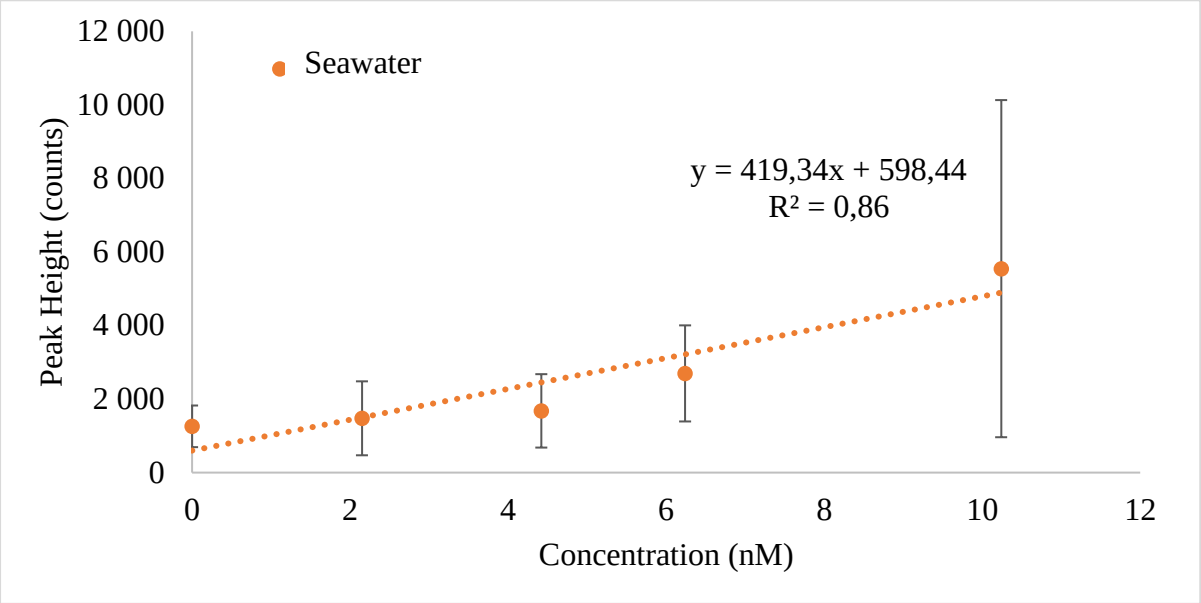

Figure 4.21: The calibration curve of low concentrations (10-0 nM) of Al standard additions in seawater with the addition of 0.02% LMG work solution and the miniSIA-2 set to 25°C.

The analysis, however, did not achieve complete stable temperatures as seen by the baseline values (Table 4.9). The baseline value as mentioned before indicates changing temperatures which the PMT voltage tries to regulate. Therefore, the increase in the manifold temperature with increasing standard analysis time can be seen by the steady increase in the baseline values from 479000 to 503000 counts (Figure 4.22; Table 4.9).

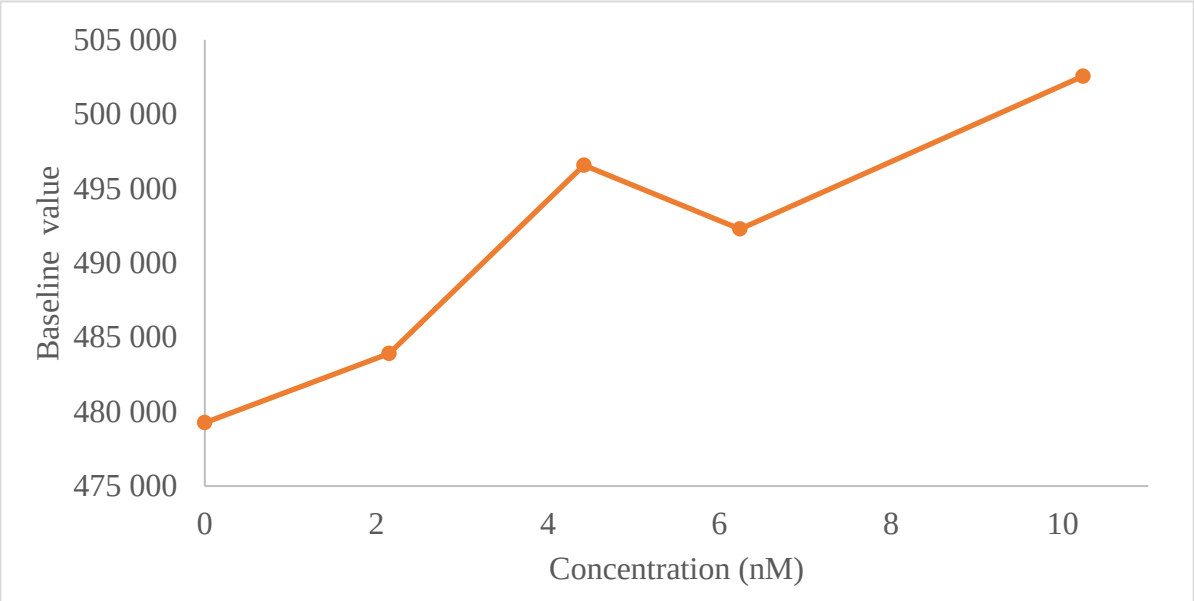

Figure 4.22: The steady increase in baseline values for low concentration standards (10-0 nM) run in seawater, with the temperature of the miniSIA-2 set at 25°C.

By increasing the manifold temperature to 25°C allows to achieve a more consistent temperature within the cell holder, which in turn decreases fluctuations in the baseline value. Instead, the baseline value increased steadily with increasing analysis time (Figure 4.22). The steady increase in the baseline value could be further the result of residual heat build-up over time, which in turn explains the partial dissociation of the chelate complex (high RSD). As the Al-LMG chelate complex is more susceptible to dissociation from the accumulation of residual heat build-up during analysis. This therefore seems to indicate that measuring the Al-LMG chelate complex at lower temperatures is more applicable to reducing the dissociation of the chelate complex (lowering the RSD) and further increasing the coefficient of regression (R^2) of the analysis.

Therefore, to limit fluctuations of self-regulation due to temperature changes (seen by the baseline values) of the miniSIA-2, the temperature of the miniSIA-2 was set at 21°C, a temperature low enough to reduce residual heat but higher than room temperature (18-19°C) to limit fluctuations of changing room temperatures. The experiment involved running the average of 6 repetitive standard additions of a concentration of (10, 8, 6, 4, 0 nM), with the exception of a 2 nM addition (outlier) in a seawater matrix. As previously the manifold was kept under an opaque box to prevent light from reaching the samples to limit any additional dissociation.

The peak shape for running the experiment at 21°C indicated a broad peak shape, with a dip in peak shape at 3-7 seconds (Figure 4.23) as seen previously for the 25°C experiment (Figure 4.20). However, with the peak height counts indicating a much clearer discrepancy among the 21°C than that of the 25°C. Therefore possibly indicating a lower dissociation of the Al-LMG chelate complex in response to temperature.

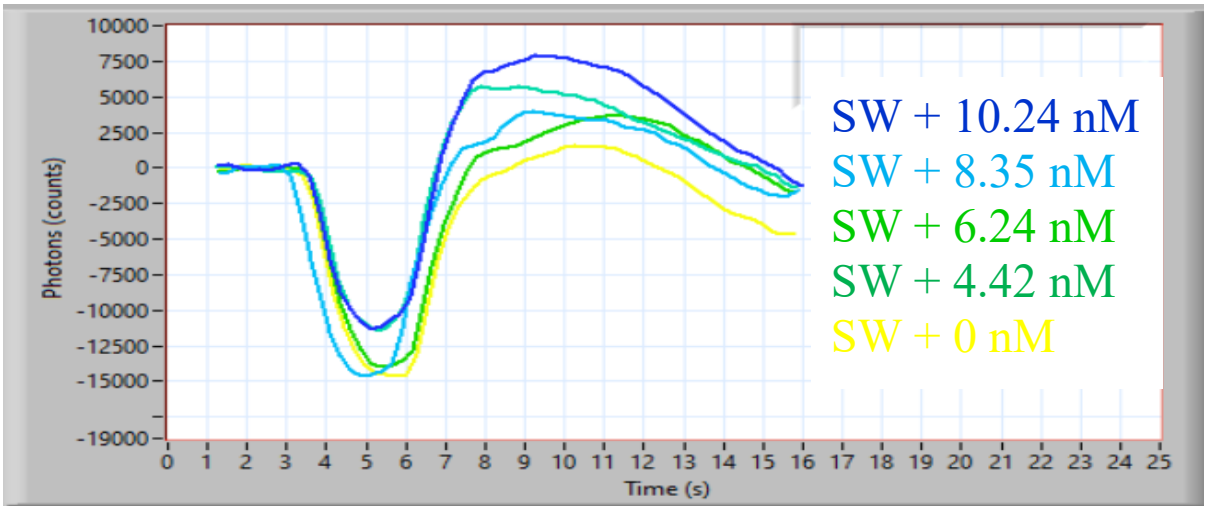

Figure 4.23: The Al standard addition in seawater with the addition the 0.02% LMG work solution indicating a broad shape.

The lower dissociation of the Al-LMG chelate complex can be further seen by the lower RSD values compared to that of 25°C. With the resulting RSD of the standards being greater than 50, with the exception of the blank. This indicates that a lower amount of residual heat was produced by the manifold during the analysis. The baseline values remained stable and fluctuated slightly between 497000 and 512000 throughout the experiment (Table 4.10).

Table 4.10: Results at an experimental temperature of 21ºC. The baseline values remained stable throughout the experiment.

Al standard concentrations in seawater						
Conc	Peak Height	Baseline value	STDEV	%rsd	Replicate sample	Sequence Name
10.24	5810	512000	1496	26	8	Al-O
8.35	5010	497000	2354	47	9	Al-O
6.24	4660	497000	2174	47	7	Al-O
4.42	3740	502000	1828	49	9	Al-O
2.15	**5480**	**496000**	**2631**	**48**	**8**	**Al-O**
0	2180	499000	779	99	6	Al-O

Derived from the peak heights of Table 4.10, a calibration curve was plotted and indicated a coefficient regression of R^2 of 0,99 and a LOD = 7 nM (Figure 4.24). By decreasing the temperature of the manifold from 25°C (Table 4.9) to 21°C (Table 4.10), the peak height increased slightly and the R^2 improved from 0.86 (Figure 4.21) to that of 0.99 (Figure 4.24). Indicating that the Al-LMG chelate complex is less susceptible to dissociation at lower and stable temperatures when compared to setting the manifold to that of room temperature (18-19°C) or 25°C. As a result, the experiment appears to be more stable.

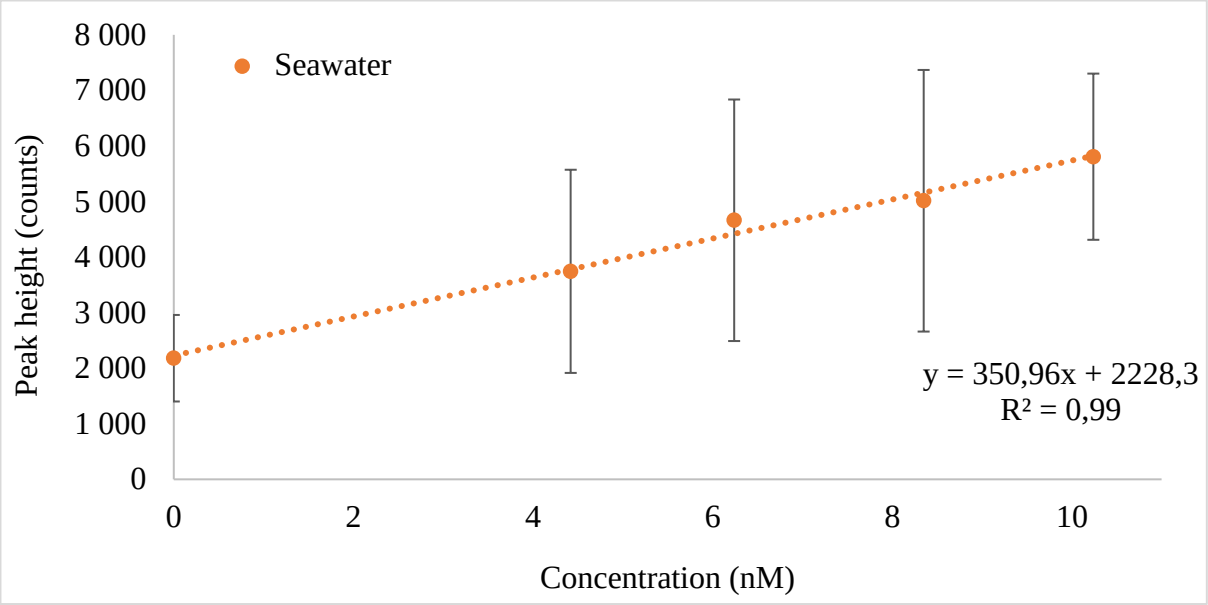

Figure 4.24: The calibration curve of Al standard additions (10-0 nM) in seawater achieving an R^2 = 0.99 and analysed at a set temperature of 21°C with the manifold covered by an opaque box to limit light.

Another indication of a stable experiment is the baseline values (Figure 4.25) which kept relatively stable and underwent minor fluctuations between 497000 and 512000 throughout the experiment. Indicating a lower amount of residual heat build-up and a lower Al-LMG chelate complex dissociation.

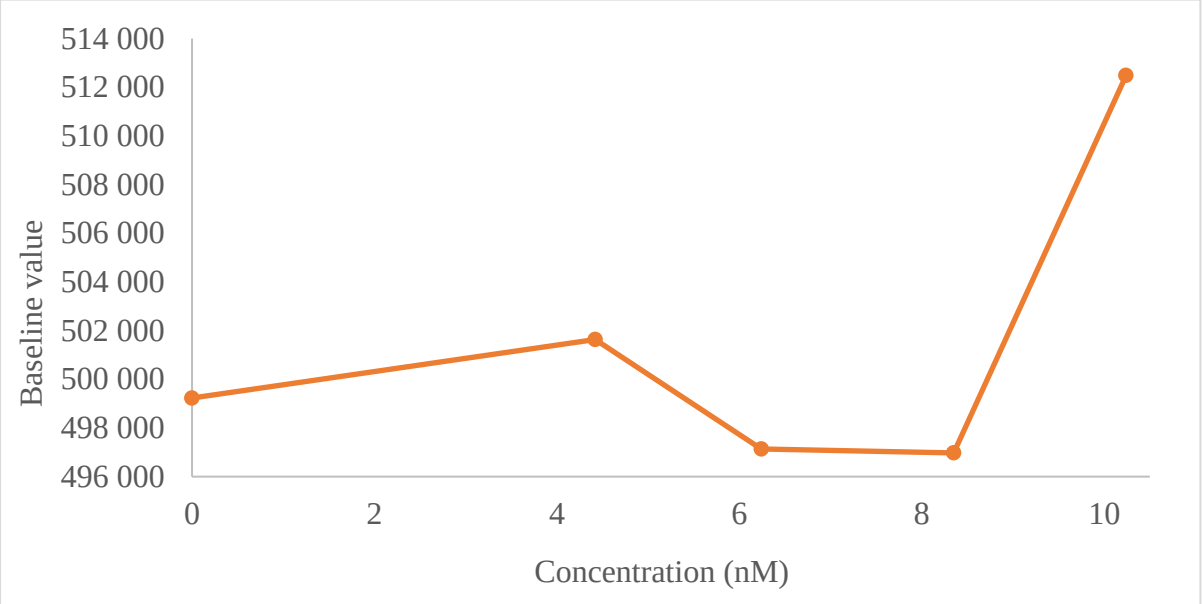

Figure 4.25: A graphical representation of the average baseline value at 21°C. The baseline values remained relatively stable throughout the analysis (496000-499000), with the exception of the 10 nM standard sample (512000).

Overall this experiment indicated that by keeping the temperature stable at 21°C, minimizing the light intensity reaching the samples during the analysis and reducing the LMG concentration to 0.02%, resulted in a stability in the linearity plot. Furthermore, analysing at 21°C kept the baseline value stable and reduced the RSD value significantly compared to that of 25°C. However, due to the high standard deviation of the blank, the lowest detection limit achieved was 7 nM Al in seawater. Which is sufficient enough to measure in oceans such as the Atlantic (19.8 -17.6 nM), Mediterranean (118-54.9 nM) and Arctic (12.3-6 nM), however, not sufficient enough to measure in the SO which requires an instrumental LOD of <0.7 nM of Al_d.

Chapter 5 Conclusion & Recommendations

This project's main aim was to establish a platform for future method development to determine the concentration of Al_d in seawater by a newly designed third generation flow analyzer (miniSIA-2). In this study, various parameters of samples prepared by the batch method were changed to determine the instrumental detection limit. These parameter changes made it possible to reduce the LOD from 242 to 7 nM. The current chapter summarizes the main findings of this study, the limitation of the measurement procedure and recommendations for future work.

5.1 Conclusions

The primary objective of this study was to develop and optimize the batch method to measure Al_d on a miniSIA-2. The first part of the analysis was to establish the Al-LMG chelate complex using the predefined sample preparation conditions in a high concentration range (800-100 nM). This experiment showed that the sample preparation for the higher concentration range was indeed adequate. Measuring samples with an Al concentration higher than 200 nM was easily achieved on the miniSIA-2 (R^2 = 0.97), with only limited interference. For concentrations with less than 200 nM Al, however, there were only minor discrepancies in their peak heights. This discrepancy was further improved by adjusting the aspiration and injected volumes of the protocol sequence. The lower volume sequence (Al-O) produced configurations with a smoother baseline and curve and in turn a smaller peak window. Matrix interference was negligible for deionised water, as was seen by the Gaussian peak shape produced. However, partial dissociation of the Al-LMG chelate complex was observed for the seawater matrix which produced a sharp pointed tailing peak and a weak chelate peak due to ionic interference. The addition of a Brij-35 solution to the seawater matrix changed the sharp, pointed tailing peaks to a gaussian peak for the higher concentrations. The lower concentration range did not exhibit these improvements and remained unaffected by the addition of the brij-35 solution. When analysing for the lower concentration range (10-0 nM), the excitation and emission wavelengths set for the miniSIA-2 were capable of measuring lower concentrations, however, required reducing the fluorophore concentration from 0.2% to 0.02% to prevent the effect of fluorescence masking. In addition, the concentration range was susceptible to fluctuating temperatures and changes in the PMT voltage, which was possibly due to the weak

Al-LMG chelate complex and the inability for the miniSIA-2 to regulate internal temperature during the experimental period. Therefore, the analysis required the addition of an opaque box and a stable manifold temperature, with 21°C exhibiting the best temperature for baseline stability and resulted in a R^2 of 0.99 and a LOD of 7 nM. Nevertheless, the batch method optimization gives a platform for future method progression to allow for a fully automated system to measuring Al_d,

5.2 Future recommendations

Several recommendations have been provided to improve the sensitivity of the "Batch method" analysis before incorporating the SHC and the SPE steps, as well as to adjust external features of the miniSIA-2 to facilitate easier analysis of Al_d. The first recommendation would be to set-up the instrument in a well ventilated, temperature controlled laboratory to facilitate with degassing and dissipate any residual heat produced by the manifold during an experimental run. Additionally, it's advised to choose a constant integration time and baseline value at the beginning of analysis. The second recommendation would be to build a customized opaque box, which contains ventilation holes and a cut out front section, with a temperature gauge. This will limit lifting the box and risking light exposure to the sample and reagents. The miniSIA-2 was shipped with PP vials, which are unfortunately not appropriate for trace Al determination, as they are believed to be manufactured by a Al co-catalyst and can therefore contribute significantly to additional Al contamination. In the meantime, acid-cleaned LDPE bottles and vials were attached to each sample or reagent port. If however, the instrument needs to be placed on a ship, attaching appropriate, well connected LDPE vials will be necessary. The bidirectional pumps are designed to run at high flow rates, but it's not advised to run them faster than 80 µL/s, as this can firstly cause O-ring slippage or grinding of the screw threads. Secondly, due to the column connected to port 5A, it cannot compensate for such a high flow rate and therefore will cause back pressure build-up.

With regards to improving the sensitivity of the analysis and possibly decrease the LOD even further by using the Batch method, would require preconcentrating the reagent (LMG) offline prior to adding to the samples which can be set-up, using a peristaltic pump. Considering that the reagent was not manufactured under trace clean conditions, therefore the reagent may be a significant contributor to contamination or ionic interference. This step can be further

optimized by incorporating another offline column for preconcentrating the samples and adding the preconcentrated LMG for reaction. In addition, to further achieve a lower blank, the Toyopearl resin should be replaced with a Nobias chelate resin, since Nobias chelate requires HNO_3 as an eluting acid instead of HCl, which in contrast is a weaker acid and therefore ensures lower instrumental blanks. Despite the fact that SPE only features in the later stages of the experimental protocol, the offline preconcentration steps will further investigate the detector's sensitivity and would represent the optimal conditions for maximum sensitivity of the miniSIA-2. In order to validate the adjusted batch method, an external fluorometer can be set up to the same wavelength as the miniSIA-2. This will make interpretation and comparing results easier, accurate and comparable. To improve the sensitivity even further collaborating with the engineers that designed the miniSIA-2 to incorporate an additional fan into the manifold to help with dissipating any residual heat build-up and modifying the excitation and emission module.

Following the optimization of the batch method, a preferable approach outlined by Hatta et al., (2018), is to start the second part of the method development (SHC) with high concentrations. Once the method is optimized for higher concentrations, the parameters are adjusted for lower concentrations. Finally, a great way of incorporating the brij-35 into the future fully automated flow scheme is by adding it directly into the carrier solution. This will leave port 1 open for online buffering of the sample.

References

1. Abdeldaim, D. & Mansour, F. 2018. Micelle-enhanced flow injection analysis. *Reviews in Analytical Chemistry*. 37(3).

2. Aldstadt, J., Olson, D., Wolcott, D., Marshall, G. & Stieg, S. 2006. Flow and Sequential Injection Analysis Techniques in Process Analysis. *Encyclopedia of Analytical Chemistry*. 1-24.

3. Alonso, A., Almendral, M., Porras, M., Curto, Y. & García de María, C. 2001. Flow-injection solvent extraction with and without phase separation. *Analytica Chimica Acta*. 447(1-2):211-217.

4. Anderson, R., Cheng, H., Edwards, R., Fleisher, M., Hayes, C., Huang, K., Kadko, D. & Lam, P. et al. 2016. How well can we quantify dust deposition to the ocean?. *Philosophical Transactions of the Royal Society A, Mathematical, Physical and Engineering Sciences*. 374(2081):20150285.

5. Brown, M. & Bruland, K. 2008. An improved flow-injection analysis method for the determination of dissolved aluminum in seawater. *Limnology and Oceanography, Methods*. 6(1):87-95.

6. Bruland, K. & Lohan, M. C. 2003. 6.02 – controls of trace metals in Seawater .*Treatise on Geochemistry* (Oxford, Pergamon), 23–47.

7. Camel, V. 2003. Solid phase extraction of trace elements. *Spectrochimica Acta Part B, Atomic Spectroscopy*. 58(7):1177-1233.

8. Cutter, G., Casciotti, K., Croot, P., Geibert,W ., Heimbürger, LE., Lohan, M., Planquette, H., & van de Flierdt, T. 2017. Sampling and Sample-handling Protocols for

GEOTRACES Cruises. Version 3, August 2017. Toulouse, France, GEOTRACES International Project Office, 139pp. & Appendices.

9. de Jong, J., Boye, M., Schoemann, V., Nolting, R. & de Baar, H. 2000. Shipboard techniques based on flow injection analysis for measuring dissolved Fe, Mn and Al in seawater. *Journal of Environmental Monitoring*. 2(5):496-502.

10. Dierssen, H., Balzer, W. & Landing, W. 2001. Simplified synthesis of an 8-hydroxyquinoline chelating resin and a study of trace metal profiles from Jellyfish Lake, Palau. *Marine Chemistry*. 73(3-4):173-192.

11. Fernández, B., Lobo, L. & Pereiro, R. 2018. Atomic Absorption Spectrometry, Fundamentals, Instrumentation and Capabilities. *Reference Module in Chemistry, Molecular Sciences and Chemical Engineering*.

12. Fratiello, A., Lee, R., Nishida, V. & Schuster, R. 1968. Proton Magnetic Resonance Coordination Number Study of Al(III), Be(II), Ga(III), In(III), and Mg(II) in Water and Aqueous Solvent Mixtures. *The Journal of Chemical Physics*. 48(8):3705-3711.

13. Gensemer, R. & Playle, R. 1999. The Bioavailability and Toxicity of Aluminum in Aquatic Environments. *Critical Reviews in Environmental Science and Technology*. 29(4):315-450.

14. Giesbrecht, T., Sim, N., Orians, K. & Cullen, J. 2013. The distribution of dissolved and total dissolvable aluminum in the Beaufort Sea and Canada Basin region of the Arctic Ocean. *Journal of Geophysical Research, Oceans*. 118(12):6824-6837.

15. Gomes, A., Lunardi, C., Rocha, F. & Patience, G. 2019. Experimental methods in chemical engineering, Fluorescence emission spectroscopy. *The Canadian Journal of Chemical Engineering*. 97(8):2168-2175.

16. Grand, M., Chocholouš, P., Růžička, J., Solich, P. & Measures, C. 2016. Determination of trace zinc in seawater by coupling solid phase extraction and fluorescence detection in the Lab-On-Valve format. *Analytica Chimica Acta*. 923:45-54.

17. Grand, M., Laes-Huon, A., Fietz, S., Resing, J., Obata, H., Luther, G., Tagliabue, A. & Achterberg, E. et al. 2019. Developing Autonomous Observing Systems for Micronutrient Trace Metals. *Frontiers in Marine Science*. 6.

18. Grand, M., Oliveira, H., Ruzicka, J. & Measures, C. 2011. Determination of dissolved zinc in seawater using micro-Sequential Injection lab-on-valve with fluorescence detection. *The Analyst*. 136(13):2747.

19. Han, Q., Moore, J., Zender, C., Measures, C. & Hydes, D. 2008. Constraining oceanic dust deposition using surface ocean dissolved Al. *Global Biogeochemical Cycles*. 22(2).

20. Harris, D. C. 2006. *Quantitative Chemical Analysis.* Eighth Edition. New York: W.H. Freeman and company.419-558.

21. Hatta, M., Measures, C. & Ruzicka, J. 2018. Programmable Flow Injection. Principle, methodology and application for trace analysis of iron in a sea water matrix. *Talanta*. 178:698-703.

22. Hoekenga, O., Vision, T., Shaff, J., Monforte, A., Lee, G., Howell, S. & Kochian, L. 2003. Identification and Characterization of Aluminum Tolerance Loci in Arabidopsis (Landsberg erecta × Columbia) by Quantitative Trait Locus Mapping. A Physiologically Simple But Genetically Complex Trait. *Plant Physiology*. 132(2):936-948.

23. Horstkotte, B., Chocholouš, P. & Solich, P. 2016. Large volume preconcentration and determination of nanomolar concentrations of iron in seawater using a renewable

cellulose 8-hydroquinoline sorbent microcolumn and universal approach of post-column eluate utilization in a Lab-on-Valve system. *Talanta*. 150:213-223.

24. Houck, M. & Siegel, J. 2010. Light and Matter. *Fundamentals of Forensic Science*. 99-122.

25. Houck, M. & Siegel, J. 2015. Separation Methods. *Fundamentals of Forensic Science*. 121-151.

26. Howard, A., Coxhead, A., Potter, I. & Watt, A. 1986. Determination of dissolved aluminium by the micelle-enhanced fluorescence of its lumogallion complex. *The Analyst*. 111(12):1379.

27. Hydes, D. & Liss, P. 1976. Fluorimetric method for the determination of low concentrations of dissolved aluminium in natural waters. *The Analyst*. 101(1209):922.

28. Koirtyohann, S. 1980. A history of atomic absorption spectroscopy. *Spectrochimica Acta Part B, Atomic Spectroscopy*. 35(11-12):663-670.

29. Kradtap Hartwell, S. 2012. Flow Injection/Sequential Injection Analysis Systems, Potential Use as Tools for Rapid Liver Diseases Biomarker Study. *International Journal of Hepatology*. 2012:1-8.

30. Kramer, J., Laan, P., Sarthou, G., Timmermans, K. & de Baar, H. 2004. Distribution of dissolved aluminium in the high atmospheric input region of the subtropical waters of the North Atlantic Ocean. *Marine Chemistry*. 88(3-4):85-101.

31. Landing, W., Haraldsson, C. & Paxeus, N. 1986. Vinyl polymer agglomerate based transition metal cation-chelating ion-exchange resin containing the 8-hydroxyquinoline functional group.*Analytical Chemistry*.58(14):3031-3035.

32. Ma, J. 2000. Role of Organic Acids in Detoxification of Aluminum in Higher Plants. *Plant and Cell Physiology*. 41(4):383-390.

33. Mahowald, N., Hamilton, D., Mackey, K., Moore, J., Baker, A., Scanza, R. & Zhang, Y. 2018. Aerosol trace metal leaching and impacts on marine microorganisms. *Nature Communications*. 9(1).

34. Marion, G., Millero, F., Camões, M., Spitzer, P., Feistel, R. & Chen, C. 2011. pH of seawater. *Marine Chemistry*. 126(1-4):89-96.

35. McKelvie, I. 2008. Principles of Flow Injection Analysis. *Advances in Flow Injection Analysis and Related Techniques*. 81-109.

36. Measures, C. & Brown, E. 1996. Estimating Dust Input to the Atlantic Ocean Using Surface Water Aluminium Concentrations. *Environmental Science and Technology Library*. 301-311.

37. Measures, C. & Edmond, J. 1989. Shipboard determination of aluminum in seawater at the nanomolar level by electron capture detection gas chromatography. *Analytical Chemistry*. 61(6):544-547.

38. Measures, C., Landing, W., Brown, M. & Buck, C. 2008. High-resolution Al and Fe data from the Atlantic Ocean CLIVAR-CO2Repeat Hydrography A16N transect, Extensive linkages between atmospheric dust and upper ocean geochemistry.*Global Biogeochemical Cycles*. 22(1).

39. Measures, C., Sato, T., Vink, S., Howell, S. & Li, Y. 2010. The fractional solubility of aluminium from mineral aerosols collected in Hawaii and implications for atmospheric deposition of biogeochemically important trace elements. *Marine Chemistry*. 120(1-4):144-153.

40. Measures, C. & Vink, S. 2000. On the use of dissolved aluminum in surface waters to estimate dust deposition to the ocean. *Global Biogeochemical Cycles*. 14(1):317-327.

41. Mendecki, L., Granados-Focil, S., Jendrlin, M., Mold, M. & Radu, A. 2020. Self-plasticized, lumogallion-based fluorescent optical sensor for the determination of aluminium (III) with ultra-low detection limits. *Analytica Chimica Acta*. 1101:141-148.

42. Menzel Barraqueta, J.-L., Klar, J. K., Gledhill, M., Schlosser, C., Shelley, R., Planquette, H. F., Wenzel, B., Sarthou, G., and Achterberg, E. P. 2019. Atmospheric deposition fluxes over the Atlantic Ocean: a GEOTRACES case study. *Biogeosciences*. 16:1525–1542.

43. Menzel Barraqueta, J., Samanta, S., Achterberg, E., Bowie, A., Croot, P., Cloete, R., De Jongh, T. & Gelado-Caballero, M. et al. 2020. A First Global Oceanic Compilation of Observational Dissolved Aluminum Data With Regional Statistical Data Treatment. *Frontiers in Marine Science*. 7:1-11.

44. Michalke, B. & Nischwitz, V. 2013. *Liquid Chromatography: Chapter 22. Speciation and Element-Specific Detection.* Germany: Elsevier Inc. 633-649.

45. Middag, R., van Slooten, C., de Baar, H. & Laan, P. 2011. Dissolved aluminium in the Southern Ocean. *Deep Sea Research Part II, Topical Studies in Oceanography*. 58(25-26):2647-2660.

46. Minami, T., Konagaya, W., Zheng, L., Takano, S., Sasaki, M., Murata, R., Nakaguchi, Y. & Sohrin, Y. 2015. An off-line automated preconcentration system with ethylenediaminetriacetate chelating resin for the determination of trace metals in seawater by high-resolution inductively coupled plasma mass spectrometry. *Analytica Chimica Acta*. 854:183-190.

47. Moore, G. 1989. Principles and history of atomic emission spectroscopy. *Introduction to Inductively Coupled Plasma Atomic Emission Spectrometry*. 1-17.

48. Nishikawa,Y ., Hiraki, K., Morishige, K. & Shigematsu, T. 1967. Fluorophotometric determination of aluminum and gallium with lumogallion. *Bunseki kagaku*. 16(7):692-697.

49. Nishikawa, Y., Hiraki, K., Morishige, K., Tsuchiyama, A. & Shigematsu, T. 1968. Fluorometric determination of trace amount of aluminum in sea-water. *Bunseki kagaku*. 17(9):1092-1097.

50. Oliveira, H., Grand, M., Ruzicka, J. & Measures, C. 2015. Towards chemiluminescence detection in micro-sequential injection lab-on-valve format, A proof of concept based on the reaction between Fe(II) and luminol in seawater. *Talanta*. 133:107-111.

51. Orians, K. & Bruland, K. 1985. Dissolved aluminium in the central North Pacific. *Nature*. 316(6027):427-429.

52. Orians, K. & Bruland, K. 1986. The biogeochemistry of aluminum in the Pacific Ocean. *Earth and Planetary Science Letters*. 78(4):397-410.

53. Pyrzynska, K. 2000. Flow-injection speciation of aluminium. *Water Research*. 34(2):359-365.

54. Ren, J., Zhang, J., Luo, J., Pei, X. & Jiang, Z. 2001. Improved fluorimetric determination of dissolved aluminium by micelle-enhanced lumogallion complex in natural waters. *The Analyst*. 126(5):698-702.

55. Resing, J. & Measures, C. 1994. Fluorometric Determination of Al in Seawater by Flow Injection Analysis with In-Line Preconcentration. *Analytical Chemistry*. 66(22):4105-4111.

56. Resing, J., Sedwick, P., German, C., Jenkins, W., Moffett, J., Sohst, B. & Tagliabue, A. 2015. Basin-scale transport of hydrothermal dissolved metals across the South Pacific Ocean. *Nature*. 523(7559):200-203.

57. Riley, J. & Roth, I. 1971. The Distribution of Trace Elements in Some Species of Phytoplankton Grown in Culture. *Journal of the Marine Biological Association of the United Kingdom*. 51(1):63-72.

58. Rudnick, R. & Gao, S. 2003. Composition of the Continental Crust. *Treatise on Geochemistry*. 1-64.

59. Ruzicka, J. 2000. Lab-on-valve, universal microflow analyzer based on sequential and bead injection. *The Analyst*. 125(6):1053-1060.

60. Ruzicka, J. 2016. From continuous flow analysis to programmable Flow Injection techniques. A history and tutorial of emerging methodologies. *Talanta*. 158:299-305.

61. Ruzicka, J. & Hansen, E. 1975. Flow injection analyses. *Analytica Chimica Acta*. 78(1):145-157.

62. Ruzicka, J. & Marshall, G. 1990. Sequential injection, a new concept for chemical sensors, process analysis and laboratory assays. *Analytica Chimica Acta*. 237:329-343.

63. Salomon, S., Giamarchi, P., Le Bihan, A., Becker-Roß, H. & Heitmann, U. 2000. Improvements in the determination of nanomolar concentrations of aluminium in

seawater by electrothermal atomic absorption spectrometry. *Spectrochimica Acta Part B, Atomic Spectroscopy*. 55(8):1337-1350.

64. Scancar, J. & Milacic, R. 2006. Aluminium speciation in environmental samples, a review. *Analytical and Bioanalytical Chemistry*. 386(4):999-1012.

65. Shrivastava, A. & Gupta, V. 2011. Methods for the determination of limit of detection and limit of quantitation of the analytical methods. *Chronicles of Young Scientists*. 2(1), 21.

66. Singh, N. 2016. Fluorescence Spectroscopy as a basic tool of analytical chemists, A review. *IOSR Journal of Applied Chemistry, 2278-5736*.9(4):37-39.

67. Smith, D. & Nordberg, M. 2015. *Handbook on the Toxicology of Metals. General Chemistry, Sampling, Analytical Methods, and Speciation.* Fourth Edition. Elsevier. 15-44.

68. Sohrin, Y. & Bruland, K. 2011. Global status of trace elements in the ocean. *TrAC Trends in Analytical Chemistry*. 30(8):1291-1307.

69. Sohrin, Y., Urushihara, S., Nakatsuka, S., Kono, T., Higo, E., Minami, T., Norisuye, K. & Umetani, S. 2008. Multielemental Determination of GEOTRACES Key Trace Metals in Seawater by ICPMS after Preconcentration Using an Ethylenediaminetriacetic Acid Chelating Resin. *Analytical Chemistry*. 80(16):6267-6273.

70. Sperling, M. 2006. *Encyclopedia of Analytical Chemistry. Flame and Graphite Furnace Atomic Absorption Spectrometry in Environmental Analysis.* Germany: John Wiley & Sons, Ltd. 1-60.

71. Stebbins, J., Zhao, P., Lee, S. & Cheng, X. 1999. Reactive Al-O-Al sites in a natural zeolite; triple-quantum oxygen-17 nuclear magnetic resonance. *American Mineralogist*. 84(10):1680-1684.

72. Tagliabue, A. 2019. Elemental Distribution, Overview. *Encyclopedia of Ocean Sciences*. 122-127.

73. Taylor, S. 1964. Abundance of chemical elements in the continental crust, a new table. *Geochimica et Cosmochimica Acta*. 28(8):1273-1285.

74. Tria, J., Butler, E., Haddad, P. & Bowie, A. 2007. Determination of aluminium in natural water samples. *Analytica Chimica Acta*. 588(2):153-165.

75. van den Berg, C., Murphy, K. & Riley, J. 1986. The determination of aluminium in seawater and freshwater by cathodic stripping voltammetry. *Analytica Chimica Acta*. 188:177-185.

76. van den Berg, M. 1989. Adsorptive cathodic stripping voltammetry of trace elements in sea water. *The Analyst*. 114(12):1527.

77. van Hulten, M., Sterl, A., Tagliabue, A., Dutay, J., Gehlen, M., de Baar, H. & Middag, R. 2013. Aluminium in an ocean general circulation model compared with the West Atlantic Geotraces cruises. *Journal of Marine Systems*. 126:3-23.

78. Wang, B., Lee, C. & Ho, T. 2014. Trace metal determination in natural waters by automated solid phase extraction system and ICP-MS, The influence of low level Mg and Ca. *Talanta*. 128:337-344.

79. Wang, J. & Hansen, E. 2003. Sequential injection lab-on-valve, the third generation of flow injection analysis. *TrAC Trends in Analytical Chemistry*. 22(4):225-231.

80. Wells, M. & Bruland, K. 1998. An improved method for rapid preconcentration and determination of bioactive trace metals in seawater using solid phase extraction and high resolution inductively coupled plasma mass spectrometry. *Marine Chemistry*. 63(1-2):145-153.

81. Wesley R. Harris, Guy Berthon, J. P. 1996. Speciation of aluminium in biological systems. *Journal of Toxicology and Environmental Health*. 48(6):543-568.

82. Wu, J., Chao Yan Zhou, Chi, H., Ming Keong Wong, Hian Kee Lee, Her Yam Ong & Choon Nam Ong. 1995. Determination of serum aluminium using an ion-pair reversed-phase high-performance liquid chromatographic-fluorimetric system with lumogallion. *Journal of Chromatography B, Biomedical Sciences and Applications*. 663(2):247-253.

83. Zagatto, E. & Worsfold, P. 2005. FLOW ANALYSIS | Overview. *Encyclopedia of Analytical Science*. 24-31.

84. Zhou, C. 1995. High performance liquid chromatographic determination of aluminium in natural waters in the form of its lumogallion chelate. *Talanta*. 42(3):415-422.